8-2016

High Throughput Phenotypic Evaluation of Drought-related Traits in Soybean

Hua Bai
University of Arkansas, Fayetteville

High Throughput Phenotypic Evaluation of Drought-related Traits in Soybean

A dissertation submitted in partial fulfillment
of the requirements for degree of
Doctor of Philosophy in Crop, Soil, and Environmental Sciences

By

Hua Bai
Kunming University of Science and Technology
Bachelor of Science in Biological Engineering, 2008
University of Arkansas
Master of Science in Biological Engineering, 2012

August 2016
University of Arkansas

This dissertation is approved for recommendation to the Graduate Council.

_____
Dr. Larry C. Purcell
Dissertation Director

_____
Dr. Christopher G. Henry
Committee Member

_____
Dr. Richard Esten Mason
Committee Member

_____
Dr. James A. Robbins
Committee Member

_____
Dr. Vaughn Skinner Jr.
Committee Member

Abstract

Drought limits crop growth and yield in soybean. Rapid and effective methods of screening large numbers of soybean lines for drought tolerance are urgently needed. Two experiments were conducted to evaluate the effects of drought in soybean during reproductive stages. In the first experiment five genotypes from maturity groups 2 through 5 were tested under well-irrigated and drought conditions. Beginning at R5, leaf samples were taken for nitrogen concentration analysis. Pictures were taken across the top of each plot to determine the intensity of greenness using the Dark Green Color Index (DGCI). Aerial photographs were also taken to determine aerial DGCI values. Leaf nitrogen concentration decreased as plants approached maturity and was closely related to ground DGCI. Additionally, ground DGCI and aerial DGCI values followed similar trends. The aerial DGCI measurements had advantages over ground DGCI measurements in that it allowed discernment between both water treatments. This opens up the possibility of using aerial DGCI to screen genotypes that senesce more slowly under drought.

In the second experiment, the effects of drought in soybean were evaluated by aerial infrared image analysis, carbon isotope discrimination ($\Delta^{13}C$) and oxygen isotope composition ($\delta^{18}O$). Five fast-and five slow-wilting genotypes derived from a cross of Benning × PI416937 were evaluated under three water treatments that included a full and two deficit-irrigation treatments of increasing severity (deficit 1, and 2). After canopy closure, aerial infrared images were taken to determine the relative canopy temperature. Soybean leaves sampled at late R5 and seed at harvest were collected to measure $\Delta^{13}C$ (leaf and seed) and $\delta^{18}O$ (seed) as surrogate measurements for water use efficiency (WUE) and transpiration, respectively. As water availability decreased, the $\Delta^{13}C$ values from leaf and seed generally decreased (i.e., higher WUE). In contrast, the $\delta^{18}O$ values and relative canopy temperature generally increased with increasing

drought stress. Moreover, slow-wilting genotypes generally had lower $\Delta^{13}C$, $\delta^{18}O$ and canopy temperature than fast-wilting genotypes. However, $\delta^{18}O$ values were not consistent over years. The results from these two experiments indicate that the determination of DGCI, $\Delta^{13}C$, and canopy temperature were promising tools for rapid characterization of drought-related traits in soybean.

Acknowledgments

I would like to thank my advisor, Dr. Larry C. Purcell, for his continued and selfless encouragement and support throughout my graduate studies. I am also very thankful for the faith that he had given me in conducting this research project. He always gave me valuable and precious advice whenever I encountered any research or personal problems. I appreciate him sharing his research experience and opinions with me. He often imparted me knowledge by example and through his dedication and passion for research. I will always keep the lessons he has taught me in mind and use them in my research career.

I would also like to thank my advisory committee members: Dr. Chris Henry, Dr. Esten Mason, Dr. Jim Robbins, and Dr. Vaughn Skinner. I appreciate their understanding, precious suggestions and patient help on my research project.

Additionally, I would like to thank the members in our research group for their support: Dr. Andy King for his help with my lab, field work, and experimental design of my research project; Marilynn Davies for her help, suggestions, and her patient guidance on my research or my personal problems; Dr. Montse Salmeron and Dr. Sadal Hwang for their help with building my research background; Avjinder Kaler, Aziz Rehezali, Alejandro Bolton, Ryan Van Roekel, Upton Siddons, Mariana Oliveira, and Pedro Antonelli for their help with my research work and for their friendship. I enjoyed the time working together with them, and I will never forget them.

I would like to thank the Department of Crop, Soil and Environmental Sciences at the University of Arkansas for supporting my graduate studies and everyone working there. Rachael Armstrong and Joda Parent were especially helpful and gave me a lot of help during my graduate studies.

Finally, I would like to thank the United Soybean Board and the Arkansas Soybean Promotion Board for their financial support of my research project.

Dedication

I dedicate my dissertation to my family. My loving parents, Ruizhen Gao and Juhai Bai, have done everything for me which I could never pay back. My brother and my sister-in-law also gave tremendous support and love to me. My husband's love and support have given me great courage to face any difficulty and hardship in my life. My lovely daughter, Lannie, brought me endless happiness and joy throughout my entire doctorate program. My grandparents have continually supported my studies not only in China but also in America. The love, support and encouragement from my family has motivated me to be the best I can be. My appreciation for them cannot be expressed adequately through words.

I also dedicate this dissertation to my uncle, Dr. Jushan Bai at Columbia University and his family. I could not start or finish my graduate research without their encouragements and financial support.

TABLE OF CONTENTS

LIST OF TABLES

CHAPTER II. Evaluation of Soybean Greenness from Ground and Aerial Platforms and the Association with Leaf Nitrogen Concentration in Response to Drought

CHAPTER III. Evaluation of Soybean Response to Drought using Infrared Thermography and Carbon and Oxygen Isotopic Methods

APPENDIX

LIST OF FIGURES

CHAPTER II. Evaluation of Soybean Greenness from Ground and Aerial Platforms and the Association with Leaf Nitrogen Concentration in Response to Drought

CHAPTER III. Evaluation of Soybean Response to Drought using Infrared Thermography and Carbon and Oxygen Isotopic Methods

APPENDIX

CHAPTER I
INTRODUCTION AND LITERATURE REVIEW

Introduction

Drought stress, from an agronomic perspective, refers to decreased soil water content, due to reduced rainfall or irrigation, resulting in abnormal plant development and yield reduction in the field (Passioura, 2007; Purcell and Specht, 2004). Drought is regarded as the most important factor restricting agricultural production worldwide (Waseem, 2011). Drought stress differs with water-deficit stress, which usually refers to the treatments established in a growth chamber or a greenhouse (Purcell and Specht, 2004). Within the last 25 years, 2012 was the most severe drought affecting agricultural productivity of the United States (USDA, 2013a). The USDA (2013a) reported that crop, livestock as well as food retail prices were influenced by the 2012 drought.

Due to world population growth and economic development, water demand is significantly increasing in industry and agriculture. The world population is predicted to increase to 9 billion by 2050 with a projected doubling in food production to feed this large population (Royal Society, 2009). To double food production, a 2.4% per year of yield increase is needed, which is much higher than current yield increase at 1.2% per year (Ray et al., 2013). Over two-thirds of water consumption worldwide is for agriculture (UN Global Compact, 2015). Freshwater demands are predicted to increase 25% by 2030 (UN Global Compact, 2015).

Approximately 51% of the U.S. land is used for agricultural production (USDA, 2014a), but only 8% of this area is irrigated (Board and Kahlon, 2011). The area planted with soybean [*Glycine max* (L.) Merrill] in 2014 accounted for 26% among the U.S. principal crops (USDA, 2015a). The United States served as the largest soybean producer and exporter worldwide, and soybean provides 90% of the U.S. oilseed production (USDA, 2012). USDA (2015a) reported that total soybean production in U.S. in 2014 was 108 million metric tons (3.97 billion bushels) in which Arkansas accounted for 4.4 million metric tons (160 million bushels). The average soybean

yield in the U.S. in 2014 was 3215 kg ha^{-1} (47.8 bu ac^{-1}), whereas the average in Arkansas was 3363 kg ha^{-1} (50 bu ac^{-1}) (USDA, 2015a). In Arkansas in 2014, non-irrigated soybean yielded 935 kg ha^{-1} (13.9 bu ac^{-1}) less than irrigated soybean (USDA, 2014b; USDA, 2014c).

Because there is little land available for expansion, projected doubling in food production requires increasing the productivity of land currently under cultivation. However, increasing global water demands restrains irrigation application, and drought stress affects crop yield potential. Although almost all plants have the ability to resist drought stress to some extent, it differs among and even within species. Improving non-irrigated crop production through breeding efforts is a sustainable way to lessen problems caused by drought. Crop breeders have made efforts to develop drought tolerant crops such as corn [*Zea mays* L.], wheat [*Triticum aestivum* L.], cotton [*Gossypium hirsutum* L.], soybean, and rice [*Oryza sativa* L.] (Basal et al., 2005; Bolanos and Edmeades, 1996; Dhanda et al., 2004; Sapra and Anaele, 2008; Sloane, 1990; Thomison et al., 2013). Great success in selecting cultivars with high yield potential under drought conditions was achieved, especially in corn. Commercially available drought tolerant corn, AQUAmax, Artesian, and DroughtGard hybrids, were recently released by DuPont Pioneer, Syngenta and Monsanto, respectively (Thomison et al., 2013). In 2012, a high yield was observed from those drought-tolerant hybrids compared to susceptible hybrids, and slightly higher or similar yields were found from more favorable conditions (Thomison et al., 2013).

However, conventional breeding programs require large number of crosses and environments for selection, which is time-consuming and dificult to identify the cultivars with specific traits. Breeders need a new strategy to complement the shortcomings that exist in traditional methods. High-throughput phenotyping overcomes the disadvantages of conventional breeding methods and is essential to provide breeders rapid, low-cost, detailed, and non-invasive

information to ensure the improvement at the gene level for future food production (Araus and Cairns, 2014).

Literature Review

A. Overview of Soybean

1. Origin and History of Soybean

Based on taxonomy, soybean [*Glycine max* (L.) Merrill] is in the family of leguminosae (ITIS, 2015); soybean was cultivated from its closest relative, the wild soybean [*Glycine soja* Sieb. & Zucc.] (Joshi et al., 2013; Tian et al., 2010). The major differences between the wild and cultivated soybean include seed color, seed size, seed oil and protein concentration, grain yield and the ability to resist stress (Joshi et al., 2013). Soybean originated in East Asia, specifically China (FAO, 2015; Qiu and Chang, 2010). Wild soybean is only found in China, Korea, Japan and far eastern part of Russia (Qiu and Chang, 2010). Soybean plants were first domesticated in China around 5000 years ago as a food crop and were then grown in several other Asian countries (NCSPA, 2014). In 1765, soybean was introduced to North America for hay by Samuel Bowen, a former sailor in the East India Company (Hymowitz and Harlan, 1983; Hymowitz and Bernard, 1991). Americans started growing soybean for food, and other industrial products in the early 20th century, and soybean became to a major crop in the U.S. over the last three decades (USSEC, 2008).

2. Soybean Today

The growth habit of soybean plants is categorized into either determinate or indeterminate; wild soybean (*Glycine soja*) is indeterminate (Tian et al., 2010). Indeterminate soybean varieties start flowering when plants are around their half final height, whereas determinate varieties bloom more uniformly in the top and bottom positions of the plant (Fehr and Caviness, 1977). Indeterminate plants are taller and have smaller leaves on the top than on the lower portion of the

plant, while determinate varieties have uppermost leaves which are similar in size with ones on the lower portion of plant (Fehr and Caviness, 1977). Determinate varieties possess a terminal raceme with a cluster of flowers along a central stem, but indeterminate plants do not have a raceme and have zigzag-pattern in the upper nodes (Fehr and Caviness, 1977). Determinate varieties were typically grown in the Southern U.S., whereas indeterminate ones are grown in the Northern U.S. (McWilliams et al., 1999), but indeterminate varieties have become more prominent in the Southern U.S. in recent years (Purcell et al., 2014).

Soybean is a short-day plant that initiates flowering under short photoperiods (Kumudini, 2000). Soybean is sensitive to the length of photoperiod, and adapted to different latitudes. Based on the adaptation for specific latitudes, soybean cultivars are classified to different maturity groups (MGs) ranging from 000 in Canada to 9 in the tropics (McWilliams et al., 1999). Arkansas typically grows MGs 3, 4 and 5 cultivars.

Today, soybean serves as one of the most important crops in the world and is commonly used for seed oil, human food, and animal feeding. Worldwide, soybean is grown on more than 90.5 million hectares with around 220 million metric tons of production (USSEC, 2008). The U.S. accounts for 32% of the soybean production, making it the largest producer worldwide, followed by Brazil (28%), Argentina (22%), China (6%) and the rest of world (12%) (USSEC, 2008; USDA, 2015b). In 2014, the United States had 108 million metric tons of soybean production (USDA, 2015a). Soybean seed contains 15 to 23% oil and 33 to 50% protein depending upon variety (Hymowitz et al., 1972). Soybean composes around 90% of the oilseed production in the United States (USDA, 2012).

B. Soybean Yield and the Impact of Drought

1. Agronomic Impact of Drought on Soybean

Specht (1999) reported that soybean yield in the U.S. linearly increased by 22.6 kg ha^{-1} $year^{-1}$ from 1924 to 1998. The increase was faster within the last 25 years (1972 to 1998) at rate of 31.2 kg ha^{-1} $year^{-1}$. The United States had an average yield of soybean production of 3215 kg ha^{-1} (47.8 bu ac^{-1}) in 2014 (USDA, 2015a). However, a report from Nebraska showed that the increasing rate of non-irrigated soybean yield from 1972 to 1997 was 40% lower than irrigated soybean, and the yield difference between irrigated and non-irrigated soybeans was 800 kg ha^{-1} in 1997 (Specht, 1999). More than 90% of the agricultural area is non-irrigated in the U.S. (Board and Kahlon, 2011), and over 18% of Arkansas soybean were grown in non-irrigated land in 2014 (USDA, 2014b; USDA, 2014c). In Arkansas in 2014, irrigated soybean had yield of 3531 kg ha^{-1} (52.5 bu ac^{-1}) whereas non-irrigated soybean yielded 2596 kg ha^{-1} (38.6 bu ac^{-1}) with a difference of 935 kg ha^{-1} (USDA, 2014b; USDA, 2014c). In 2012, the year with most severe drought within last 25 years, non-irrigated soybean yield in Arkansas was 1594 kg ha^{-1} (23.7 bu ac^{-1}) less than irrigated yield (USDA, 2013b; USDA, 2013c). Therefore, drought stress is a severe problem for agricultural systems and is considered one of the most important abiotic factors restricting soybean yield (Heatherly and Elmore, 1986).

2. Physiological Responses of Soybean to Drought

Response of Yield, Seed Mass, Seed Number to Drought at Different Developmental Stages

Drought stress is considered as the most adverse abiotic factors for soybean (Heatherly, 2009). Soybean yield, seed mass, and seed number are affected by drought at different stages of development to varying degrees. Cell expansion, seed germination, and seedling establishment were some of the major factors that contribute to soybean yield loss (Raper and Kramer, 1987). Poor emergence and seedling establishment due to drought stress can lead to a poor plant

population that is insufficient for an optimal yield (Board and Kahlon, 2011). Drought stress occurring after successful stand establishment during vegetative development diminishes cell and leaf expansion because of declined turgor pressure, which subsequently decreases light interception (LI) and leaf area index (LAI), and the decreased LI may limit crop growth rate (CGR) and yield (Raper and Kramer, 1987). LAI of soybean under drought during vegetative stages (emergence to R5) is significantly less than that under well-watered conditions (Cox and Jolliff, 1987). Decreased water availability during the period from emergence to R5 reduces rooting depth resulting in short plants (Mayaki et al., 1976). Drought during the seed filling stages shortens the seedfill period by accelerating senescence, which results in decreased average seed mass and yield (De Souza et al., 1997). Drought starting from the R1 stage mainly reduces pod and seed numbers instead of average seed mass (Ball et al., 2000; Neyshabouri and Hatfield, 1986). Eventually, soybean yield loss occurs from a combination of reduced seed number and/or average seed mass.

Response of Leaf Gas Exchange and Water Use Efficiency to Drought

Water is a major component in plant tissues, and plant growth greatly depends on water. Water moves from the soil into the roots, and through the xylem tissue to leaves. When water reaches the leaves, it moves through stomata and diffuses into the atmosphere through transpiration. Meanwhile, CO_2 in the atmosphere diffuses into the leaf through stomata and is used for photosynthesis. Therefore, stomatal conductance is an essential variable affecting CO_2 and water vapor exchange (Manavalan et al., 2009). Water use efficiency (WUE) is a significant factor affecting crop productivity under drought, and increasing WUE is one strategy to increase agricultural production under drought stress (Araus et al., 2002). WUE refers to the ratio of biomass (BM) produced per unit water transpired (T) (g biomass g water^{-1}). Passioura (1977) provided a function of grain yield under drought conditions:

$$Y = T \times WUE \times HI \quad [1]$$

where Y is the grain yield (g grain m^{-2}), and T is the total amount of water (g water m^{-2}) transpired over the growing season from emergence to physiological maturity, and HI (harvest index) is the ratio of grain weight to the total biomass. WUE at the leaf-level, often referred to transpiration efficiency (TE, mmol mol^{-1}), is defined as the ratio of CO_2 assimilation (A, µmol CO_2 m^{-2} s^{-1}) to transpiration rate (E, µmol H_2O m^{-2} s^{-1}) (Farquhar and Richards, 1984).

CO_2 assimilation, A, may be expressed as stomatal conductance to CO_2 (G_c, µmol m^{-2} s^{-1}) multiplied by the CO_2 concentration gradient between the air (C_a, µmol mol^{-1}) and inside (C_i, µmol mol^{-1}) of the leaf:

$$A = G_c (C_a - C_i) \quad [2]$$

In an analogous way, leaf transpiration rate, E, is equal to stomatal conductance to water vapor (G_w, mmol m^{-2} s^{-1}) multiplied by the concentration gradient of water vapor between inside (W_i, µmol mol^{-1}) of the leaf and the air (W_a, µmol mol^{-1}) (Condon et al., 2004)

$$E = G_w (W_i - W_a) \quad [3]$$

The concentration of CO_2 outside the leaf is greater than that inside the leaf, while water vapor is greater inside the leaf than in the air. Therefore,

$$TE = A/E = [G_c (C_a - C_i)] / [G_w (W_i - W_a)] \quad [4]$$

The ratio of the conductance terms (G_c / G_w) is equal to 0.6, and Eq. [4] can be simplified to Eq. [5] (Condon et al., 2004) indicating that TE is inversely related to C_i/C_a.

$$TE \approx 0.6\ C_a (1 - C_i/C_a) / (W_i - W_a) \quad [5]$$

Based on Eq. [5], TE can be increased by decreasing C_i or ($W_i - W_a$) or by increasing C_a.

Under water-limited conditions, plant cells lose turgor because water movement from the xylem to adjacent cells is inhibited (Nonami, 1998). Turgor loss of plant cells under drought leads to stomatal closure, which decreases diffusion of CO_2 into leaves (decreased stomatal conductance) causing a decreased intercellular CO_2 concentration (Waseem et al., 2011), and thereby, decreasing the rate of photosynthesis as well as transpiration (Mittelheser and Steveninck, 1969). Eventually, turgor loss suppresses cell enlargement and plant growth (Anjum et al., 2003). Soybean plants under CO_2 enrichment have reduced transpiration and increased leaf area and photosynthesis rate under either ideal or water-limited conditions, hence increased TE (WUE at leaf level), compared to plants that were grown in a normal CO_2 condition (Allen et al., 1994; Serraj et al., 1999). Some soybean cultivars such as 'Young' and 'Jackson' show the characteristics of high WUE compared to 'PI416937' (Mian et al., 1996; Purcell et al., 1997). Increased WUE, under water-limited conditions, may increase biomass production sufficiently to improve yield.

Response of Nitrogen Fixation to Drought and Importance of Nitrogen for Seed Production

Soybean seeds contain around 40% protein. Hence, a large amount of nitrogen is required for soybean plants in order to obtain the high protein concentration in the grain. In soybean, nitrogen fixation plays a critical role in providing nitrogen to the plant by reducing gaseous N_2 to biologically useful ammonia (NH_3). This process is mediated by *Bradyrhizobium japonicum* bacteria living in nodules on soybean roots, forming a symbiotic relationship. Young nodules are inactive and are white or gray in color; pink or reddish nodules are actively fixing nitrogen, and nodules that have lost the ability to fix nitrogen usually become green (Lindemann and Glover, 2003). Mastrodomenico and Purcell (2012) found that under well-watered conditions nitrogen fixation continued until the end of seedfill. During the pod filling stage, large amounts of nutrients

are used to develop seeds instead of nodules, and nodules fix nitrogen till grain filling stage finishes and nitrogen is remobilized from leaves to seed (Board and Kahlon, 2011; Lindemann and Glover, 2003; Mastrodomenico and Purcell, 2012).

The amount of nitrogen derived from fixation is inversely related to the nitrogen availability in soil (Harper, 1987), which means that soybean grown in soils with low amount of mineral nitrogen fix more nitrogen than those in soils with large amount of mineral nitrogen. Nitrogen fixation can provide up to 90% of the soybean seed nitrogen when soil nitrogen is minimal (Mastrodomenico and Purcell, 2012). Although nitrogen fixation is an important advantage for soybean and other legumes, it is negatively impacted under drought stress (Djekoun and Planchon, 1991; Purcell, 2009). Nitrogen fixation has high sensitivity to drought compared to photosynthesis, transpiration, total biomass accumulation, or soil nitrogen absorption (Purcell and Specht, 2004). During drought the uptake and assimilation of mineral nitrogen from soil is greater than the rate of nitrogen fixation, indicating that nitrogen fixation is highly sensitive to drought (Purcell and King, 1996). Sinclair et al. (1987) found that nitrogen accumulation rate was 0.31 g N m^{-2} day^{-1} for an irrigated treatment while the rate was 0.003 g N m^{-2} day^{-1} for drought treatment. A 70% reduction in nitrogenase activity was confirmed in soybean during the early stage of water stress (Durand et al., 1987).

C. Ameliorating Effects of Drought on Soybean

1. Management Options

Avoiding Drought

In U.S. Midsouth water deficits usually start sometime in June and extend until September (Heatherly et al., 1998). In Arkansas, the conventional planting date for determinate cultivars is

between April 25 and June 30 (Ashlock et al., 1998a). Typical cultivars grown during this period are in their reproductive stages from mid-July through mid-September and require large amounts of water.

However, dry and hot weather usually occurs during this time span (Healtherly et al., 1998). To avoid drought and heat, soybean may be planted in late March to mid-April in the midsouthern U.S. (Heatherly, 2015). An early planting allows plants to reach full canopy quicker, absorb more sunlight, and transpire more water so that more nodes and pods may be produced, resulting in high yield potential (Specht et al., 2012). Early closed soybean canopy with early planting produces high humidity around the canopy, reduces soil water evaporation and conserves soil moisture for transpiration (Specht et al., 2012). Early planting plus early MGs have advantages of avoiding drought, disease, and insects late in the season (Purcell et al., 2014). Prior to 1985, the predominate MGs in Arkansas were 5, 6 and 7, and more currently MG 4 and 5 are widespread in Arkansas (Purcell et al., 2014). Research conducted at Pine Tree Experiment Station from 1995 to 1998 reported that early planting from April 25 to May 6 with MGs 4, 5 and 6 had significantly higher yield compared to planting from May 25 to June 5 and late planting from July 1 from July 10 (Ashlock et al., 1998b). Nebraska research showed that every single day delayed for planting after May 1 had a yield loss ranging from 0.25 to 0.63 bu ac^{-1}, which again illustrates the importance of selecting an appropriate planting date (Specht et al., 2012). Recent work by Salmeron et al. (2014) found that early planting had highest yield in MG 4 and MG 5, whereas late planting had its greatest yield in MG 3 and MG 4. However, early planting may leave soybean open to risks like low temperature, frost and insects, which can cause germination failure, plant death or injury. Thus, some recommendations offered for early planting include: a seed vigor test and seed fungicide treatments to ensure successful germination, knowing the probability and timing of killing frost in

the area and planting 7-10 days after the potential risk, and use of insecticide and fungicide treatments if needed (Heatherly, 2015; Specht et al., 2012).

Tillage

Soil structure is critical to support plants and to provide crops with water and nutrients (Bronick and Lal, 2005). Soil water availability, flow and storage are affected by soil structure (Pachepsky and Rawls, 2003). Tillage is an essential factor influencing sustainable use of soil by changing soil properties and crop production (Lal and Stewart, 2013). Among the factors that contribute to crop production, tillage accounts for as high as 20% of total yield variability (Khurshid et al., 2006). However, conventional tillage disturbs macropores in soil, which are responsible for water storage and for the diffusion of air, water, and chemicals in soil (Khan et al., 2001).

The soil surface on a tilled field may form crusts with rainfall that reduces infiltration and increases runoff (Triplett et al., 2008). No tillage or reduced tillage can reduce soil erosion and conserve soil-moisture availability for crops and may contribute to increased crop production during drought seasons (Triplett et al., 2008). Yet, Khairul et al. (2014) reported that among no tillage, minimum tillage, conventional tillage, and deep tillage, no tillage has shown the highest reduction in soil particle density, bulk density, and permanent wilting point after four years study, while deep tillage had the lowest reduction in those area. Likewise, the maximum and minimum available water contents were in deep tillage and no tillage, respectively. Available water content constrains productivity, but deep tillage may breakup hard subsoil layers and increase infiltration and allow roots access to soil moisture deep in the profile (Baumhardt and Jones, 2005). With deep tillage, a 10% crop yield increase was found compared to other tillage practices (Baumhardt and Jones, 2005). Deep tillage allows wheat and rice plants to produce a higher root mass density in

deeper soil layers compared with other tillage practices (Khairul et al., 2014), which may be particularly important during drought stress.

2. Genetic Differences in Traits Related to Drought Tolerance

Fast/Slow Wilting

One of the aims for breeders is to select soybean cultivars with drought tolerance. Slow-wilting, considered as one characteristic of drought tolerance, has been found in several soybean genotypes including PI 416937, PI 471938, PI 567690 and PI 567731 (King et al., 2009; Pathan et al., 2014; Sloane et al., 1990). PI 416937 is a Japanese accession that exhibits minimal yield loss under drought and has the slow-wilting characteristic (King et al., 2009; Sloane et al., 1990), which may result from its soil moisture conservation under drought conditions (Sadok and Sinclair, 2010). This genotype limits stomatal conductance (Tanaka et al., 2010) and has constant transpiration rate at vapor pressure deficits (VPDs) over 2.0 kPa (Fletcher et al., 2007). In contrast, transpiration for commercial cultivars continues to increase linearly as VPD values increase above 2.0 kPa (Fletcher et al., 2007). The results above indicate that the slow-wilting trait might be favorable when evaporative demand is extremely high, resulting in increased water use efficiency.

Genotypic Differences in Nitrogen Fixation

Nitrogen fixation is negatively affected by drought stress (Purcell, 2009; Djekoun and Planchon, 1991). There are numerous articles that reported the sensitivity of nitrogen fixation to drought stress in soybean (King et al., 2014; King and Purcell, 2006; Purcell and King, 1996; Sprent, 1972; Vadez and Sinclair, 2001; Weisz et al., 1985). Nitrogen fixation under water-limited conditions has been reported to be associated with ureide concentration in plant tissues (Serraj and

Sinclair, 1997; Vadez et al., 2000; Vadez and Sinclair, 2001). Ureides are the final product of nitrogen fixation that are produced in nodules and transported to the shoot. Ureide accumulation in soybean leaf tissues during drought stress was correlated with decreased nitrogen fixation (de Silva et al., 1996). Under drought conditions, plants with low ureide accumulation in leaves had enhanced nitrogen fixation, whereas plants with high ureide in leaf tissue reduced the nitrogen fixation activity (Serraj and Sinclair, 1997; Vadez et al., 2000; Vadez and Sinclair, 2001). 'Jackson', the drought-tolerant soybean cultivar, accumulated less ureide than drought-sensitive cultivars (Serraj and Sinclair, 1996) indicating Jackson may have greater nitrogen fixation than drought-susceptible cultivars.

Besides shoot ureide concentration, shoot nitrogen concentration can also indicate the differences of nitrogen fixation sensitivity. Under drought stress conditions, the ureide concentration is inversely related to the activity of nitrogen fixation (Serraj and Sinclair, 1997; Vadez et al., 2000; Vadez and Sinclair, 2001), which indicates that leaf/shoot nitrogen concentration would decrease if nitrogen fixation decreased due to drought during seedfill. King and Purcell (2006) found that soybean genotypes with high well-watered nitrogen concentration had lower shoot nitrogen concentration under drought stress than under well-watered conditions. Under well-watered conditions, both shoot nitrogen and ureides concentrations are strongly correlated with genotypic differences for the sensitivity of nitrogen fixation; under drought stress, only shoot ureide concentration is correlated with continued nitrogen fixation (King et al., 2014). Sall and Sinclair (1991) found that soybean genotype Jackson was drought-tolerant for nitrogen fixation among six genotypes in a greenhouse study and eight genotypes in field tests.

The acetylene reduction activity (ARA) assay has been used in numerous articles to study drought tolerance of nitrogen fixation. Fraction of transpirable soil water (FTSW) is defined as the

ratio of the transpirable soil water left in soil to the total amount of transpirable soil water (Sinclair and Ludlow, 1986). In a greenhouse experiment, soybean genotypes with low well-watered shoot ureide concentration had a lower FTSW threshold at which ARA started to decrease compared with genotypes with a high well-watered shoot ureide concentration (Vadez and Sinclair, 2001). King et al. (2014) conducted a growth chamber experiment and found that different soybean genotypes responded differently for sensitivity of nitrogen fixation under drought stress. Most drought tolerant lines had a lower FTSW of 0.11 compared with the drought sensitive genotypes KS4895 with a FTSW of 0.19. Normalized ARA can be affected by soil moisture when FTSW reached 0.4; at FTSW values less than 0.4, normalized ARA decreased linearly (Serraj et al., 1998). Purcell et al. (1997) found that under moderate drought conditions, Jackson, drought-resistant genotype, maintained twice the ARA as KS4895, a drought-sensitive genotype, indicating Jackson fixes more nitrogen under drought than KS4895. Although the ARA assay is a simple and an economical way for quantification of nitrogen fixation activity, it is difficult to use in field environments and cannot be used for seasonal estimates (Hardarson and Danso, 1993; Kagabo, 1986).

Deep Rooting

Soybean root system responds differently for drought-tolerant and drought-sensitive genotypes due to drought. Roots distribution is critical to evaluate the response of plants to absorb soil water and nutrients, especially for roots that can reach deeper soil (Fenta et al., 2014). Thus, crop development and productivity can be influenced by root architecture. Plants develop deeper taproots in order to adapt to drought stress (Taylor et al, 1978). Deeper roots and greater root mass provide a better chance to extract moisture in deeper soil (Garay and Wilhelm, 1982).

Because roots first perceive soil water limitation, water stress can trigger increased ratio of root to shoot mass (Manavalan et al., 2009). Rainfed soybean had longer roots than well-watered plants (Huck et al., 1983). Soybean exposed to drought at later vegetative stages and/or early reproductive stages had greater root growth than plants exposed to drought at R4 stage (Hoogenboom et al., 1987). Soybean drought stressed prior to blooming had yields greater than soybean drought stressed after blooming (Hirasawa et a., 1994). One interpretation of these results is that increased root development occurred during vegetative stages allowing plants to reach more moisture deep in soil when drought occurred.

Root distribution and architecture for drought-tolerant soybean has also been explored in some research. Fenta et al. (2014) reported that a drought-susceptible cultivar, A5409RG, possessed shallow roots with a root angle of <40º; Jackson, a drought-tolerant cultivar, had deeper roots with a root angle of >60º; an intermediate drought-tolerant cultivar, Prima 2000, had intermediate root depth with a root angle of 40º-60º, and greatest shoot biomass and yield. PI416937, with the slow-wilting trait, possesses an extensive, fibrous root system, large root surface area and large number of nodules (Pantalone et al., 1996).

D. Breeding for Drought Tolerance in Soybean

1. Current Cultivars are Closely Related (lack of genetic diversity)

Superior soybean cultivars with high yield are developed from segregating population, and lines with high yield and favorable traits are selected as parents to produce segregating populations (Sneller, 1994). A large number of public soybean cultivars have been generated within the last several decades in North America (Gizlice et al., 1996). However, elite soybean populations in North American lack genetic diversity. Approximately, 95% of the genes in current soybean

cultivars comes from only 35 genotypes (Gizlice et al., 1994) indicating that modern cultivars are closely related. Low genetic diversity places big challenges for soybean breeders to develop superior lines. Genetic diversity and agronomic value have to be taken into account to introduce new sources of germplasm into breeding program for increase of genetic variation and crop productivity (Ude et al., 2003).

2. Selection of Physiological Traits of Interest from Widely Diverse Germplasm

Fast/Slow Wilting

Canopy wilting in soybean is one of the first signs observed for water stress (King et al., 2009). Canopy wilting is first observed during drought, and the intensity of canopy wilting varies among soybean genotypes (Sloane et al., 1990). Visual rating of canopy wilting has been used to identify fast/slow-wilting genotypes (Abdel-Haleem et al., 2012; King et al., 2009). Although visual rating has been accepted by researchers, it is objective and dependent on one's experience. Additionally, wilting severity may change due to rapidly changing environmental conditions during the time that wilting data are being collected. Thereby, a rapid and objective technique is needed to quantify slow wilting.

Water Use Efficiency

Water use efficiency (WUE) is an important factor affecting crop productivity under drought. WUE at leaf level can be described as the ratio of CO_2 accumulation to leaf water loss through transpiration (Farquhar and Richards, 1984); WUE at plant level is the ratio of dry biomass accumulation to the water transpired (Jones, 1992).

Soybean genotypes differ in WUE. Mian et al. (1996) found in a greenhouse experiment that 'Young' had a high WUE (4.4 g dry matter L^{-1}) relative to PI416937 (3.7 g dry matter L^{-1}). Purcell et al. (1997) reported that with similar water losses by transpiration, Jackson gained more nitrogen and biomass than did PI416937. High WUE is one strategy to increase crop production under drought conditions (Araus et al., 2002). However, it is difficult to measure WUE. Biomass accumulation is easy to calculate, but determining transpiration has traditionally been done gravimetrically, which is not amenable to large-scale evaluations. Therefore, WUE at leaf level with photosynthetic/transpiration measurements are tedious and not amenable to large-scale evaluations.

Nitrogen Fixation

Up to 90% of soybean grain nitrogen was obtained through nitrogen fixation when soil nitrogen was low (Mastrodomenico and Purcell, 2012). However, nitrogen fixation is significantly reduced under drought, even though nitrogen fixation plays a critical role in soybean and other legumes (Djekoun and Planchon, 1991; Purcell, 2009). Purcell et al. (1997) conducted a greenhouse experiment to compare nitrogen and biomass accumulation in six soybean genotypes including Jackson and PI416937. They found that Jackson continued accumulating nitrogen and biomass during drought conditions relative to drought-sensitive cultivar and that Jackson accumulated more biomass than PI416937 when they had similar transpirational losses. Sall and Sinclair (1991) found that Jackson was drought-tolerant for nitrogen fixation among six genotypes in a greenhouse study and eight genotypes in field tests. A growth chamber study compared the nitrogen fixation rate of PI416937 and Forrest, a commercial cultivar, and concluded that PI416937 accumulated more nitrogen than Forrest and yielded more during drought stress (Patterson and Hudak, 1996). Herridge et al. (1990) were able to use ureide- and natural-^{15}N-

abundance methods to assess soybean nitrogen fixation in field studies among six genotypes. However, measurements for genetic differences of nitrogen fixation allow only a few genotypes to be measured at a time.

3. High Throughput Selection

Color Image Analysis during Seedfill

During the seedfill period in soybean, nitrogenous compounds from vegetative tissues are broken down to supply seed with nitrogen (Sinclair and deWitt, 1976; Mastrodomenico and Purcell, 2012). In the absence of soil nitrogen, most of the seed nitrogen is derived from biological nitrogen fixation. Hence, decreased nitrogen fixation in soybean due to drought during the seedfill period results in a shortage of nitrogen and accelerated senescence. Nitrogen is a key element of chlorophyll, the green pigment in plants responsible for photosynthesis. Consequently, lack of nitrogen leads to a decline of chlorophyll and leaf yellowing. Therefore, canopy color is associated with nitrogen status in crops, which is amenable to measurement by remote sensing.

Karcher and Richardson (2003) reported a method of digital image analysis in which the hue (H), saturation (S), and brightness (B) values from a digital image were converted into a dark green color index (DGCI) value as shown in the equation below:

$$\text{DGCI value} = [(H - 60) / 60 + (1 - S) + (1 - B)] / 3 \quad [6]$$

DGCI is a composite number on a scale of 0 to 1 with higher values related to a darker green color and lower values corresponding to a yellow color.

Rorie et al. (2011a; 2011b) reported that DGCI values were closely associated with leaf N concentration. In this regard, corn [*Zea mays L.*] leaf photographs were taken against a pink felt

background with yellow and green color disks that served as known internal standards. Based on their research, the internal standards were used to calibrate differences among cameras and lighting conditions. Images were saved as joint photographic experts group (JPEG), reordered and renamed by FastStone Image viewer (www.faststone.org), and analyzed by Sigma Scan Pro 5.0 (https://systatsoftware.com/products/sigmascan/) which were used to calculate DGCI (Rorie et al., 2011a; Rorie et al., 2011b). In soybean, differences in DGCI between well-watered and drought conditions may reflect the activity of nitrogen fixation (King et al., 2014).

Carbon Isotope Discrimination as a Surrogate Measure of Water Use Efficiency

The isotopes that are commonly used in natural abundance studies include carbon (C), nitrogen (N), and oxygen (O). Stable isotope analysis is a powerful tool assessing plant tissue. During the last decades, stable isotope techniques have witnessed the achievements to understand several biochemical and physiological mechanisms in plants (Barbour, 2007; Cernusak et al., 2003; Werner et al., 2012). Stable isotope ratios are one tool for describing the performance of plants under drought.

The carbon in the ecosystem is comprised of 98.89% ^{12}C, 1.1% ^{13}C, and a trace of ^{14}C. ^{13}C is a stable isotope whereas ^{14}C is radioactive, which means the nuclei are unstable and dissipate by emitting radiation. Hence, ^{14}C is usually regarded as negligible. The distribution of isotopes are uneven in different materials. The ratio of ^{13}C to ^{12}C in plant tissue is usually less than that in the atmosphere (as CO_2) indicating there is an isotope discrimination when carbon is assimilated into plant tissue (Farquhar and Richards, 1984; Farquhar et al., 1989). The variation in discrimination against ^{13}C is due to two factors. First, ^{13}C is a heavier molecule and diffuses more slowly as CO_2 into plant tissues than ^{12}C. Second, the enzymatic reaction of ribulose bisphosphate carboxylase oxygenase (RuBisCo) reacts more readily with $^{12}CO_2$ than $^{13}CO_2$ (Farquhar et al., 1989).

Carbon isotope discrimination ($\Delta^{13}C$) is defined as the deviation of carbon isotopic abundance in the air and plant (Farquhar et al., 1989)

$$\Delta^{13}C = (R_a - R_p)/R_p = (R_a/R_p) - 1 \quad [7]$$

where R_a is the carbon isotopic abundance, $^{13}C/^{12}C$, in the air, and R_p is the carbon isotopic abundance, $^{13}C/^{12}C$, in the plant tissue.

Farquhar et al. (1982) described a simple equation of carbon isotope discrimination for C3 plants:

$$\Delta^{13}C = a + (b - a)\, C_i/C_a \quad [8]$$

where a is the discrimination that occurs due to diffusion of $^{12}CO_2$ and $^{13}CO_2$ through stoma (~4.4‰), and b is the discrimination affected by RuBisCo within the process of CO_2 carboxylation into the first products in photosynthesis (~27‰). Ci/Ca is the ratio of CO_2 inside the leaf and in the atmosphere, respectively, as described in Eq. [4] and Eq. [5]. Thus, Eq. [8] can be simplified by substituting terms a and b with 4.4 (‰) and 27 (‰):

$$\Delta^{13}C\ (‰) \approx 4.4 + 22.6\, C_i/C_a \quad [9]$$

$\Delta^{13}C$ is positively related to C_i/C_a from Eq. [9] whereas TE, WUE at leaf level, is negatively related to C_i/C_a from Eq. [5]. Based on that, $\Delta^{13}C$ and TE are inversely related.

Numerous research publications have confirmed the relationship between $\Delta^{13}C$ and WUE as an indicator for the degree of drought stress. Farquhar and Richards (1984) described the inverse relationship between WUE and $\Delta^{13}C$ in leaves of C3 plants. Condon et al. (1990) reported the positive relationship between $\Delta^{13}C$ and C_i/C_a, and negative relationship between WUE and $\Delta^{13}C$

for 13 and 16 wheat genotypes, respectively. Crop productivity of bread wheat and durum wheat was also reported to be closely associated with $\Delta^{13}C$ (Araus et al., 1998; Condon et al., 2004).

Oxygen Isotope Composition as a Surrogate Measure of Transpiration

Three stable oxygen isotopes exists in the ecosystem: ^{16}O (99.76%), ^{17}O (0.04%), and ^{18}O (0.20%). The $^{18}O/^{16}O$ ratios are usually the focus of research since the large quantity and great mass difference between ^{16}O and ^{18}O (Rohling, 2007). The ^{18}O isotope can be found in a small proportion of water molecules, so the oxygen isotope composition of plant tissue can be used to reflect the isotopic changes in water composition due to transpiration and photosynthesis. Measurements of ^{18}O composition have great potential for understanding physical and biochemical processes within plants (Robinson et al., 1995).

Numerous articles have reported the applications and importance of oxygen isotope enrichment (Barbour et al, 2004; Gessler et al., 2007; Madhava et al., 2010; Rohling, 2007; Sheshshayee et al., 2005;). Most research publications used leaf water to assess oxygen isotope enrichment (Barbour et al, 2004; Gessler et al., 2007). A few reports have used leaf dry matter in evaluations (Madhava et al., 2010). A positive correlation between $\delta^{18}O$ in leaf water or leaf dry biomass and stomatal conductance as well as transpiration were reported so that $\delta^{18}O$ can reflect the ^{18}O enrichment over a long-term plant development (Madhava et al., 2010).

Water is needed in the Calvin cycle of photosynthesis in which CO_2 and H_2O are needed to synthesize hexoses. The H_2O molecule is added to 2-Carboxy-3-keto-D-arabinitol 1, 5-bisphosphate to form two 3-phosphoglycerate, one of which contains the oxygen from H_2O (Berg et al., 2005). These two 3-phosphoglycerate are then be used to form hexoses in following reactions (Berg et al., 2005). Thus, the use of leaf dry biomass to assess oxygen isotope enrichment is feasible. Increased stomatal conductance resulted in increased transpiration rate, and increased

$\delta^{18}O$ in leaf water because $H_2{}^{18}O$ diffuses much more slowly than $H_2{}^{16}O$ from the leaf (Farquhar and Lloyd, 1993).

Carbon isotope discrimination ($\Delta^{13}C$) has been used as a surrogate measure of WUE, but the value of increased WUE for agronomic crops is questionable. Generally, low values of $\Delta^{13}C$ (high WUE) could result from two scenarios. Firstly, low stomatal conductance at a constant C_i/C_a which decreases transpiration, resulting in increased WUE due to the negative relationship between transpiration and WUE shown in Eq. [5]. However, increased WUE from decreased stomatal conductance would also expectantly decrease crop growth because of decreased CO_2 diffusion into leaves (Eq. [4]). Secondly, decreased C_i/C_a at any given stomatal conductance would result in increased WUE (Eq. [5]). Eq. [5] indicates that a plant with a decreased C_i/C_a would assimilate more carbon at a given conductance value, resulting in a higher WUE than a plant with a higher C_i/C_a at the same conductance.

By combining $\Delta^{13}C$ and $\delta^{18}O$ analysis it offers the possibility of identifying genotypes with high WUE from $\Delta^{13}C$ analysis and determining if high WUE is due to low conductance or low C_i/C_a from $\delta^{18}O$ analysis. Xu et al. (2000) reported a negative relationship between $\Delta^{13}C$ and $\delta^{18}O$ in leaf of pine tree.

However, the disadvantages of isotope analysis also have to be considered, including (a) $\delta^{18}O$ method cannot directly determine grain yield and water use efficiency, (b) carbon and oxygen analysis requires very small sample size, requiring extreme care in obtaining a representative sample (e.g., grinding, sample preparation and sample weighing), (c) cost of isotope analysis is high around $20 per sample, (d) and higher WUE at the leaf level may not result in higher WUE and yield at the crop level (Condon et al., 2004; Ebdon et al., 1998).

Infrared Imaging as a Surrogate Measure for Slow-wilting

Temperature is one of the most frequently measured physical quantities. All objects in the landscape with a temperature greater than absolute zero emit thermal infrared energy (Jensen, 2007). Vegetation becomes stressed due to lack of water, and the spectral reflectance of vegetation changes according to the severity of the stress. Infrared thermography is now a developed tool with agricultural applications. Measurements of canopy temperature using thermal IR imaging mainly focuses on plant water relations such as stomata conductance, because canopy temperature can reflect the conditions of transpiration rate (Jones et al., 2009). Aerial imaging techniques have been using in the United States since 1930s to assist agricultural management (Rundquist and Samson, UNL). Over the past decade, IR thermal imaging was well developed in a variety of studies. French et al. (2000) proposed a method using remote thermal infrared imagery to distinguish senescent vegetation from bare soil. Handcock et al. (2006) used thermal IR remote sensing to detect stream temperature. Jones et al. (2002) applied infrared thermal imaging to monitor stomata conductance of grapevines in a field study. A wireless infrared thermometer was used to identify wheat genotypes with drought tolerance in the US Southern high plains and found that genotypes with a cool canopy tended to have greater yield under drought conditions (Rudd et al., 2013). Aerial imaging is more rapid compared with ground measurements because one image can include a large number of plots (Jones et al., 2009; Guilioni et al., 2008). Additionally, aerial imaging does not have to contact plant leaves, which may be destructive to stomatal responses (Guilioni et al., 2008).

As discussed previously, the slow-wilting trait in soybean has been found in some genotypes including PI 416937 (King et al., 2009), PI 471938 (Fletcher et al., 2007; Sadok et al., 2012), PI 567690 (Pathan et al., 2014), and PI 567731 (Pathan et al., 2014). King et al. (2009) found that slow wilting was due to conservation of moisture when soil moisture was plentiful that

could then be utilized during drought when fast wilting genotypes had exhausted their soil moisture. Canopy wilting has been measured by visual rating on a scale of 0 to 100 (0=no wilting; 100=plant death) (Abdel-Haleem et al., 2012; King et al., 2009). However, rating plots is subjective and time-consuming. Aerial thermal imaging can overcome the disadvantages of visual rating and supply a rapid, precise, and objective method to screen for a cool canopy in soybean.

Several different aerial platforms have been used for remote sensing applications including unmanned aerial vehicle (UAV), balloon, and kite platforms (Aber et al., 2002; Boike and Yoshikawa, 2003; Miyamoto et al., 2004; Primicerio et al., 2012; Chapman et al., 2014). Chapman et al. (2014) used a UAV for high throughput field-based phenotyping to estimate ground cover in sorghum [*Sorghum bicolor* (L.) Moench], canopy temperature in sugarcane [*Saccharum officinarum* L.], and crop lodging in wheat. Primicerio et al. (2012) reported a UAV platform for precision agriculture application in small crops. Miyamoto et al. (2004) used aerial imaging with a balloon platform to classify the wetland vegetation of Kushiro in Japan. Boike and Yoshikawa (2003) applied balloon and kite aerial imaging method to collect the glacial features and vegetation in Alaska. Aber et al. (2002) have applied unmanned, kite-based, small-format remote sensing methods for diverse applications such as assessment of forests and wetlands.

Objective

This research was aimed to develop aerial imaging tools to rapidly screen large number of soybean lines for drought tolerance traits in field environments, characterize differences in seed-fill duration among soybean lines during drought from the association of DGCI and shoot nitrogen, and characterize $\Delta^{13}C$, $\delta^{18}O$, canopy temperature in genotypes that have known differences in how quickly they wilt under drought conditions.

Literature Cited

Abdel-Haleem, H., T.E. Carter Jr., L.C. Purcell, C.A. King, L.L. Ries, P. Chen, W. Schapaugh Jr., T.R. Sinclair, and H.R. Boerma. 2012. Mapping of quantitative trait loci for canopy-wilting trait in soybean (Glycine max L. Merr). Theor. Appl. Genet. 125:837-846.

Aber, J.S., S.W. Aber, and F. Pavri. 2002. Unmanned small-format aerial photography from kites for acquiring large-scale, high-resolution, multiview-angle imagery. In: The International Archives of the Photogrammetry, Remote Sensing and Spatial Information Sciences, Pecora 15/Land Satellite Information IV/ISPRS Commission I/FIEOS, Denver, CO, USA.

Alam, M.K., M.M. Islam, N. Salahin, and M. Hasanuzzaman. 2014. Effect of tillage practices on soil properties and crop productivity in wheat-mungbean-rice cropping system under subtropical climatic conditions. Sci. World J. doi: 10.1155/2014/437283.

Allen, L.H., R.R. Valle, J.W. Mishoe, and J.W. Jones. 1994. Soybean leaf gas-exchange responses to carbon dioxide and water stress. Agron. J. 86:625-636.

Allen, R.G., L.S. Pereira, D. Raes, and M. Smith. 1998. Crop evapotranspiration - Guidelines for computing crop water requirements - FAO Irrigation and drainage paper 56. http://www.fao.org/docrep/X0490E/X0490E00.htm (accessed 31 May 2016).

Anjum, F., M. Yaseen, E. Rasul, A. Wahid, and S. Anjum. 2003. Water stress in barley (*Hordeum vulgare* L.). I. Effect on morphological characters. Pakistan J. Agric. Sci. 40:43-44.

Araus, J.L., T. Amaro, J. Casadesus, A. Asbati, and M.M. Nachit. 1998. Relationships between ash content, carbon isotope discrimination and yield in durum wheat. Aust. J. Plant Physiol. 25:835-842.

Araus, J.L., and J.E. Cairns. 2014. Field high-throughtput phenotyping: the new crop breeding frontier. Trends Plant Sci. 19:52-61.

Araus, J.L., G.A. Slafer, M.P. Reynolds, and C. Royo. 2002. Plant breeding and drought in C3 cereals: what should we breed for? Annals of Botany 89:925–940.

Ashlock, L., R. Klerk, G. Huitink, T. Keisling, and E. Vories. 1998a. Planting practices. p. 42-48. In: Arkansas soybean handbook, MP197. Arkansas Cooperation Extension Service, Little Rock, AR.

Ashlock, L., W. Mayhew, T. Windham, T. Keisling, R. Klerk, D. Beaty, and G. Lorenz. 1998b. Production systems and economics. p. 122-128. In: Arkansas soybean handbook, MP197. Arkansas Cooperation Extension Service, Little Rock, AR.

Ball, R. A., L.C. Purcell, and E.D. Vories. 2000. Short-season soybean yield compensation in response to population and water regime. Crop Sci. 40:1070-1078.

Barbour, M.M. 2007. Stable oxygen isotope composition of plant tissue: a review. Funct. Plant Biol. 34. doi: 10.1071/FP06228.

Barbour, M.M, J.S. Roden, G.D. Farquhar, and J.R. Ehleringer. 2004. Expressing leaf water and cellulose oxygen isotope ratios as enrichment above source water reveals evidence of a Péclet effect. Oecologia. 138:426-435.

Basal, H., C.W. Smith, P.S. Thaxton, and J.K. Hemphill. 2005. Seedling drought tolerance in upland cotton. Crop Sci. 45:766-771.

Baumhardt, R.L., and O.R. Jones. 2005. Long-term benefits of deep tillage on soil physical properties and crop yield. p. 95–101. In: Proceedings of the 27th Southern Conservation Tillage Systems Conference, Florence, KY, USA. http://www.ag.auburn.edu/auxiliary /nsdl/scasc/Proceedings/2005/Baumhardt.pdf (accessed 1 Jun. 2016).

Berg, J.M., J.L. Tymoczko, and L. Stryer. 2005. The Calvin cycle and the pentose phosphate pathway. p. 565-591. In: (eds. K. Ahr et al.) Biochemistry, 6th Edition. Freeman, New York, NY.

Board, J.E., and C.S. Kahlon. 2011. Soybean yield formation: what controls it and how it can be improved. p. 1-36. In: (eds. A. Hany, El-Shemy) Soybean Physiology and Biochemistry, InTech, doi: 10.5772/17596. http://www.intechopen.com/books/soybean-physiology-and-biochemistry/soybean-yield-formation-what-controls-it-and-how-it-can-be-improved (accessed 31 May 2016).

Boike, J., and K. Yoshikawa. 2003. Mapping of periglacial geomorphology using kite/balloon aerial photography. Permafrost Periglac. 14:81-85.

Bolanos, J., and G.O. Edmeades. 1996. The importance of the anthesis-silking interval in breeding for drought tolerance in tropical maize. Field Crops Res. 48:65-80.

Bronick, C.J., and R. Lal. 2005. Soil structure and management: a review. Geoderma. 124:3-22.

Cernusak, L.A., D.J. Arthur, J.S. Pate, and G.D. Farquhar. 2003. Water relations link carbon and oxygen isotope discrimination to phloem sap sugar concentration in *Eucalyptus globulus*. Plant Physiol. 131:1544-1554.

Chapman, S.C., T. Merz, A. Chan, P. Jackway, S. Harbar, M. F. Dreccer, E. Holland, B. Zheng, T.J. Ling, and J. Jimenez-Berni. 2014. Pheno-copter: a low-altitude, autonomous remote-sensing robotic helicopter for high-throughput field-based phenotyping. Agron. 4:279-301.

Condon, A.G., G.D. Farquhar, and R.A. Richards. 1990. Genotypic variation in carbon isotope discrimination and transpiration efficiency in wheat leaf gas exchange and whole plant studies. Aust. J. Plant Physiol. 17:9-22.

Condon, A.G., R.A. Richards, G.J. Rebetzke, and G.D. Farquhar. 2004. Breeding for high water-use efficiency. J. Exp. Bot. 55:2447-2460.

Cox, W.J., and G.D. Jolliff. 1987. Crop-water relations of sunflower and soybean under irrigated and dryland conditions. Crop Sci. 27:553-557.

de Souza, P.I., D. B. Egli, and W.P. Bruening. 1997. Water stress during seed filling and leaf senescence in soybean. Agron. J. 89:807-812.

Dhanda, S.S., S.G. Sethi, and R.K. Behl. 2004. Indices of drought tolerance in wheat genotypes at early stages of plant growth. J. Agron Crop Sci. 190:6-12.

Dilworth, M.J. 1966. Acetylene reduction by nitrogen fixing preparations from Clostridium pasteurianum. Biochem. Biophys. Acta. 127:285-294.

Djekoun, A., and C. Planchon. 1991. Water status effect on dinitrogen fixation and photosynthesis in soybean. Agron. J. 83:316-322.

Durand, J.L., J.E. Sheehy, and F.R. Minchin. 1987. Nitrogenase activity, photosynthesis and nodule water potential in soyabean plants experiencing water deprivation. J. Exp. Bot. 38:311-321.

Ebdon, J.S., A.M. Petrovic, and T.E. Dawson. 1998. Relationship between carbon isotope discrimination, water use efficiency, and evapotranspiration in Kentucky Bluegrass. Crop Sci. 38:157-162.

FAO. 2015. Glycine max L. Food and Agriculture Organization of the United Nations. http://www.fao.org/ag/agp/AGPC/doc/gbase/data/soybean.htm (accessed 29 May 2016).

Farquhar, G.D., J.R. Ehleringer, and K.T. Hubick. 1989. Carbon Isotope discrimination and photosynthesis. Plant Mol. Biol. 40:503-537.

Farquhar, G.D., M.H. O'leary, and J.A. Berry. 1982. On the relationship between carbon isotope discrimination and the intercellular carbon dioxide concentration in leaves. Aust. J. Plant Physiol. 9:121-137.

Farquhar, G.D., and R.A. Richards. 1984. Isotopic composition of plant carbon correlates with water-use efficiency of wheat genotypes. Aust. J. Plant Physiol. 11:539–552.

Fehr, W.R., and C.E. Caviness. 1977. Stages of soybean development. Cooperative Extension Service, Agriculture and Home Economics Experiment Station, Iowa State University, Ames, Iowa.

Fenta, B.A., S.E. Beebe, K.J. Kunert, J.D. Burridge, K.M. Barlow, J.P. Lynch, and C.H. Foyer. 2014. Field phenotyping of soybean roots for drought stress tolerance. Agron. 4:418-435.

Fletcher, A.L., T. R. Sinclair, and L.H. Allen Jr. 2007. Transpiration responses to vapor pressure deficit in well watered 'slow-wilting' and commercial soybean. Environ. Exp. Bot. 61:145-151.

French, A.N., T.J. Schmugge, and W.P. Kustas. 2002. Discrimination of senescent vegetation using thermal emissivity contrast. Remote Sens. Environ. 74:249-254.

Garay, A.F., and W.W. Wilhelm. 1982. Root system characteristics of two soybean isolines undergoing water stress conditions. Agron. J. 75:973–977.

Gessler, A., A.D. Peuke, C. Keitel, and G.D. Farquhar. 2007. Oxygen isotope enrichment of organic matter in *Ricinus communis* during the diel course and as affected by assimilate transport. New Phytol. 174:600-613.

Gizlice, Z., T.E. Carter Jr., and J.W. Burton. 1994. Genetic base for North American public soybean cultivars released between 1947 and 1988. Crop Sci. 34:1143-1151.

Gizlice, Z., T.E. Carter Jr., T.M. Gerig, and J.W. Burton. 1996. Genetic diversity patterns in North American public soybean cultivars based on coefficient of parentage. Crop Sci. 36:753-765.

Gonfiantini, R. 1983. Advisory group meeting on stable isotope reference samples for geochemical and hydrological investigations. IAEA, Vienna. http://www-naweb.iaea.org/naalihl/docs /pub/iaea-1984-gonfiantini_agmeeting-stableisotoperm.pdf (accessed 31 May 2016).

Gonzalez-dugo, M.P., M.S. Moran, L. Mateos, and R. Bryant. 2005. Canopy temperature variability as an indicator of crop water stress severity. Irri. Sci. doi: 10.1007/s00271-005-0023-7.

Guilioni, L., H.G. Jones, I. Leinonen, and J.P. Lhomme. 2008. On the relationships between stomatal resistance and leaf temperatures in thermography. Agric. For. Meteorol. 148:1908-1912.

Handcock, R.N., A. Gillespie, K.A. Cherkauer, J.E. Kay, S.J. Burges, and S.K. Kampf. 2006. Accuracy and uncertainty of thermal-infrared remote sensing of stream temperatures at multiple spatial scales. Remote Sens. Environ. 100:427–440.

Hardarson, G., S.K.A. Danso. 1993. Methods for measuring biological nitrogen fixation in grain legumes. Plant Soil 152:19-23.

Harper, J.E. 1987. Nitrogen metabolism. p. 498-533. In: (ed. J.R. Wilcox) Soybeans: improvement, production, and uses. American Society of Agronomy, Madison, WI.

Heatherly, L.G. 2009. Sustainability of U.S. soybean production: conventional, transgenic, and organic production systems. CAST, Ames, IA. http://unitedsoybean.org/wp-content/ uploads/CAST_Special_Publication.pdf (accessed 31 May 2016).

Heatherly, L.G. 2015. Tips for early soybean planting. Mississippi Soybean Promotion Board. http://mssoy.org/blog/tips-for-early-soybean-planting/ (accessed 17 Sep. 2015).

Heatherly, L.G., G. Bowers, D. Boethel, M. Baur, J. Rabb, J. Rupe, J. Tyler, M.O. Way, and L. Ashlock. 1998. Early soybean production system handbook. Mississippi Soybean

Promotion Board. http://mssoy.org/uploads/2014/03/ESPS-HANDBOOK.pdf (accessed 29 May 2016).

Heatherly, L.G., and C.D. Elmore. 1986. Irrigation and planting date effects on soybean grown on clay soil. Agron. J. 78:576-580.

Herridge, D.F., F.J. Bergersen, and M.B. Peoples. 1990. Measurement of nitrogen fixation by soybean in the field using the ureide and natural ^{15}N abundance methods. Plant Physiol. 93:0708-0716.

Hoogenboom, G., C.M. Peterson, and M.G. Huck. 1987. Shoot growth rate of soybeans as affected by drought stress. Agron. J. 79:598–607.

Huck, M.G., K. Ishihara, C.M. Peterson, and T. Ushijima. 1983. Soybean adaptation to water stress at selected stages of growth. Plant Physiol. 73:422–427.

Hymowitz, H., and R.L. Bernard. 1991. Origin of the soybean and germplasm introduction and development in North America. p. 147–164. In: (H.L. Shands and L.E. Wiesner) Use of plant introductions in cultivar development. Part I CSSA Special Publication, 17. Crop Science Society of America, Madison, WI.

Hymowitz, H., and J.R. Harlan. 1983. Introduction of soybean to North America by Samuel Bowen in 1765. Econ. Bot. 37:371-379.

Hymowitz, T., F.I. Collins, J. Panczner, and W.M. Walker. 1972. Relationship between the content of oil, protein and sugar in soybean seed. Agron. J. 64:613-616.

ITIS. 2015. *Glycine max*. Taxonomic serial No.: 26716. Integrated Taxonomic Information System. http://www.itis.gov/servlet/SingleRpt/SingleRpt?search_topic=TSN&search_value=26716 (accessed 13 May 2015).

Jensen, A.M., M. Baumann, and Y.Q. Chen. 2008. Low-cost multispectral aerial imaging using autonomous runway-free small flying wing vehicles. Geoscience and Remote Sensing Symposium, IGARSS, IEEE International, Boston, MA. 5:506-509.

Jensen, J.R. 2007. Remote sensing of the environment: an Earth resource perspective, 2nd edition. Pearson Prentice Hall, NJ.

Jones, H.G. 1992. Plant and microclimate: a quantitative approach to environmental plant physiology, 2nd edition. Cambridge University Press, Cambridge, U.K

Jones, H.G., R. Serraj, B.R. Loveys, L.Z. Xiong, A. Wheaton, and A.H. Price. 2009. Thermal infrared imaging of crop canopies for the remote diagnosis and quantification of plant responses to water stress in the field. Funct. Plant Biol. 36:978-989.

Joshi, T., B. Valliyodan, J.H. Wu, S.H. Lee, D. Xu, and H.T. Nguyen. 2013. Genomic differences between cultivated soybean, *G. max* and its wild relative *G. soja*. BMC Genomics 14 (Suppl):S5.

Kagabo, W.E. 1986. Nitrogen fixation in field-grown legumes measured by the ^{15}N isotope dilution and the difference methods. MS thesis. University of Hawaii. http://www.ctahr.hawaii.edu/bnf/Downloads/Dissertations/Kagabo%20Thesis.htm (accessed 17 Sep. 2015).

Karcher, D.E., and M.D. Richardson. 2003. Quantifying turfgrass color using digital image analysis. Crop Sci. 43:943-951.

Khan, F.U.H., A.R. Tahir, and I.J. Yule. 2001. Intrinsic implication of different tillage practices on soil penetration resistance and crop growth. Int. J. Agric. Biol. 1:23-26.

Khurshid, K., M. Iqbal, M.S. Arif, and A. Nawaz. 2006. Effectof tillage and mulch on soil physical properties and growth of maize. Int. J. Agric. Biol. 8:593-596.

King, C.A., and L.C. Purcell. 2006. Genotypic variation for shoot N concentration and response to water deficits in soybean. Crop Sci. 46:2396–2402.

King, C.A., L.C. Purcell, A. Bolton, and J.E. Specht. 2014. A possible relationship between shoot N concentration and the sensitivity of N_2 fixation to drought in soybean. Crop Sci. 54:746-756.

King, C.A., L.C. Purcell, and K.R. Brye. 2009. Differential wilting among soybean genotypes in response to water deficit. Crop Sci. 49:290-298.

Kumuduni, S. 2000. Soybean phenology. University of Guelph. https://www. uoguelph.ca/plant /research/homepages/ttollena/research/soy.html (accessed 11 Aug. 2015).

Lal, R., and B.A. Stewart. 2013. Principles of Sustainable Soil Management in Agroecosystems. p. 568. In: (ed. B.A. Stewart) Advances in Soil Science. CRC Press. 20. FL, USA.

Lindemann, W.C., and C.R. Glover. 2003. Nitrogen fixation by legumes. New Mexico State University. Guide A-129. http://aces.nmsu.edu/pubs/_a/A129/ (accessed 29 May 2016).

Madhava, H.B., M.S. Sheshshayee, R. Devendra, T.G. Prasad, and M. Udayakumar. 2010. Oxygen (^{18}O) isotopic enrichment in the leaves as a potential surrogate for transpiration and stomatal conductance. http://www.iisc.ernet.in/currsci/jun10/articles12.htm (accessed 17 Sep. 2015).

Manavalan, L.P., S.K. Guttikonda, L.P. Tran, and H.T. Nguyen. 2009. Physiological and molecular approaches to improve drought resistance in soybean. Plant Cell Physiol. 50:1260-1276.

Mastrodomenico, A.T., and L.C. Purcell. 2012. Soybean nitrogen fixation and nitrogen remobilization during reproductive development. Crop Sci. 52:1281-1289.

Mayaki, W.C., I.D. Teare, and L.R. Stone. 1976. Top and root growth of irrigated and nonirrigated soybeans. Crop Sci. 16:92-94.

Mcwilliams, D.A., D.R. Berglund, and G.J. Endres. 1999. Soybean growth and management quick guide-A1174. North Dakota State University Extension Service. https://www.ag.ndsu.edu/pubs/plantsci/rowcrops/a1174.pdf (accessed 29 May 2016).

Mian, M.A.R., M.A. Mailey, D.A. Ashley, R. Wells, T.E. Carter, W.A. Parrot and H.R. Boerma. 1996. Molecular markers associated with water use efficiency and leaf ash in soybean. Crop Sci. 36:1252-1257.

Mittelheuser, C.J., and R.F.M. Van Steveninck. 1969. Stomatal closure and inhibition of transpiration induced by (RS)-abscisic acid. Nature 221:281-282.

Miyamoto, M., K. Yoshino, T. Nagano, T. Ishida, and Y. Sato. 2004. Use of balloon aerial photography for classification of Kushiro wetland vegetation, northeastern Japan. Wetlands 24:701-710.

NCSPA. 2014. History of soybeans. North Carolina Soybean Producers Association, INC. http://ncsoy.org/media-resources/history-of-soybeans/ (accessed 17 Sep. 2015).

Neyshabouri, M.R., and J.L. Hatfield. 1986. Soil water deficit effects on semi-determinate and determinate soybean growth and yield. Field Crops Res. 15:73-84.

Nonami, H. 1998. Plant water relations and control of cell elongation at low water potentials. J. Plant Res. 111:373-382.

O'leary, M.H. 1988. Carbon isotope in photosynthesis. BioSci. 38:325-336.

Pachepsky, Y.A., and W.J. Rawls. 2003. Soil structure and pedotransfer functions. Eur. J. Soil Sci. 54:443– 451.

Pantalone, V.R., G.J. Rebetzke, J.W. Burton, and T.E. Carter Jr. 1996. Phenotypic evaluation of soybean root traits and applicability to plant breeding. Crop Sci. 36:456-459.

Passioura, J.B. 1977. Grain yield, harvest index and water use of wheat. J. Aust. Inst. Agric. Sci. 43:117-120.

Passioura, J.B. 2007. The drought environment: physical, biological and agricultural perspectives. J. Exp. Bot. 58:113-117.

Pathan, S.M., J.D. Lee, D.A. Sleper, F.B. Fritschi, R.E. Sharp, T.E. Carter Jr., R.L. Nelson, C.A. King, W.T. Schapaugh, M.R. Ellersieck, H.T. Nguyen, and J.G. Shannon. 2014. Two soybean plant introductions display slow leaf wilting and reduced yield loss under drought. J. Agron. Crop Sci. 200:231-236.

Patterson, R.P., and C.M. Hudak. 1996. Drought-avoidant soybean germplasm maintains nitrogen-fixation capacity under water stress. Plant Soil 186:39-43.

Primicerio, J., S.F.D. Gennaro, E. Fiorillo, L. Genesio, E. Lugato, A. Matese, and F.P. Vaccari. 2012. A flexible unmanned aerial vehicle for precision agriculture. Precision Agric. 13:517-523.

Purcell, L.C. 2009. Physiological responses of N_2 fixation to drought and selecting genotypes for improved N_2 fixation. p. 211-238. In: (eds. H.B. Krishnan and D.W. Emerich) Nitrogen Fixation in Crop Production. Agronomy Monograph. 52. ASA CSSA SSSA, Madison, WI.

Purcell, L.C., and C.A. King. 1996. Drought and nitrogen source effects on nitrogen nutrition, seed growth, and yield in soybean. J. Plant Nutr. 196:969-993.

Purcell, L.C., M. DeSilva, C.A. King, and W.H. Kim. 1997. Biomass accumulation and allocation in soybean associated with genotypic differences in tolerance of nitrogen fixation to water deficits. Plant Soil 196:101-113.

Purcell, L.C., M. Salmeron, and L. Ashlock. 2014. Soybean growth and development. In: Arkansas soybean production handbook, MP197. University of Arkansas Division of Agriculture Research & Extension. https://www.uaex.edu/publications/pdf/mp197/chapter2.pdf (accessed 29 May 2016).

Purcell, L.C., and J.E. Specht. 2004. Physiological traits for ameliorating drought stress. p. 569-620. In: (eds. J.E. Specht and H.R. Boerma) Soybeans: Improvement, Production, and Uses. Agronomy Monographs, 3rd edition. 16. ASA CSSA SSSA, Madison, WI.

Qiu, L.J., and R.Z. Chang. 2010. The origin and history of soybean. In: (ed. G. Singh) The soybean: botany, production and uses. doi: 10.1079/9781845936440.0001.

Raper, C.D., and P.J. Kramer. 1987. Stress physiology. p. 589-641. In: (ed. J.R. Wilcox) Soybeans: improvement, production, and uses. American Society of Agronomy, Madison, WI.

Ray, D.K., N.D. Mueller, P.C. West, and J.A. Foley. 2013. Yield trends are insufficient to double global crop production by 2050. PLOS ONE 8: e66428. doi: 10.1371/ journal.pone.0066428.

Robinson, S.A., M. Ribas-Carbo, D. Yakir, L. Giles, Y. Reuveni, and J.A. Berry. 1995. Beyond SHAM and cyanide: opportunities for studying the alternative oxidase in plant respiration using oxygen isotope discrimination. Aust. J. Plant Physiol. 22:487-496.

Rohling, E.J. 2007. Oxygen isotope composition of seawater. p. 1748–1756. In: (ed. S.A. Elias) Encyclopedia of Quaternary Science, 3, Elsevier.

Rorie, R.L., L.C. Purcell, D.E. Karcher, and C.A. King. 2011a. The assessment of leaf nitrogen in corn from digital images. Crop Sci. 51:2174-2180.

Rorie, R.L., L.C. Purcell, M. Mozaffari, D.E. Karcher, C.A. King, M.C. Marsh, and D.E. Longer. 2011b. Association of "greenness" in corn with yield and leaf nitrogen concentration. Agron. J. 103:529-535.

Royal Society. 2009. Reaping the benefits: science and the sustainable intensification of global agriculture. Royal Society, London. https://royalsociety.org/~/media /Royal_Society_ Content/policy/publications/2009/4294967719.pdf (accessed 29 May 2016).

Rudd, J., Q. Xue, S. Liu, J. Mahan, and K. Jessup. 2013. Identifying drought tolerant wheat genotypes using wireless infrared thermometer in the US Southern high plains. American Society of Animal Science abstract 368-7. https://www.animalscience publications.org/publications/meetings/2013am/12530/79206 (accessed 29 May 2016).

Rundquist, D.C., and S.A. Samson. UNL. A guide to the practical use of aerial color-infrared photography in agriculture. Educational Circular 8. University of Nebraska-Lincoln. http://www.casde.unl.edu/activities/cir-uses/ (accessed 17 Sep. 2015).

Sadok, W., and T.R. Sinclair. 2010. Transpiration response of 'slow-wilting' and commercial soybean (Glycine max (L.) Merr.) genotypes to three aquaporin inhibitors. J. Exp Bot. 61:821-829.

Salmeron, P., E.E. Gbur, F.M. Bourland, N.W. Buehring, L. Earnest, F.B. Fritschi, B.R. Golden, D. Hathcoat, J. Lofton, T.D. Miller, C. Neely, G. Shannon, T.K. Udeigwe, D.A. Verbree, E.D. Vories, W.J. Wiebold, and L.C. Purcell. 2014. Soybean maturity group choices for early and late plantings in the Midsouth. Agron. J. 106:1893-1901.

Sapra, V.T., and A.O. Anaele. 1991. Screening soybean genotypes for drought and heat tolerance. J. Agron Crop Sci. 167:96-102.

Serraj, R., L.H. Allen, and T.R. Sinclair. 1999. Soybean leaf growth and gas exchange response to drought under carbon dioxide enrichment. Global Change Biol. 5:283-291.

Serraj, R., T.R. Sinclair. 1997. Variation among soybean cultivars in nitrogen fixation response to drought. Agron. J. 89:963–969.

Sheshshayee, M.S., H. Bindumadhava, R. Ramesh, T.G. Prasad, M.R. Lakshminarayana, and M. Udayakumar. 2005. Oxygen isotope enrichment ($\Delta^{18}O$) as a measure of time-averaged transpiration rate. J. Exp. Bot. 56:3033-3039.

Sinclair, T.R. 2012. Is transpiration efficiency a viable plant trait in breeding for crop improvement? Funct. Plant Biol. 39:359-365.

Sinclair, T.R., and C.T. Dewit. 1976. Analysis of the carbon and nitrogen limitations to soybean yield. Agron. J. 68:319-324.

Sinclair, T.R., and M.M. Ludlow. 1986. Influence of soil water supply on the plant water balance of four tropical grain legumes. Aust. J. Plant Physiol. 13:329-341.

Sinclair, T.R., R.C. Muchow, J.M. Bennett, and L.C. Hammond. 1987. Relative sensitivity of nitrogen and biomass accumulation to drought in field-grown soybean. Agron. J. 79:986-991.

Sloane, R.J., R.P. Patterson, and T.E. Carter. 1990. Field drought tolerance of a soybean plant introduction. Crop Sci. 30:118-123.

Sneller, G.H. 1994. Pedigree analysis of elite soybean lines. Crop Sci. 34:1515-1522.

Specht, J.E., D.J. Hume, and S.V. Kumudnini. 1999. Soybean yield potential-a genetic and physiological perspective. Crop Sci. 39:1560-1570.

Specht, J. E., J.M. Rees, G.L. Zoubek, K.L. Glewen, R.S. VanDeWalle, J.W. Schneider, D.L. Varner, and A.R. Vyhnalek. 2012. Soybean planting date-when and why. University of Nebraska, Lincoln, Extension. http://extensionpublications.unl.edu/assets/pdf/ec145.pdf (accessed 29 May 2016).

Sprent, J.L. 1972. The effects of water stress on nitrogen fixing root nodules. III. Effects of osmotically applied stress. New Phytol. 71:451–460.

Tanaka, Y., K. Fuji, and T. Shiraiwa. 2010. Variability of leaf morphology and stomatal conductance in soybean [Glycine max (L.) Merr.] cultivars. Crop Sci. 50:2525-2532.

Thomison, P., A. Lindsey, A. Geyer, and R. Minyo. 2013. Drought tolerant corn hybrids. The Ohio State University Extension. Crop Observation and recommendation network. http://ohioline.osu.edu/factsheet/agf-516 (updated 14 Oct. 2015).

Tian, Z.X., X.B. Wang, R. Lee, Y.H. Li, J.E. Specht, R.L. Nelson, P.E. Mcclean, L.J. Qiu, and J.X. Ma. 2010. Artificial selection for determinate growth habit in soybean. Proceedings of the National Academy of Sciences of the United States of America. 107:8563-8568.

Triplett, G.B., W. Kingery, and M. Shankle. 2008. Tillage Effects on the Soil Moisture Regime. Mississippi State University. http://www.ag.auburn.edu/auxiliary/nsdl/scasc/Proceedings/2008/Triplett.pdf (accessed 17 Sep. 2015).

Ude, G.N., W.J. Kenworthy, J.M. Costa, P.B. Cregan, and J. Alvernaz. 2003. Genetic diversity of soybean cultivars from China, Japan, North America, and North American ancestral lines determined by amplified fragment length polymorphism. Crop Sci. 43:1858-1867.

UN Global Compact, 2015. Increasing water demand. CEO Water Mandate, United Nations Global Compact. http://ceowatermandate.org/business-case/global-water-trends/increasing-water-demand/ (accessed 17 Sep. 2015).

USDA. 2012. Economic Research Service: Soybeans & oil crops, background. United States Department of Agriculture. http://www.ers.usda.gov/topics/crops/soybeans-oil-crops/background.aspx (updated 10 Oct. 2012).

USDA. 2013a. Economic Research Service: U.S. drought 2012: farm and food impacts. United States Department of Agriculture. http://ers.usda.gov/topics/in-the-news/us-drought-2012-farm-and-food-impacts.aspx#.VDMwNvldVrU (updated 26 Jul. 2013).

USDA. 2013b. Soybean-irrigated, crop acreage, yield, and production, by county, 2012-2013. United States Department of Agriculture, National Agricultural Statistics Service, Delta Regional Office: Arkansas. http://www.nass.usda.gov/Statistics_by_State/Arkansas/Publications/County_Estimates/13_AR_soybean_irrigated.pdf (accessed 17 Sep. 2015).

USDA. 2013c. Soybean-nonirrigated, crop acreage, yield, and production, by county, 2012-2013. United States Department of Agriculture, National Agricultural Statistics Service, Delta Regional Office: Arkansas. http://www.nass.usda.gov/Statistics_by_State/Arkansas/Publications/County_Estimates/13_AR_soybean_nonirrigated.pdf (accessed 17 Sep. 2015).

USDA. 2014a. Economic Research Service: Land use, land value & tenure. United States Department of Agriculture. http://ers.usda.gov/topics/farm-economy/land-use,-land-value-tenure.aspx (updated 21 Feb. 2014).

USDA. 2014b. Soybean-irrigated, crop acreage, yield, and production, by county, 2013-2014. United States Department of Agriculture, National Agricultural Statistics Service, Delta Regional Office: Arkansas. http://www.nass.usda.gov/Statistics_by_State /Arkansas/Publications/County_Estimates/14_AR_soybean_irrigated.pdf (accessed 17 Sep. 2015).

USDA. 2014c. Soybean-nonirrigated, crop acreage, yield, and production, by county, 2013-2014. United States Department of Agriculture, National Agricultural Statistics Service, Delta Regional Office: Arkansas. http://www.nass.usda.gov/Statistics_by_State/Arkansas/Publications/County_Estimates/14_AR_soybean_nonirrigated.pdf (accessed 17 Sep. 2015).

USDA. 2015a. Crop production 2014 summary. United States Department of Agriculture. http://www.usda.gov/nass/PUBS/TODAYRPT/cropan15.pdf (updated 5 Feb. 2015).

USDA. 2015b. Economic Research Service: Soybeans & oil crops, trade. United States Department of Agriculture. http://www.ers.usda.gov/topics/crops/soybeans-oil-crops/trade.aspx (updated 7 May 2015).

USSEC. 2008. How the global oilseed and grain trade works. US Soybean Export Council. Soyatech, LLC, Southwest Harbor, Maine, US.

Vadez, V., and T.R. Sinclair. 2001. Leaf ureide degradation and N_2 fixation tolerance to water deficit in soybean. J. Exp. Bot. 52:153-159.

Vadez, V., T. R. Sinclair, and R. Serraj, 2000. Asparagine and ureide accumulation in nodules and shoots as feedback inhibitors of N_2 fixation in soybean. Physiol. Plant. 110:215–223.

Waseem, M., A. Ali, M. Tahir, M.A. Nadeem, M. Ayub, A. Tanveer, R. Ahmad, and M. Hussain. 2011. Mechanism of drought tolerance in plant and its management through different methods. Continental J. Agricultural Science 5:10-25.

Weisz, P.R., R.F. Denison, and T.R. Sinclair. 1985. Response to drought stress of nitrogen fixation (acetylene reduction) rates of field-grown soybeans. Plant Physiol. 78:725–730.

Werner, C., H. Schnyder, M. Cuntz, C. Keitel, M.J. Zeeman, T.E. Dawson, F.W. Badeck, E. Brugnoli, J. Ghashghaie, T.E.E. Grams, Z.E. Kayler, M. Lakatos, X. Lee, C. Maguas, J. Ogee, K.G. Rascher, R.T.W. Siegwolf, S. Unger, S. Welker, L. Wingate, and A. Gessler. 2012. Process and challenges in using stable isotopes to trace plant carbon and water relations across scales. Biogeosci. 9:3083-3111.

Xu, Z.H., P.G. Saffigna, G.D. Farquhar, J.A. Simpson, R.J. Haines, S. Walker, D.O. Osborne, and D. Guinto. 2000. Carbon isotope discrimination and oxygen isotope composition in clones of the F1 hybrid between slash pine and Caribbean pine in relation to tree growth, water-use efficiency and foliar nutrient concentration. Tree Physiol. 20:1209-1218.

CHAPTER II

EVALUATION OF SOYBEAN GREENNESS FROM GROUND AND AERIAL PLATFORMS AND THE ASSOCIATION WITH LEAF NITROGEN CONCENTRATION IN RESPONSE TO DROUGHT

Abstract

Conventional breeding methods for developing drought-tolerant soybean genotypes have difficulties in screening large number of soybean lines. Drought effects were evaluated on soybean during reproductive stages in an experiment where the greenness of the canopy was quantified using digital-image analysis. Five genotypes including maturity groups (MGs) 2 to 5 were planted in the field with drought (DR) and well-irrigated (WI) treatments. When seed filling began for the MG 2 genotypes, leaf samples were taken to measure the nitrogen concentration every 7 days. Pictures from the ground were also made throughout the season for each plot against a pink board including yellow and green disks that served as internal standards to calculate the Dark Green Color Index (DGCI). Moreover, aerial photographs were taken from a height of 50 to 75 m to determine the aerial DGCI values. Leaf nitrogen concentration was closely related to ground DGCI, and ground DGCI measurements were highly associated with aerial DGCI. The aerial DGCI measurements were able to identify more rapid senescence for the drought treatment compared to the irrigated treatment. This ensures the possibility for characterizing soybean genotypes with quick senescence because of water stress. The results demonstrated that aerial DGCI measurements have the promise to quantify sensitivity of drought among soybean genotypes.

Introduction

By the middle of this century, the global population is expected to reach to 9 billion (Godfray et al., 2010). To feed this large population, food production needs are predicted to be doubled by 2050 (Royal Society, 2009). However, the current yield increase each year (1.2%) is only half of the predicted rate (2.4%) necessary to meet this demand (Ray et al., 2013), which presents a big challenge to everyone in the food production pipeline. The main crops worldwide include maize [*Zea mays* L], wheat [*Triticum aestivum* L.], rice [*Oryza sativa* L.], soybean [*Glycine max* (L.) Merr] and potato [*Solanum tuberosum* L.]. Soybean is mainly used for vegetable oil, human food, and animal feeding. The top four countries for soybean production are the United States., Brazil, Argentina, and China, successively (USSEC, 2008).

The average soybean yield in 2014 in U.S. was 3215 kg ha^{-1} (47.8 bu ac^{-1}) (USDA, 2015). For Arkansas in 2014, the average yield was 3363 kg ha^{-1} (50 bu ac^{-1}), and there was a yield difference of 935 kg ha^{-1} between irrigated (3531 kg ha^{-1}, 52.5 bu ac^{-1}) and non-irrigated (2596 kg ha^{-1}, 38.6 bu ac^{-1}) soybean (USDA, 2014a; USDA, 2014b). However, the average yield in U.S. and Arkansas from 2005 to 2014 was 2892 kg ha^{-1} (43 bu ac^{-1}), and 2636 kg ha^{-1} (39.2 bu ac^{-1}), respectively (NASS, 2015). In Arkansas, this average yield in last ten years was 2892 kg ha^{-1} (43 bu ac^{-1}) for irrigated fields, and 1809 kg ha^{-1} (26.9 bu ac^{-1}) for non-irrigated field (NASS, 2015). The U.S. agricultural area is mainly composed of rainfed fields (> 90%) (Board and Kahlon, 2011). The existence of large non-irrigated areas and large yield differences between irrigated and non-irrigated production indicate the severe problem caused by drought stress.

Soybean ranks among the top ten crops with the highest production in the world (FAO, 2015). Over 90% of oilseed production in the United States is from soybean (USDA, 2012). Additionally, soybean grain is composed of approximately 40% of protein, and hence, nitrogen is

a major component in the seeds. In the absence of soil nitrogen, soybean plants obtain nitrogen through biological nitrogen fixation mediated by *Bradyrhizobium japonicum* bacteria living in soybean root nodules. When the soil nitrogen is poor, biological nitrogen fixation contributes up to 85% of the nitrogen in the soybean plant (Mastrodomenico and Purcell, 2012). Water stress negatively impacts the rate of nitrogen fixation. Soil nitrogen uptake and assimilation under water stress was greater than nitrogen fixation, which shows the high sensitivity of nitrogen fixation to water stress (Purcell and King, 1996) although there are genotypic differences in the sensitivity of nitrogen fixation to drought (King and Purcell, 2006).

Chlorophyll, functioning in photosynthesis, contains nitrogen. Nitrogen is remobilized from soybean leaves to seeds during seedfill (Sinclair and Dewitt, 1976; Mastrodomenico and Purcell, 2012). Nitrogen deficiency, thus, results in decreased chlorophyll concentration, causing leaf yellowing, and leaf color can be used as an indicator of nitrogen status of plants. Rorie et al. (2011a; 2011b) found that the greenness of corn leaves from digital color images was closely related with nitrogen concentration. The greenness of leaves can be expressed by the dark green color index (DGCI), which can be determined from hue, saturation and brightness (HSB) values from standard digital photographs.

When soil contains minimal nitrogen, biological nitrogen fixation can provide the majority of nitrogen to soybean plants (Mastrodomenico and Purcell, 2012). However, drought had a negative impact on nitrogen fixation (Purcell, 2009). Drought stress during seedfill results in remobilization of nitrogen from leaves to seed, leading to rapid senescence and decreased yield. DGCI measurements have the potential to identify the changes in nitrogen remobilization in soybean.

Unfortunately, ground-level measurements have several disadvantages, such as they are time-consuming, not suitable for measuring large number of plots, and they are not representative due to small imaging areas. Aerial imaging techniques have been widely used in global agricultural systems, especially in the United States since 1930s (Rundquist and Samson, UNL). Many researchers have applied remote sensing techniques in their studies (Aber et al., 2002; Boike and Yoshikawa, 2003; French et al., 2000; Handcock et al., 2006; Jones et al., 2009; Miyamoto et al., 2004; Primicerio et al., 2012). In this study, an aerial photographic method for measuring DGCI was evaluated that overcomes the shortcomings that exist in the ground method. The hypothesis of this research is that under drought, the greenness of a soybean canopy will decrease faster than under well-watered conditions as N is remobilized to seed. The objective was to characterize differences in seed-fill duration in response to drought among soybean genotypes from the DGCI decrease during seedfill.

Materials and Methods

A field experiment was conducted at the Main Experiment Station in Fayetteville, Arkansas (36º05' N, 94º10' W) on a Captina silt loam soil (Fine-silty, siliceous, active, mesic Typic Fragiudults) during the summers of 2012, 2013, and 2014. This experiment was divided into well-irrigated (WI) and drought (DR) experiments that were grown side by side. Four different soybean maturity groups (MGs) from MG 2 to MG 5 were selected for evaluation of WI and DR experiments. The soybean genotypes are shown in **Table 2_1**. Genotypes differed among years due to the rapid turnover of cultivars by seed companies.

The experiment was conducted using a randomized complete block design with five replications. Soybean was planted on June 2, June 8, and June 17 for 2012 through 2014. Plots consisted of four rows 6.1 m in length and 0.46 m between rows. The seeding density was 30 seed m^{-2}. An overhead sprinkler irrigation system was installed for both WI and DR sections. Irrigation was applied to the WI field when the estimated soil-water deficit (Purcell et al., 2007) reached 30 mm. The drought portion of the field was kept fully irrigated until canopy closure (approximately 4 weeks after emergence) and then received irrigation approximately every third time the fully irrigated treatment received water. A total of 10 rain gauges were placed in the field (5 in WI treatment and 5 in DR treatment) to record the irrigation amount and rainfall. The total irrigation amount per rain gauge for each water treatment for the growing season was calculated based on the rain gauge amounts. The percent of deficit for individual water treatment was calculated using Eq [10]

$$\text{Deficit (\%)} = 100 - [(\text{Irrigation amount/rain-gauge for individual water treatment} + \text{rainfall}) \times 100 / (\text{Irrigation amount/rain-gauge for full irrigation} + \text{rainfall})] \quad [10]$$

Table 2_1 Maturity groups (MGs) and genotypes selected for Greenness study from 2012 to 2014.

Year	MG 2	MG 3	MG 4	MG 5
2012	AG24-30, S25-T8	S33-K5	P94Y40	P95Y50
2013	S25-E5	S35-C3, P93Y72	P94Y40	P95Y50
2014	S25-E5	S35-A5, R2 36X82N	P46T21R	AG5532

Approximately, 1 week after emergence, stand counts were made in each plot by counting the number of plants in 1 m of two central rows and averaging the two measurements. Light interception was measured twice a week after emergence until canopy closure using a digital-imaging method (Purcell, 2000). Soybean phenological development was also recorded twice a week for each variety after R1 using the staging method of Fehr and Caviness (1977).

The greenness of the canopy was determined once a week after R5 by taking digital color pictures of the canopy at ground level of each plot, similar to the method described by Rorie et al. (2011a; 2011b). A pink board (1.2 m by 0.6 m) with both yellow and green disks (11 cm in diameter) that served as internal standards to correct for differences in lighting conditions (Rorie et al., 2011a) was positioned vertically at about one third of the plot length, and a picture was taken against the pink board from the other end of the plot across the top of the canopy. The pictures were usually taken between 10 am and 2 pm on sunny days to minimize shadows. Known Munsell color values for green and yellow disks were 6.7GY 4.2/4.1 and 5Y 8/11.1, and the corresponding DGCI values were 0.5722 and 0.0733, respectively (Rorie et al., 2011a).

A Canon Power Shot S5 IS camera with a resolution of 3264 x 2448 (Canon U.S.A., Inc. Lake Success, NY), was used for taking ground images. The camera had a f stop of ¼, a focal length of 6 mm, and an ISO of 80 with no flash. The images were saved as Joint Photographic Experts Group (JPEG) files with dimensions of 640×480, reordered by FastStone Image Viewer (v4.2 FastStone Soft), and analyzed by Sigma Scan Pro (v5.0 SPSS, Inc., Chicago, IL) with hue values ranging from 30 to 115, and saturation values ranging from 0 to 100. A macro working with Sigma Scan Pro (Rorie et al., 2011b) allowed batch analysis for determining DGGI values using the given ranges of hue and saturation. On the same day ground images were taken, three leaves were sampled from three different plants in each plot for nitrogen concentration analysis using the

Dumas method with a Leco FP-428 Determinator (Leco corporation, St. Joseph, MO) at the Soil Testing and Plant Analysis Laboratory at the University of Arkansas. The three leaves were the third fully developed leaf from the top of the plant.

On the same day ground images and leaf samples were taken, measurements of DGCI were made from the air. A digital camera was mounted on balloon or kite platforms to take aerial photographs from heights of 50 to 75 m. The aerial DGCI values were compared with the DGCI values from the ground color images. Two identical boards (1.2×2.4m) painted with a pink background and painted with both yellow and green internal standards (~1 m in diameter) were positioned on one side of the field. Eighteen white boards around 0.5 m^2 were laid in known positions in the field and served as reference points in 2012 and 2013. A GPS map of the field was then created based on the reference points. The GPS reference points were used in ArcGIS 10.2 (Redlands, CA: Environmental Systems Research Institute) as a base map to coordinate the reference points in the images. In 2014, GIMP 2.8 (www.gimp.org) software was used for analyzing images and this procedure did not require reference points.

The tethered balloon (approximately 1 m in diameter) was purchased from Southern Balloon (www.southernballoon.com). Helium was used to inflate the balloon. Three strings were fixed onto the balloon, and each of the strings was attach to a winding mechanism. The balloon was used as the aerial platform on calm days. A parafoil kite (2 m^2 in area) bought from Peter Lynn (www.peterlynn.com) kites was used when wind speeds were greater than 8.9 m s^{-1}. A Levitation Delta kite with a 2.75 m wing span from Into The Wind (www.intothewind.com) was used at intermediate winds ranging from 1.7 to 8.9 m s^{-1}. It has an oversized keel and trailing edge flap for stability.

A GoPro camera (Hero, DCIM/100GOPRO, https://gopro.com/) with a f stop of 1/3.6 and a focal length of 5 mm was used for the aerial images in 2012. The GoPro camera was set to take photos every 2 seconds. The images were saved as JPEG files with dimensions of 2592 x 1944, but the images were distorted due to the 'Fisheye' lens of the camera. The original GoPro lens (2.5 mm) was replaced with a lens with a narrower field of view (6 mm) to lessen the distortion (www.ragecams.com). A Canon PowerShot S100 camera with a f stop of ¼ and a focal length of 5 mm was used in 2013 and 2014, which ensured less distortion. The images were saved as JPEG files with dimensions of 1600 x 1064. Using this camera, three images were taken in a sequence at three different exposures. An intervalometer was installed on the camera's SD memory card from the Canon Hack Development Kit (CHDK, www.chdk.wikia.com) which allowed the sequence of three pictures to be taken continuously at 2 s intervals. The camera was suspended from one of the balloon tether lines or from the kite line using a picavet (http://www.armadale.org.uk/kitebasic.htm), which dampened the movement of the camera while suspended.

After the kite or balloon with the camera were lifted about 5 m high, the picavet was attached to the string of the kite or one string of the balloon, and camera was turned on. Then the aerial platform was lifted to a height that allowed the entire width of the field to be captured. After the camera was centered above the field, the camera was walked slowly through the field. Selected color digital images were then processed using ArcGIS10.2 (2012 and 2013) and GIMP 2.8 (2014) to obtain the RGB values for individual plots. The RGB values were converted to HSB values using an online RGB to HSB convertor (http://www.rags-int-inc.com/PhotoTechStuff/Acr Calibration/RGB2HSB.html), and HSB values were then used to calculate DGCI values. Those DGCI values were considered as observed disk or leaf DGCI. The yellow and green disks were

used as internal standards to correct for differences in lighting conditions (Rorie et al., 2011a). The DGCI values for green (0.5722) and yellow (0.0733) disks were considered as known values and used to correct observed DGCI values. A simple linear response was assumed between known DGCI and observed DGCI values (Rorie et al., 2011a):

$$\text{Slope} = (\text{Known Green disk DGCI} - \text{Know Yellow disk DGCI}) / (\text{Observed Green disk DGCI} - \text{Observed Yellow disk DGCI}) \quad [11]$$

$$\text{Intercept} = \text{Known Yellow disk DGCI} - (\text{Slope} \times \text{Observed Yellow disk DGCI}) \quad [12]$$

$$\text{Corrected leaf DGCI} = (\text{Slope} \times \text{Observed leaf DGCI}) + \text{Intercept} \quad [13]$$

The procedure using ArcGIS to analyze the aerial image is complex. First, by selecting "Add Base Map", "Imagery" and "Add Data", the aerial image that was taken on the experiment was imported. The image was rotated under "Georeferencing" to align the plots horizontally on the screen. Next, the GPS reference point map was added as another layer. The control points in the GPS reference layer (i.e. georeferenced) and the aerial image layer (i.e. ungeoreferenced) were then linked by selecting "Add control points". The more control points between these two layers were linked, the more accurate the plots between these two layers matched. After all possible points were linked, by selecting "2nd order polynomial" in "Transformation" under "Georeferencing", the distorted aerial image was transformed into an undistorted one. Then, the image was saved as "GRID" format. Under "Georeferencing", by selecting "Update Georeferencing", the lines linking aerial image layer and GPS reference layer disappeared.

"Export Raster Data" table displayed by selecting the name of the aerial image under "Layers" in the "Table of Contents", then "Data", and "Export Data". "Raster dataset" was selected for extent and spatial reference. The default "Location" in the raster data table was replaced with

the folder that was being used by selecting “Add”. “GRID” format was then used. Two more windows displayed after saving, and closed by choosing “Yes”. Then, a new layer with a similar name with the original image was shown.

The two center rows of each plot were selected by making a polygon in the new layer. Under “Catalog”, by selecting the folder the image was in, a drop down menu displayed. Shapefile window was shown by selecting “Shapefile” under “New”. A name for the new shapefile was given such as “samplebox_image xxxx”. “Polygon” was chosen for feature type. “NAD 1983 HARN StatePlane Arkansas North FIPS 0301 (US Feet)” was chosen by selecting “Edit”, opening “Projected Coordinate Systems”, “State Plane”, and then “NAD 1983 HARN (US Feet)”. Now, a new shapefile layer with the name “Samplebox_image xxxx” displayed under “Layer”. The properties of the sample box can be changed, such as the fill color, outline width and color, by double clicking the box under the shapefile. By clicking “Sample box_image xxxx”, “Edit features”, and selecting “Start Editing”, and then “Create Features” icon, “Sample box_image xxxx” in the window of “Create features” was then selected. “Polygon” was selected under the “construction tools”. Then, a polygon was created around the two center rows of each plot, and saved by clicking “Save Edits” and “Stop Editing”. Polygons can be copied and pasted for other plots by selecting “Start Editing”. Once all polygons are made, the attribute table was opened by right clicking “Sample box_image xxxx” under layer. In the attribute table, the polygon ID was changed to the corresponding plot number by using “Start Editing” and “Stop editing” tools.

The final step was to get the RGB values. Under ArcToolbox, “Zonal Statistical as Table” was opened. In this table, the input raster was “Sample box_image xxxx”, and the input value raster was the band 1 (Red). The “Zone field” and “Output table” were default. Then, a zonalSta_Shp file displayed, and the name can be change, such as image xxxxRed. In this file, the

ID is the plot number, the “Mean” is the Red values for each plot. The same procedure was used to get Green and Blue values.

In 2014, images were analyzed using GIMP because of its simplicity. After an image was imported into GIMP, it was rotated to align the plots horizontally on the screen. Once the plots in the image were in the horizontal direction, the central two rows of individual four-row plots were cropped. By selecting “Colors”, “Info” functions in sequence a histogram window displays the distribution and mean of red, green, or blue value for all pixels in the selected area. Depending upon the height at which the image was taken, aerial DGCI measurements for each plot was based upon an average of 5000 to 10000 pixels, which was about half of the total pixels for an individual plot.

At the end of the R5 developmental stage, a harvest index (HI) sample was taken for each plot by cutting three to four plants at the soil surface from the border rows. The pods were removed from the plants, and remaining plant material and pods were dried separately. After drying, soybean seeds were shelled from the pods, weighed, counted, and ground for nitrogen analysis. Shells were added to the corresponding bag with plant material and ground with the plant material for nitrogen analysis. Approximately 10 to 14 days later, in the middle of the R6 stage, a second HI sample was taken and analyzed as described for first HI. At maturity, a final HI sample was taken from the two central rows for each plot. Whole plant samples were dried, weighed, and threshed for seeds. Seeds were weighed and counted. At R8, plants from the middle 4.9 m of the two central rows were harvested, weighed, and yields were expressed at 13% moisture content. A representative sample was used to determine 100 seed weight.

DGCI and leaf N concentration were evaluated as a function of the estimated HI as well as days after R5 (DAR5) separately after photographs and samples were analyzed. To estimate HI, a

two-point regression of HI versus the day of year was used (**Figure 2_1**); the regression line was extended until it crossed the X axis (beginning of seed-fill) and until the trend line intersected the mature HI value (end of seed-fill). The estimated HI values for other sampling days were determined by solving the regression equation of HI for the day of year that samples were taken (**Figure 2_1**).

Statistical Analysis

Data were analyzed by year using analysis of covariance (ANOCVA) for leaf N concentration vs days after R5 (DAR5), ground DGCI (G_DGCI) vs DAR5, aerial DGCI vs DAR5, G_DGCI vs leaf N, aerial DGCI vs leaf N, aerial DGCI vs G_DGCI, leaf N vs estimated harvest index (est_HI), G_DGCI vs est_HI, and aerial DGCI vs est_HI. The factors in the whole model for leaf N concentration vs DAR5 included irrigation, genotype, DAR5, DAR5*DAR5, and all possible two- and three-way combinations. The non-significant factors were eliminated one at a time from the highest order interaction to the lowest order interaction but keeping the main factors, irrigation and genotype. The whole models for the other pairs of dependent and independent variables listed above were similar to leaf N concentration vs DAR5, with similar rules for removing non-significant factors.

Yield data were analyzed with analysis of variance (ANOVA). The whole model was irrigation, genotype, and irrigation*genotype.

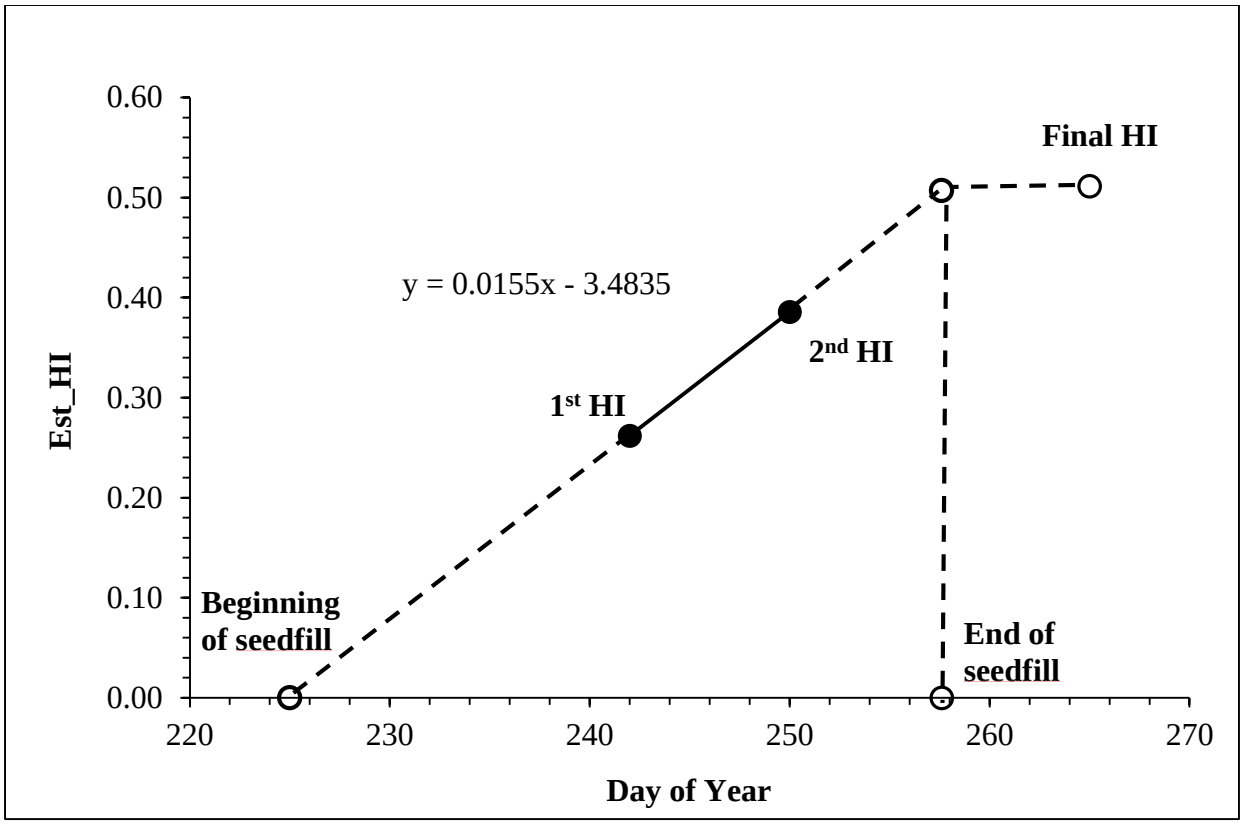

Figure 2_1 Example of method to determine estimated harvest index (Est_HI) versus day of year. For each plot, three to five plants were harvested at mid-seedfill (1st HI) and then again 10 to 14 days later (2nd HI). Samples were dried, weighed, and seeds shelled from pods, and HI was calculated as the quotient of seed mass and plant mass. For other days of the year, Est_HI was determined assuming that HI was linear from the beginning of seedfill till reaching the final HI.

Results

A. Environmental Data and Calculation of Deficit for Different Water Treatments

The environmental conditions on measurement dates including daily maximum and minimum temperature, total solar radiation and soil water deficit for well-irrigated treatment are summarized in **Table 2_2**. **Table 2_3** shows the deficit percentage for both water treatments. The estimated deficit percentage ranged from 22% (2013) to 30% (2012) for the DR treatment. Monthly averages of maximum and minimum temperature (T_{max}, T_{min}), rainfall, and solar radiation for the growing season (June through September) from 2012 to 2014 versus 30-year average values from 1981 to 2010 (NCDC, 2016) are shown in **Table 2_4**. During the growing season, the average maximum temperatures in 2012 was greater than 30ºC for all three months whereas the average maximum temperatures exceeded 30ºC for 2 months (2013), 1 month (2014), and 2 months for 30-year average (**Table 2_4**). Similarly, solar radiation was higher in 2012 than the other two years, and similar to the 30-year average (**Table 2_4**). Though 2014 had the least precipitation for the growing season, the average maximum temperature in 2014 was less than those observed in 2012.

Soil water deficits during the growing season for WI and DR treatments from 2012 through 2014 are shown in **Figure 2_2 A**, **B**, and **C**. Soil water deficits were much greater in 2012 compared with 2013 and 2014. High temperature, high solar radiation and a long period of high soil water deficit could possibly impact the measurements of greenness, N concentration and yield in 2012.

B. G_DGCI and Aerial DGCI versus Leaf N Concentration

Before discussing the comparison between G_DGCI and aerial DGCI, the aerial DGCI values from ArcGIS and GIMP were compared. Six different aerial images with a total of 56 DGCI

Table 2_2 Environmental conditions on measurement dates including daily maximum and minimum temperature (T_{max}, T_{min}), total solar radiation, and soil water deficit for well-irrigated treatment.

Date	T_{max} (°C)	T_{min} (°C)	Solar Radiation (MJ m^{-2} d^{-1})	Soil Water Deficit (mm)
08/02/12	37.4	28.1	19.17	6.58
08/06/12	36.4	22.9	22.83	13.91
08/13/12	27.1	19.3	16.84	0.14
08/22/12	31.1	18.2	20.98	3.00
08/29/12	33.0	19.7	20.56	13.30
09/05/12	36.2	22.1	20.29	19.48
09/13/12	29.9	16.8	18.61	30.00
09/20/12	30.3	17.0	17.85	4.96
09/27/12	27.9	17.8	14.68	30.00
09/28/12	27.4	17.1	14.72	30.00
10/08/12	15.2	1.7	15.49	16.57
10/09/12	18.5	5.8	14.87	19.86
10/18/12	17.9	6.8	12.78	5.15
08/07/13	34.3	24.4	19.48	17.27
08/12/13	29.4	20.9	17.74	3.45
08/16/13	25.1	15.7	18.36	8.72
08/23/13	32.3	18.3	21.72	30.00
08/30/13	35.2	23.2	19.45	5.82
09/06/13	32.2	13.3	23.38	22.01
09/13/13	28.9	16.7	17.96	0.00
09/19/13	31.0	22.7	14.17	23.27
09/28/13	26.3	16.5	14.36	0.00
10/01/13	28.0	16.0	15.52	9.34
10/04/13	19.4	3.5	17.41	19.13
10/11/13	23.7	13.8	12.91	24.11
08/12/14	27.0	14.0	21.93	22.12
08/13/14	28.0	11.0	24.99	28.82
08/22/14	34.0	24.0	18.44	31.85
08/28/14	33.0	18.0	21.92	29.71
09/04/14	32.0	23.0	16.98	11.34
09/09/14	31.0	19.0	18.28	15.42
09/25/14	27.0	8.0	20.51	0.00
10/01/14	23.9	8.9	17.35	29.36
10/09/14	28.0	11.1	17.17	18.96

Table 2_3 Irrigation amounts, rainfall, and estimated deficit irrigation amounts for different water treatments from 2012 through 2014.

Year	Irrigation Amount/Rain Gauge (mm)		Rainfall (mm)	Deficit (%)	
	WI	DR		WI	DR
2012	443	224	276	0	30
2013	322	177	335	0	22
2014	228	102	237	0	27

Table 2_4 Monthly averages of maximum and minimum temperature (T_{max}, T_{min}), rainfall, and solar radiation from June through September for 2012 to 2014 versus 30-year average values from 1981 to 2010 (NCDC, 2016).

Year	Month	T_{max} (°C)	T_{min} (°C)	Rainfall (mm)	Solar Radiation (MJ m^{-2} d^{-1})
2012	June	31.8	19.0	58	23.8
	July	35.6	22.3	62	23.7
	August	32.4	20.1	101	20.8
	September	28.0	16.7	56	16.7
2013	June	29.8	19.6	32	21.4
	July	31.6	19.9	94	22.3
	August	30.5	20.2	138	18.8
	September	29.4	17.0	92	17.7
2014	June	28.4	20.4	102	18.6
	July	29.2	18.6	37	21.1
	August	32.1	20.5	70	20.3
	September	27.3	16.0	101	16.8
30-year average (1981-2010)	June	28.7	16.8	127	23.0
	July	31.4	19.2	88	22.8
	August	31.7	18.4	82	21.8
	September	26.9	13.7	122	18.4

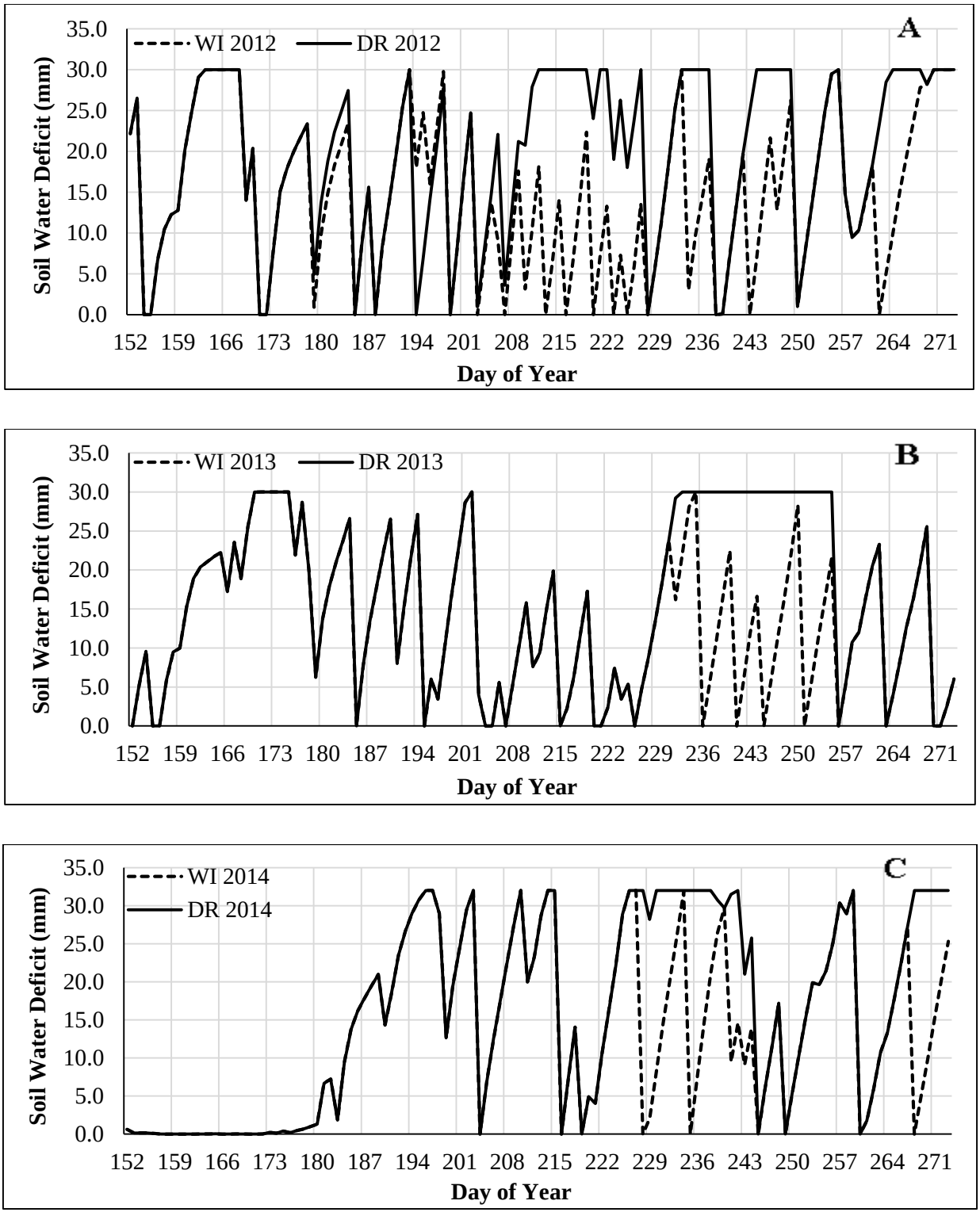

Figure 2_2 Soil water deficit from June through September for well-irrigated (WI) and drought (DR) treatments for 2012 (A), 2013 (B), and 2014 (C). Irrigation was applied for the WI treatment when the soil water deficit reached 30 mm. No attempt was made to estimate deficit greater than 30 mm.

values were analyzed using both methods (**Figure 2_3**). DGCI values from GIMP were nearly identical with the values from ArcGIS ($R^2 = 0.99$).

As expected, G_DGCI increased with increasing leaf N concentration in all 3 years (**Figure 2_4**, **2_5**, and **2_6**) with ANCOVA accounting for between 67 and 74% of all variation (**Table 2_5**, **2_6**, and **2_7**). In all 3 years, G_DGCI was not affected by either irrigation or genotype. G_DGCI values increased with increasing leaf N concentration between 1.5% and 4.5% for 2012 and 2014 (**Figure 2_4** and **2_6**). At leaf N concentrations above 4.5%, there was a slight decrease in G_DGCI. In contrast, in 2013, G_DGCI increased linearly with increasing leaf N concentration ranging from 2% to 6.5% (**Figure 2_5)**.

In 2012, in analyzing aerial DGCI corresponding to leaf N concentration, Only MG5 (P95Y50) was included in this model because the other MGs had only a few data points. Similar to G_DGCI, aerial DGCI increased with increasing leaf N concentration in all 3 years (**Figure 2_7**, **2_8**, and **2_9**) with ANCOVA accounting for between 87 and 99% of all variation (**Table 2_8**, **2_9**, and **2_10**). Likewise, aerial DGCI values increased with increasing leaf N concentration from 1.5% to 5% for all 3 years. At leaf N concentration over 5%, there was a slight decrease in aerial DGCI for 2013 and 2014 (**Figure 2_8** and **2_9**). In 2012, aerial DGCI increased linearly, and was not affected by irrigation treatment for genotype P95Y50 (**Table 2_8**). In 2013, aerial DGCI was affected by both irrigation and genotype (**Table 2_9**). In **Figure 2_8** the response of P94Y40 illustrates the general response of aerial DGCI to leaf N concentration; similar responses were observed for the other genotypes (not included in the **Figure 2_8**). The WI treatment had significantly higher aerial DGCI values at a given leaf N concentration than the DR treatment for each genotype in 2013. In contrast, in 2014, neither irrigation nor genotype had significant effects

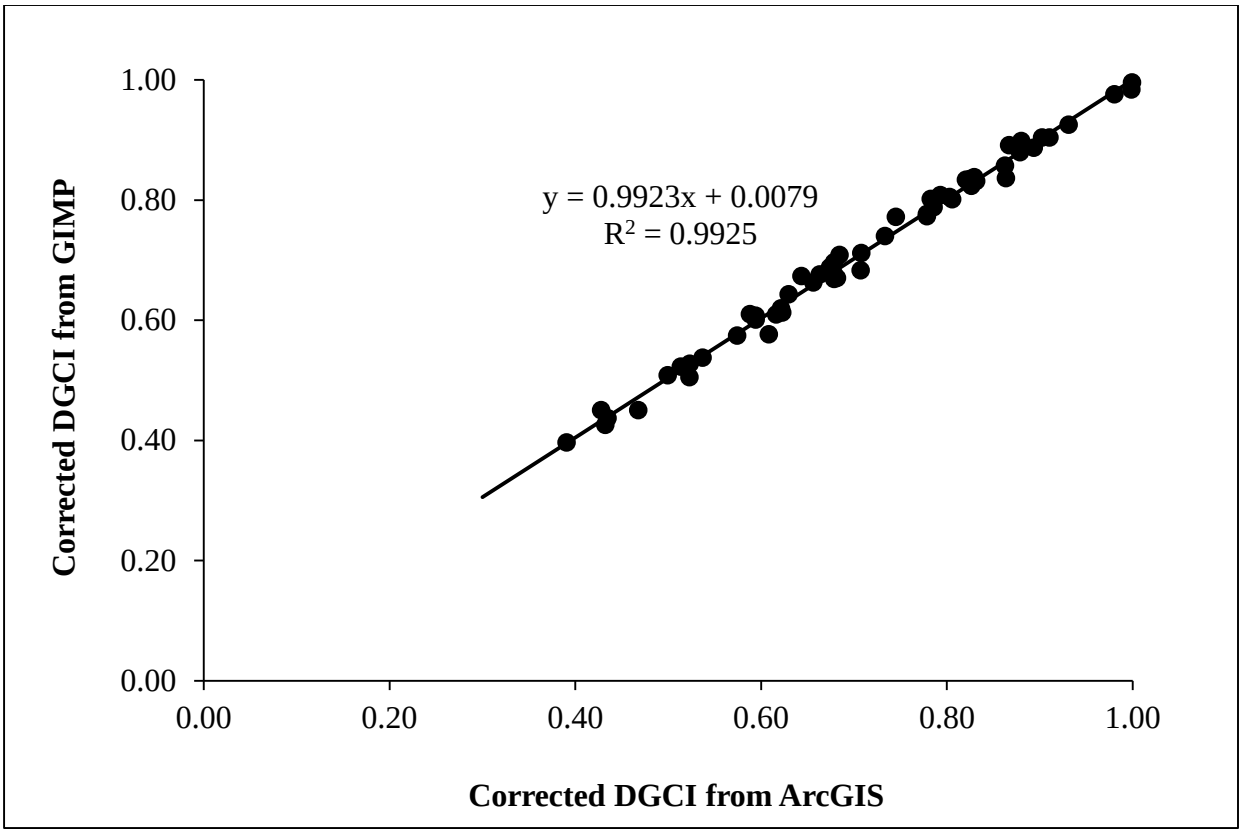

Figure 2_3 Comparison of Dark Green Color Index values (DGCI) values determined with GIMP versus DGCI values determined with ArcGIS. A total of 56 data points from six different aerial images were processed with both GIMP and ArcGIS.

Table 2_5 ANCOVA for ground DGCI (G_DGCI) associated with the linear and quadratic interactions of leaf N concentration in Fayetteville 2012. Non-significant interactions were removed from the model stepwise.

G_DGCI

Source	DF	Mean Square	F Value	Pr > F	Adj. R^2
Irri	1	0.0092	1.30	0.2589	0.74
Geno	4	0.0062	0.87	0.4860	
Leaf_N	1	0.2554	36.14	<.0001	
Leaf_N*leaf_N	1	0.1438	20.35	<.0001	

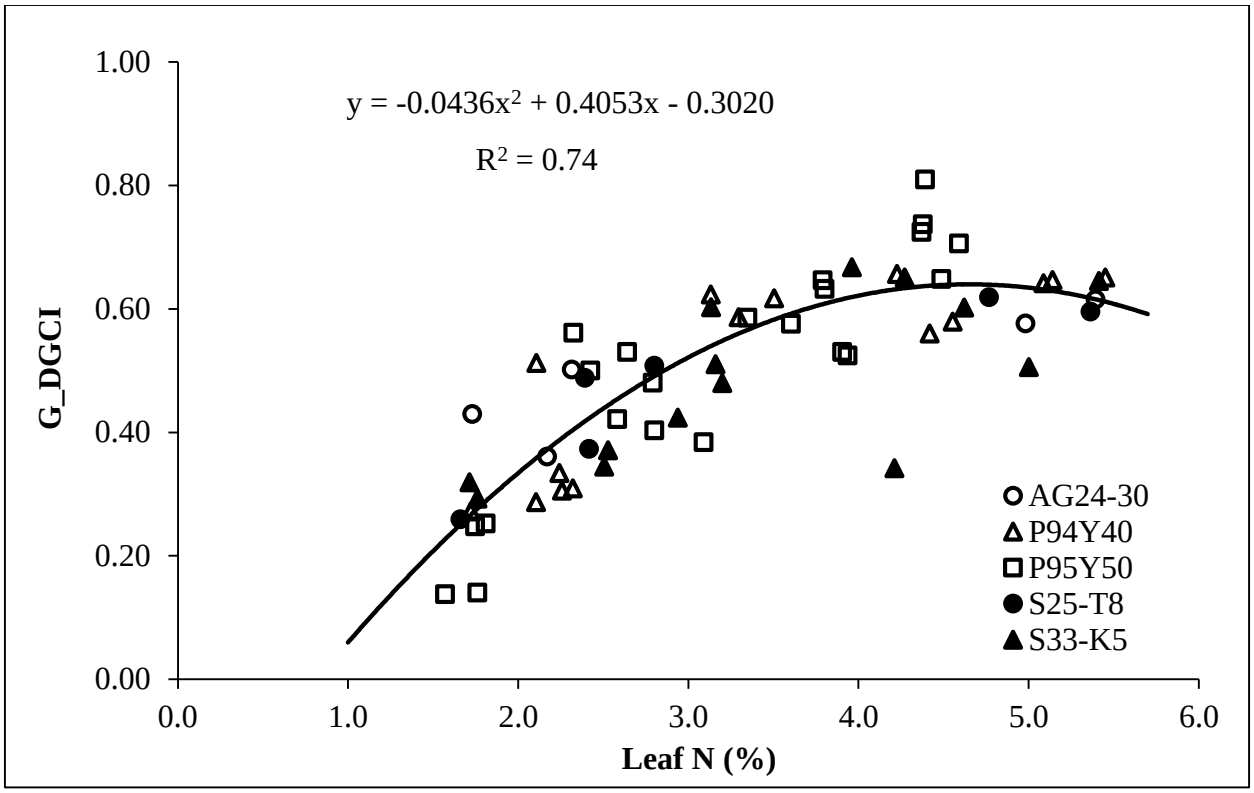

Figure 2_4 Ground DGCI (G_DGCI) versus leaf N concentration across genotypes and water treatments (genotype × water treatment interaction, NS) in Fayetteville 2012.

Table 2_6 ANCOVA for ground DGCI (G_DGCI) associated with leaf N concentration in Fayetteville 2013. Non-significant interactions were removed from the model stepwise.

G_DGCI

Source	DF	Mean Square	F Value	Pr > F	Adj. R^2
Irri	1	0.0019	0.10	0.7520	
Geno	4	0.0206	1.07	0.3791	0.67
Leaf_N	1	2.0521	106.27	<.0001	

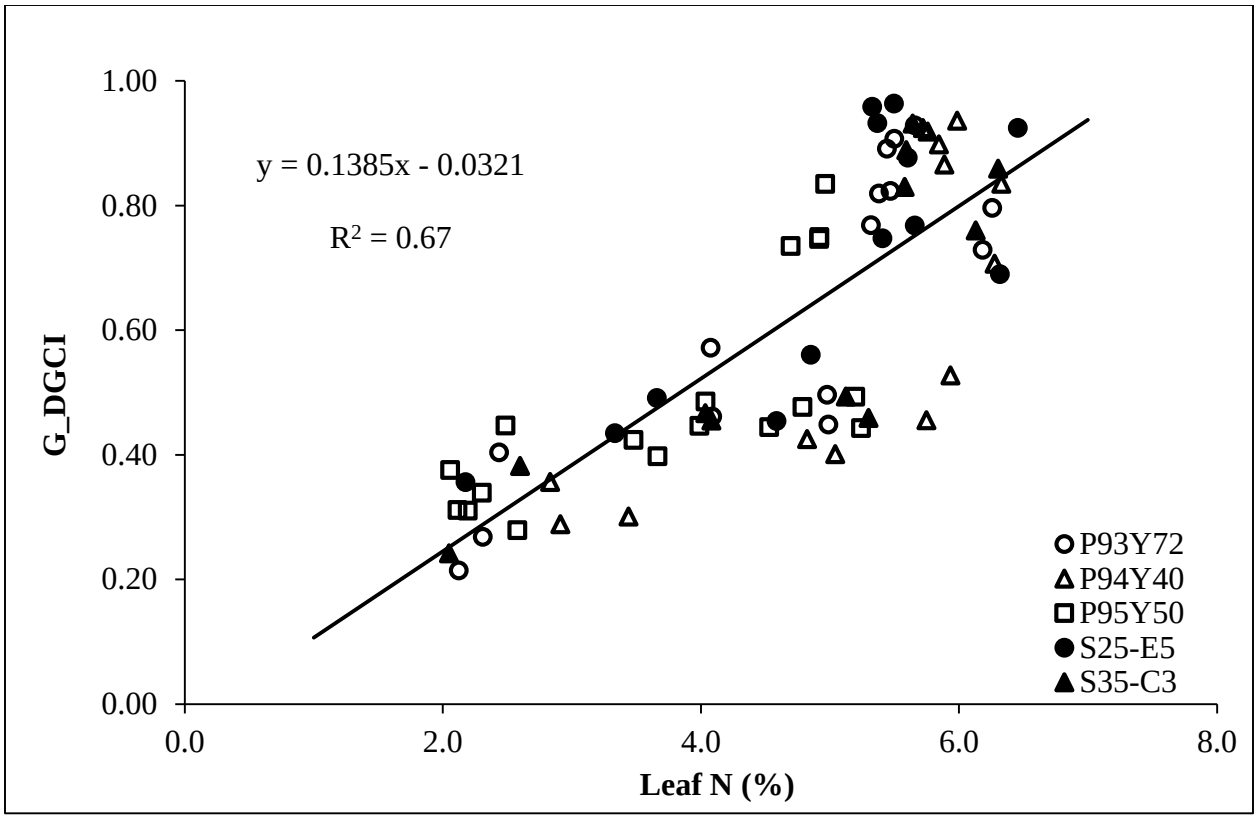

Figure 2_5 Ground DGCI (G_DGCI) versus leaf N concentration across genotypes and water treatments (genotype × water treatment interaction, NS) in Fayetteville 2013.

Table 2_7 ANCOVA for ground DGCI (G_DGCI) associated with leaf N, and leaf N*leaf N in Fayetteville 2014. Non-significant interactions were removed from the model stepwise.

G_DGCI

Source	DF	Mean Square	F Value	Pr > F	Adj. R^2
Irri	1	0.0003	0.03	0.8583	0.67
Geno	4	0.0046	0.54	0.7094	
Leaf_N	1	0.6103	71.26	<.0001	
Leaf_N*leaf_N	1	0.4557	53.21	<.0001	

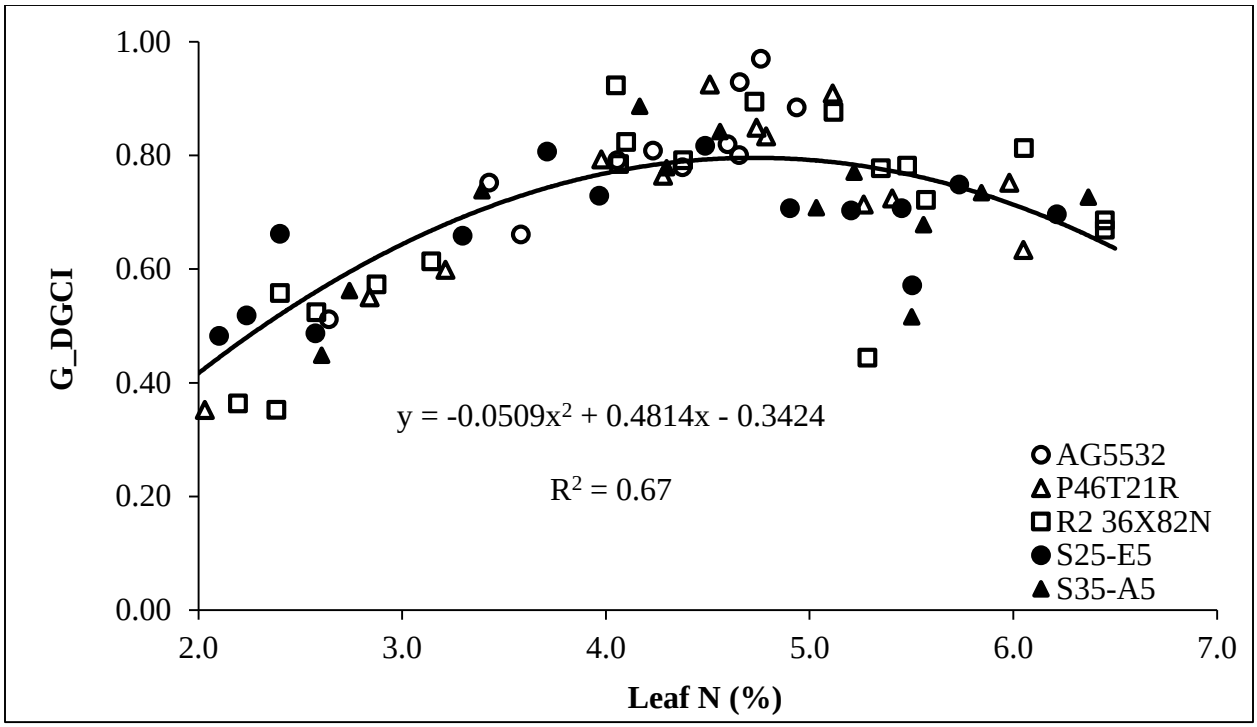

Figure 2_6 Ground DGCI (G_DGCI) versus leaf N concentration across genotypes and water treatments (genotype × water treatment interaction, NS) in Fayetteville 2014.

Table 2_8 ANCOVA for aerial DGCI associated with leaf N concentration in Fayetteville 2012. Non-significant interactions were removed from the model stepwise. Only MG 5 was included in this model because the other MGs did not have enough data points.

Aerial DGCI

Source	DF	Mean Square	F Value	Pr > F	Adj. R^2
Irri	1	0.0018	1.19	0.3039	0.99
Leaf_N	1	1.0656	689.44	<.0001	

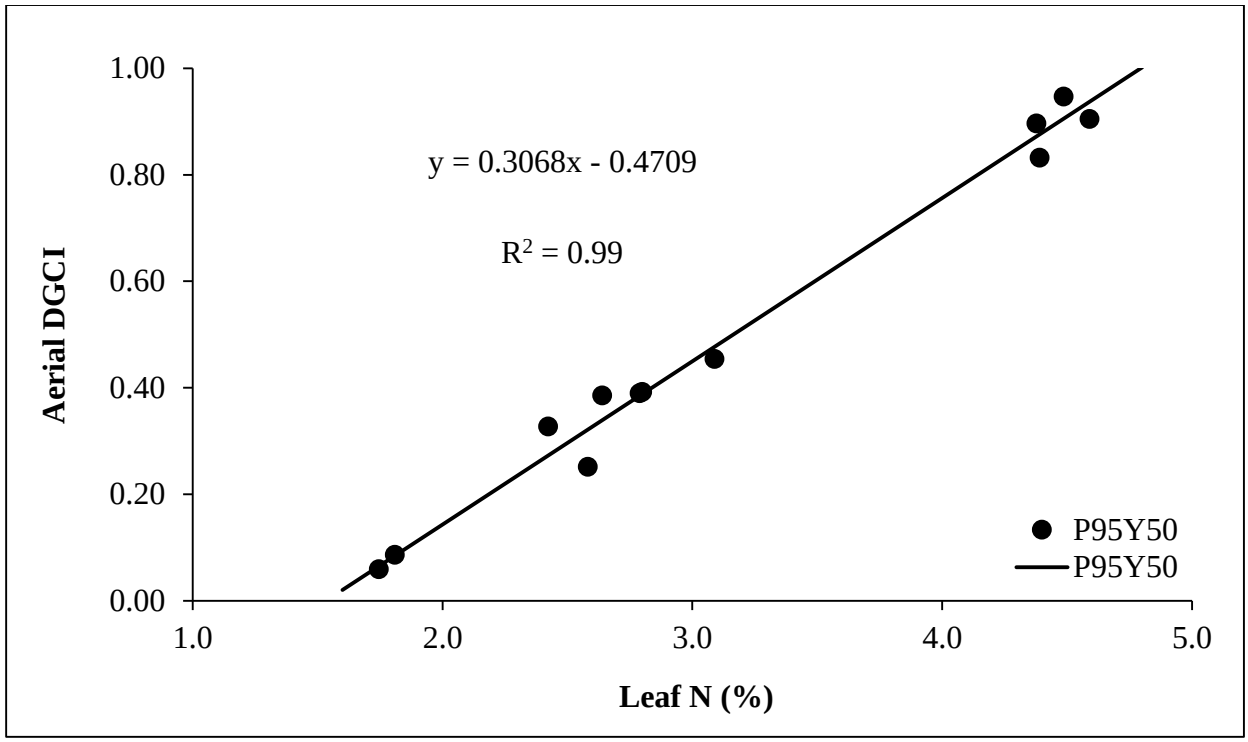

Figure 2_7 Aerial DGCI versus leaf N concentration across water treatments (NS) in Fayetteville 2012.

Table 2_9 ANCOVA for aerial DGCI associated with irrigation, genotype, leaf N concentration, and leaf N*leaf N in Fayetteville 2013. Non-significant interactions were removed from the model stepwise. Letters a, b and c represented the quadratic and linear slopes and intercept for each genotype under different water treatments in this model.

Aerial DGCI

Source	DF	Mean Square	F Value	Pr > F	Adj. R^2
Irri	1	0.0583	11.83	0.0019	0.87
Geno	4	0.0261	5.29	0.0028	
Leaf_N	1	0.1237	25.11	<.0001	
Leaf_N*leaf_N	1	0.0566	11.49	0.0022	

$y = ax^2 + bx + c$

Geno	Relative MG	Irri	a	b	c
S25-E5	2.5	DR	-0.0344	0.3868	-0.2885
		WI	-0.0344	0.3868	-0.2043
S35-C3	3.5	DR	-0.0344	0.3868	-0.1983
		WI	-0.0344	0.3868	-0.1142
P93Y72	3.7	DR	-0.0344	0.3868	-0.1893
		WI	-0.0344	0.3868	-0.1052
P94Y40	4.4	DR	-0.0344	0.3868	-0.1977
		WI	-0.0344	0.3868	-0.1136
P95Y50	5.5	DR	-0.0344	0.3868	-0.1170
		WI	-0.0344	0.3868	-0.0329

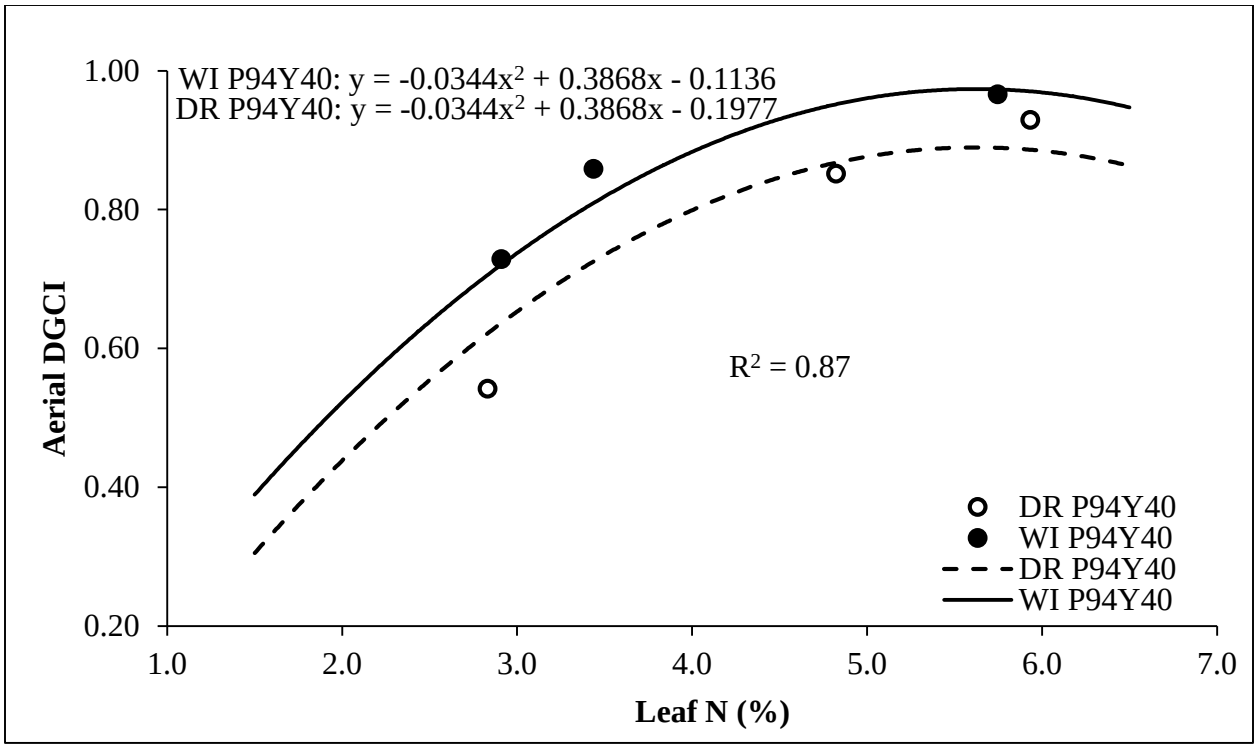

Figure 2_8 Aerial DGCI versus leaf N concentration in Fayetteville 2013. The WI and DR had the same quadratic and linear slopes, but different intercepts. Genotype P94Y40 was used to represent the response of aerial DGCI to leaf N concentration, which was similar to other genotypes (not included in the figure).

Table 2_10 ANCOVA for aerial DGCI associated with leaf N, and leaf N*leaf N in Fayetteville 2014. Non-significant interactions were removed from the model stepwise.

Aerial DGCI

Source	DF	Mean Square	F Value	Pr > F	Adj. R^2
Irri	1	0.0057	1.21	0.2761	0.90
Geno	4	0.0065	1.37	0.2533	
Leaf_N	1	0.7784	165.29	<.0001	
Leaf_N*leaf_N	1	0.4615	98.01	<.0001	

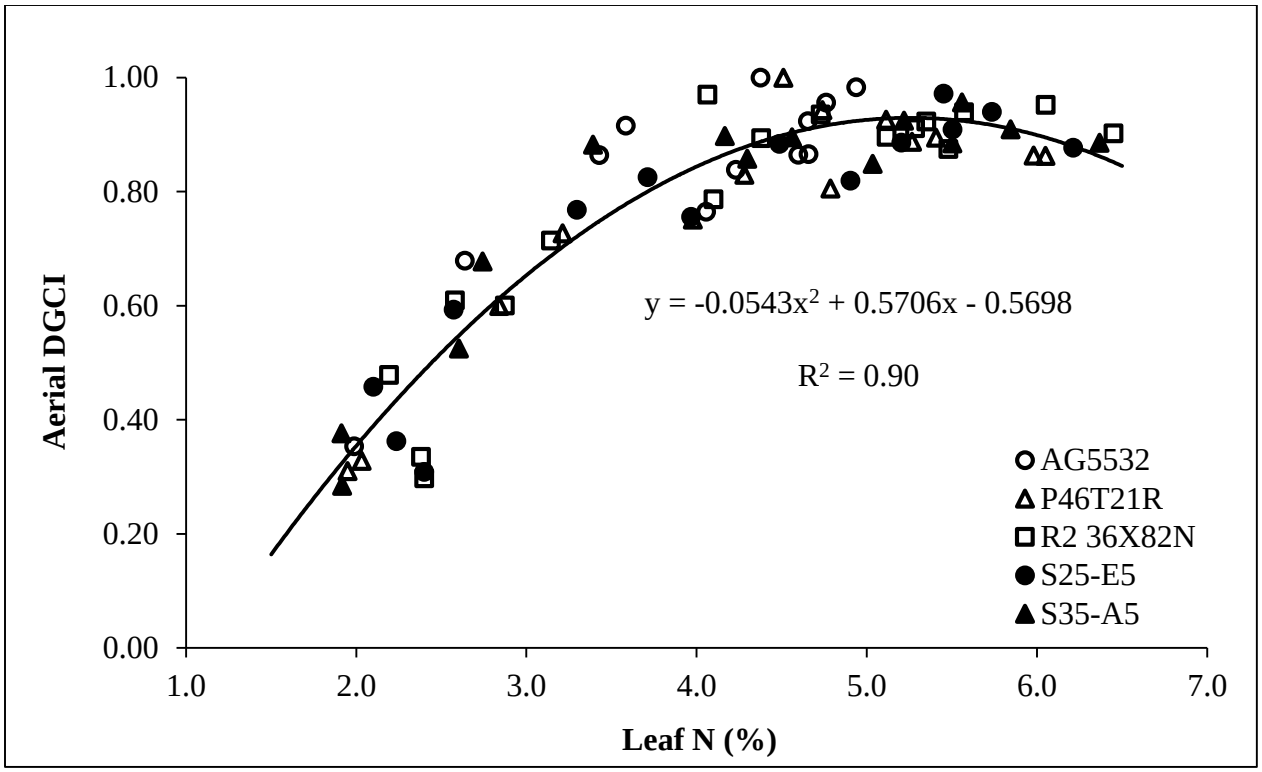

Figure 2_9 Aerial DGCI versus leaf N concentration across genotypes and water treatments (genotype × water treatment interaction, NS) in Fayetteville 2014.

on aerial DGCI (**Table 2_10**), but aerial DGCI values increased linearly as leaf N concentration increased, similar to the response in 2013.

Based upon the analysis above, color analysis of DGCI is sensitive to N concentration in leaves. Leaf N concentration measurements were made on top-most leaves, which likely had the highest N concentration in canopy. Whereas, DGCI measurements captured much more of the canopy than the top-most leaves. Similar to research in corn by Rorie et al. (2011a; 2011b), the DGCI values reached a plateau at high leaf N concentration (2012 and 2014 for G_DGCI; 2013 and 2014 for aerial DGCI).

C. G_DGCI and Aerial DGCI versus DAR5

G_DGCI decreased with increasing DAR5 in all years (**Figure 2_10, 2_11**, and **2_12**) with ANCOVA accounting for between 68 and 82% of variation (**Table 2_11**, **2_12**, and **2_13**). In 2012, G_DGCI decreased quadratically and was not affected by either irrigation or genotype. In contrast, in 2013, there was a linear decrease in G_DGCI that differed among genotypes but was similar between irrigation treatments. In 2014, G_DGCI decreased quadratically and was affected by genotypes but not irrigation treatments.

As expected, aerial DGCI decreased with increasing DAR5 in all years (**Figure 2_13**, **2_14**, and **2_15**) with ANCOVA accounting for between 84 and 89% of the variation (**Table 2_14**, **2_15**, and **2_16**). In 2012, aerial DGCI decreased quadratically, and the rate of decrease differed among genotypes and between irrigation treatments. In 2013, a quadratic decrease in aerial DGCI differed between irrigation treatments but was similar among genotypes. In contrast, in 2014, aerial DGCI decreased quadratically and was not affected by either irrigation or genotype, but was affected by the interaction between irrigation and DAR5. For all years, the WI treatment had higher aerial DGCI than the DR treatment.

Table 2_11 ANCOVA for ground DGCI (G_DGCI) associated with DAR5* DAR5 in Fayetteville 2012. Non-significant interactions were removed from the model stepwise.

G_DGCI

Source	DF	Mean Square	F Value	Pr > F	Adj. R^2
Irri	1	0.0000	0.00	0.9891	
Geno	4	0.0162	1.70	0.1556	0.68
DAR5*DAR5	1	1.9584	205.60	<.0001	

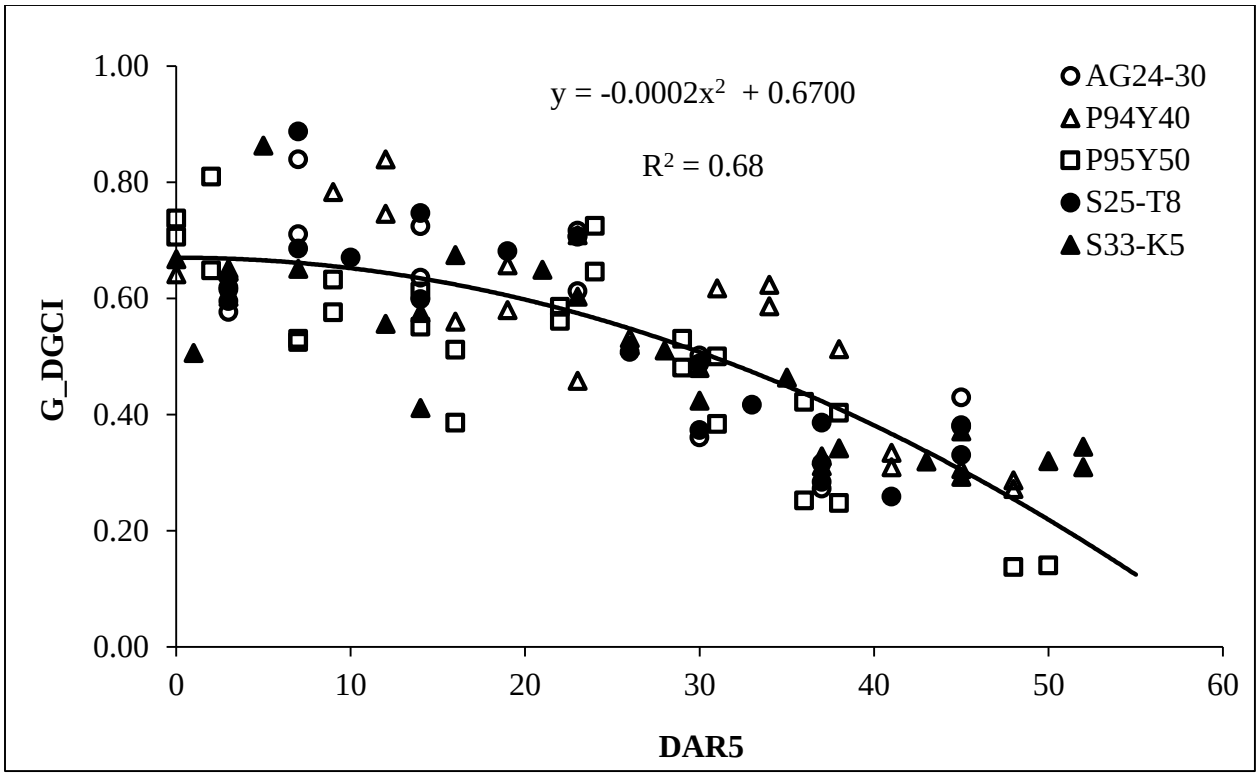

Figure 2_10 Ground DGCI (G_DGCI) versus days after R5 (DAR5) across genotypes and water treatments (genotype × water treatment interaction, NS) in Fayetteville 2012.

Table 2_12 ANCOVA for ground DGCI (G_DGCI) associated with genotype, days after R5 (DAR5), and their interaction in Fayetteville 2013. Non-significant interactions were removed from the model stepwise. Letters b and c represented the slope and intercept for each genotype across water treatments in this linear model.

G_DGCI

Source	DF	Mean Square	F Value	Pr > F	Adj. R^2
Irri	1	0.0000	0.00	0.9826	0.82
Geno	4	0.1261	10.58	<.0001	
DAR5	1	2.7800	233.28	<.0001	
DAR5*geno	4	0.0705	5.91	0.0005	

y = bx + c

Geno	Relative MG	Irri	b	c
S25-E5	2.5	DR/WI	-0.0169	1.0618
S35-C3	3.5	DR/WI	-0.0161	0.9666
P93Y72	3.7	DR/WI	-0.0143	0.9393
P94Y40	4.4	DR/WI	-0.0199	1.0220
P95Y50	5.5	DR/WI	-0.0072	0.6290

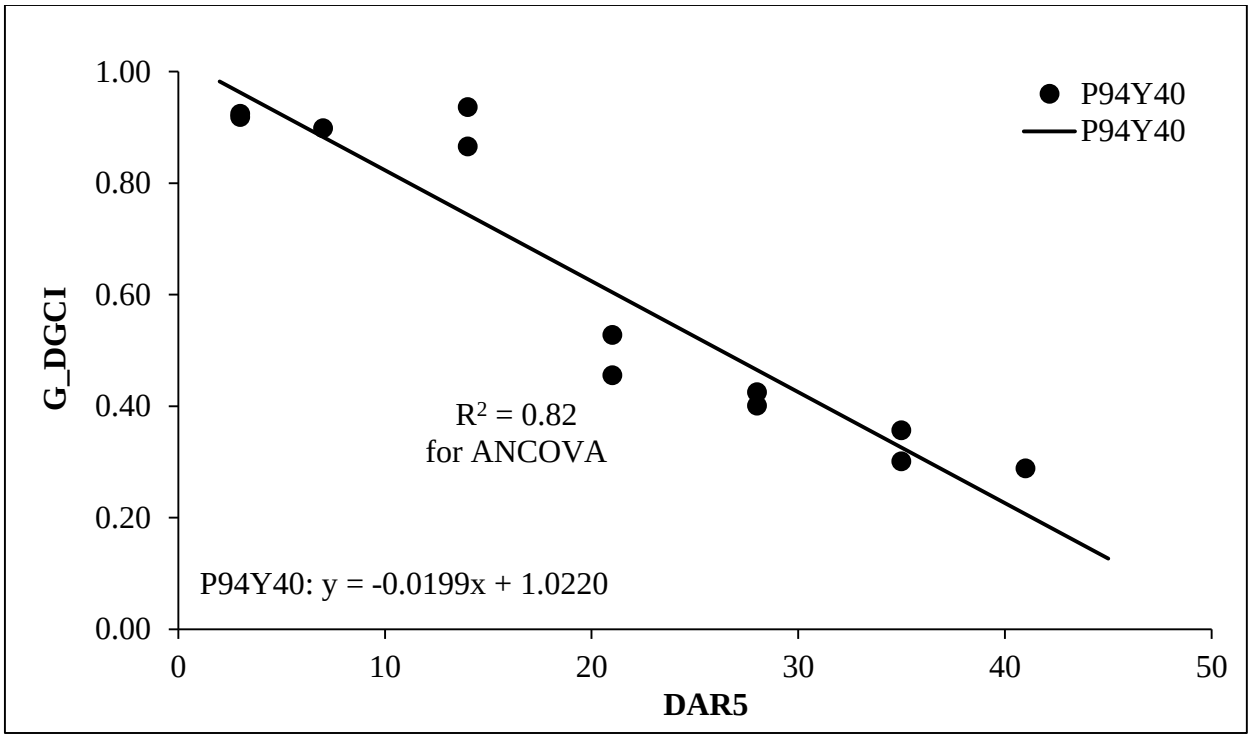

Figure 2_11 Ground DGCI (G_DGCI) versus days after R5 (DAR5) across water treatments (NS) in Fayetteville 2013. Genotype P94Y40 was used to represent the response of G_DGCI to DAR5, which was similar to other genotypes (not included in the figure).

Table 2_13 ANCOVA for ground DGCI (G_DGCI) associated with genotype, days after R5 (DAR5), DAR5*genotype, DAR5*DAR5, and DAR5*DAR5*genotype in Fayetteville 2014. Non-significant interactions were removed from the model stepwise. Letters a, b and c represented the quadratic and linear slopes and intercept for each genotype across water treatments in this model.

G_DGCI

Source	DF	Mean Square	F Value	Pr > F	Adj. R^2
Irri	1	0.0036	0.65	0.4251	0.81
Geno	4	0.0261	4.66	0.0025	
DAR5	1	0.3416	61.01	<.0001	
DAR5*geno	4	0.0196	3.51	0.0125	
DAR5*DAR5	1	0.5663	101.14	<.0001	
DAR5*DAR5*geno	4	0.0213	3.80	0.0083	

$y = ax^2 + bx + c$

Geno	Relative MG	Irri	a	b	c
S25-E5	2.5	DR/WI	-0.0003	0.0126	0.5985
S35-A5	3.5	DR/WI	-0.0006	0.0225	0.5660
R2 36X82N	3.6	DR/WI	-0.0008	0.0303	0.5407
P46T21R	4.6	DR/WI	-0.0008	0.0379	0.4328
AG5532	5.5	DR/WI	-0.0004	0.0066	0.8693

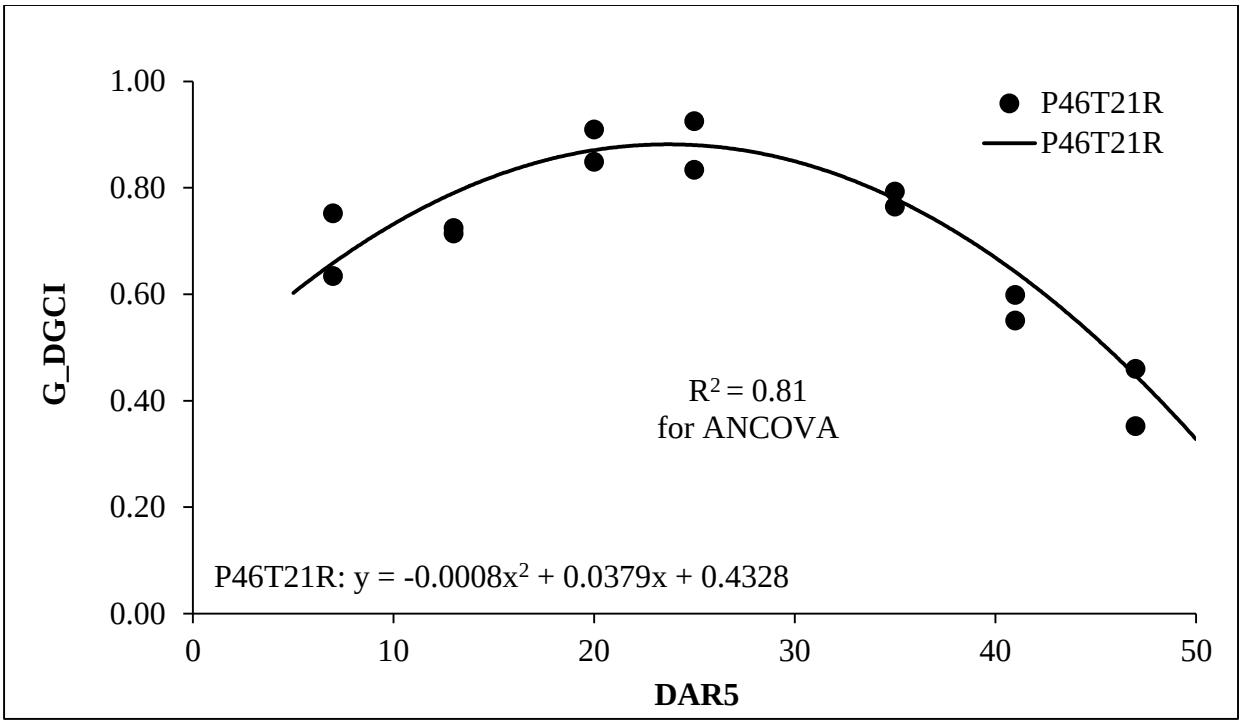

Figure 2_12 Ground DGCI (G_DGCI) versus days after R5 (DAR5) across water treatments (NS) in Fayetteville 2014. Genotype P46T21R was used to represent the response of G_DGCI to DAR5, which was similar to other genotypes (not included in the figure).

Table 2_14 ANCOVA for aerial DGCI associated with irrigation treatment, genotype, days after R5 (DAR5), DAR5*genotype, DAR5*DAR5, and DAR5*DAR5*genotype in Fayetteville 2012. Non-significant interactions were removed from the model stepwise. Letters a, b and c represented the quadratic and linear slopes and intercept for each genotype under different water treatments in this model.

Aerial DGCI

Source	DF	Mean Square	F Value	Pr > F	Adj. R^2
Irri	1	0.1114	9.60	0.0034	0.89
Geno	4	0.3786	32.61	<.0001	
DAR5	1	0.3154	27.17	<.0001	
DAR5*geno	4	0.2386	20.55	<.0001	
DAR5*DAR5	1	0.8253	71.09	<.0001	
DAR5*DAR5*geno	4	0.1835	15.81	<.0001	

$y = ax^2 + bx + c$

Geno	Relative MG	Irri	a	b	c
AG24-30	2.4	DR	-0.0017	0.0623	0.0837
		WI	-0.0017	0.0623	0.1732
S25-T8	2.5	DR	-0.0021	0.0748	0.0739
		WI	-0.0021	0.0748	0.1634
S33-K5	3.3	DR	-0.0012	0.0449	0.1781
		WI	-0.0012	0.0449	0.2676
P94Y40	4.4	DR	0.0001	-0.0305	1.2544
		WI	0.0001	-0.0305	1.3438
P95Y50	5.5	DR	0.0001	-0.0208	0.8601
		WI	0.0001	-0.0208	0.9496

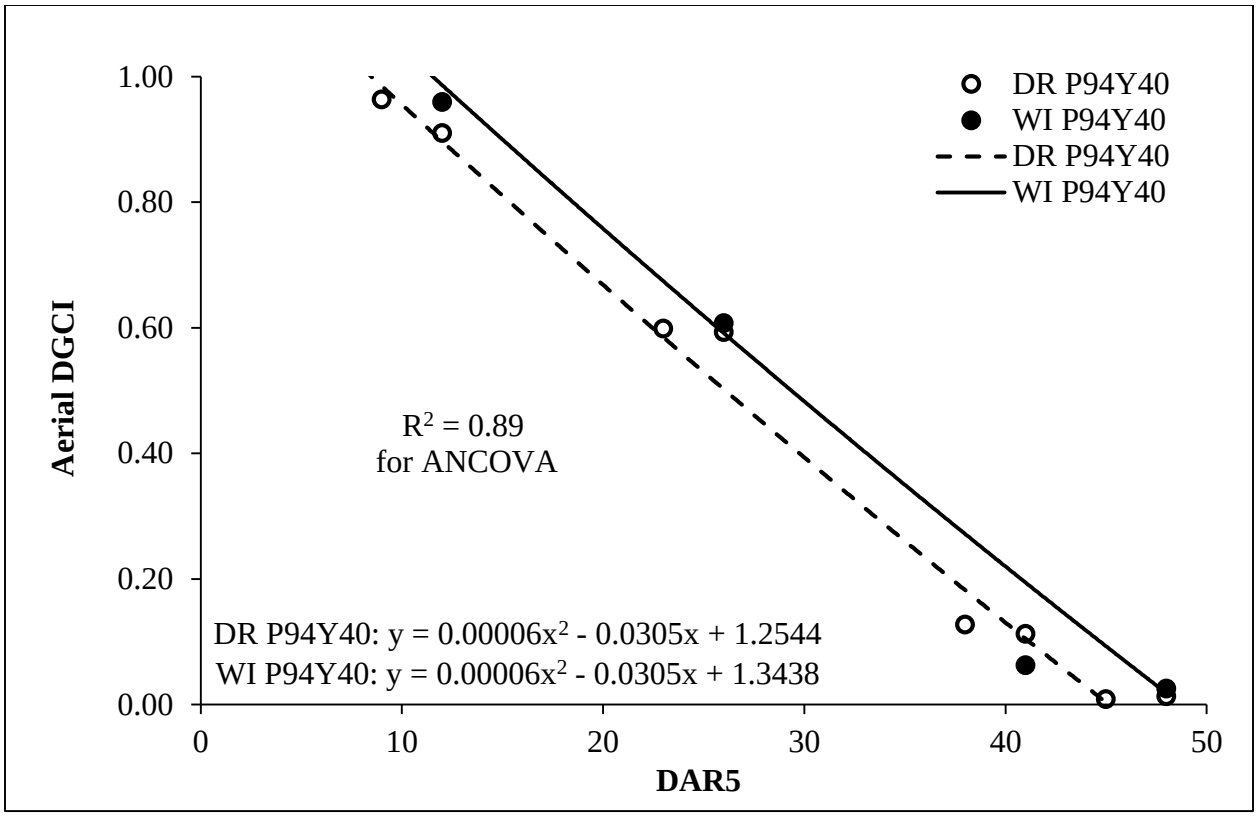

Figure 2_13 Aerial DGCI versus days after R5 (DAR5) under different water treatments in 2012. Genotype P94Y40 was used to represent the response of aerial DGCI to DAR5, which was similar to other genotypes (not included in the figure).

Table 2_15 ANCOVA for aerial DGCI associated with irrigation treatment, days after R5 (DAR5), and DAR5*DAR5 in Fayetteville 2013. Non-significant interactions were removed from the model stepwise. Letters a, b and c represented the quadratic and linear slopes and intercept for each water treatments in this model.

Aerial DGCI

Source	DF	Mean Square	F Value	Pr>F	Adj. R^2
Irri	1	0.1109	18.94	0.0002	0.84
Geno	4	0.0040	0.68	0.6135	
DAR5	1	0.0510	8.72	0.0064	
DAR5*DAR5	1	0.1644	28.08	<.0001	

$y = ax^2 + bx + c$

Irri	a	b	c
DR	-0.0006	0.0200	0.7483
WI	-0.0006	0.0200	0.8674

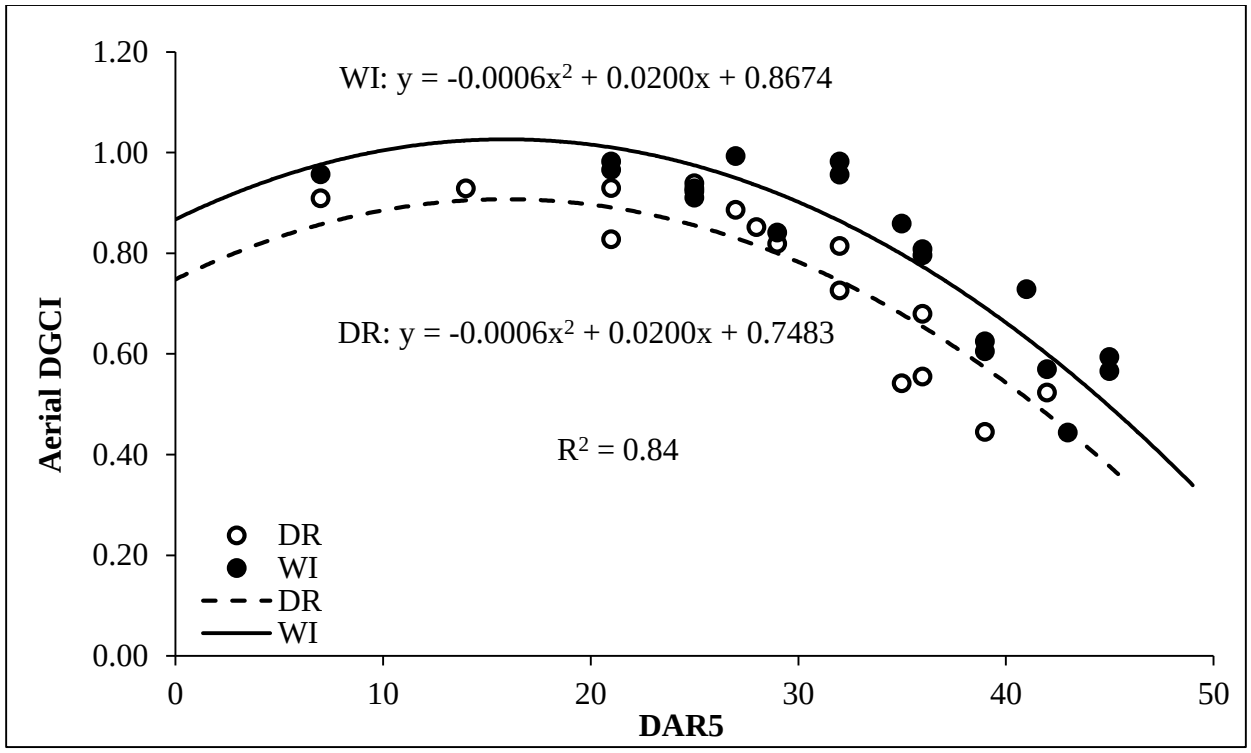

Figure 2_14 Aerial DGCI versus days after R5 (DAR5) across genotypes (NS) in Fayetteville 2013.

Table 2_16 ANCOVA for aerial DGCI associated with days after R5 (DAR5), DAR5*irrigation, and DAR5*DAR5 in Fayetteville 2014. Non-significant interactions were removed from the model stepwise.

Aerial DGCI

Source	DF	Mean Square	F Value	Pr > F	Adj. R^2
Irri	1	0.0048	0.77	0.3825	
Geno	4	0.0014	0.22	0.9254	
DAR5	1	0.1409	22.53	<.0001	0.87
DAR5*irri	1	0.0382	6.12	0.0162	
DAR5*DAR5	1	0.5636	90.13	<.0001	

$y = ax^2 + bx + c$

Irri	a	b	c
DR	-0.0005	0.0111	0.8635
WI	-0.0005	0.0144	0.8635

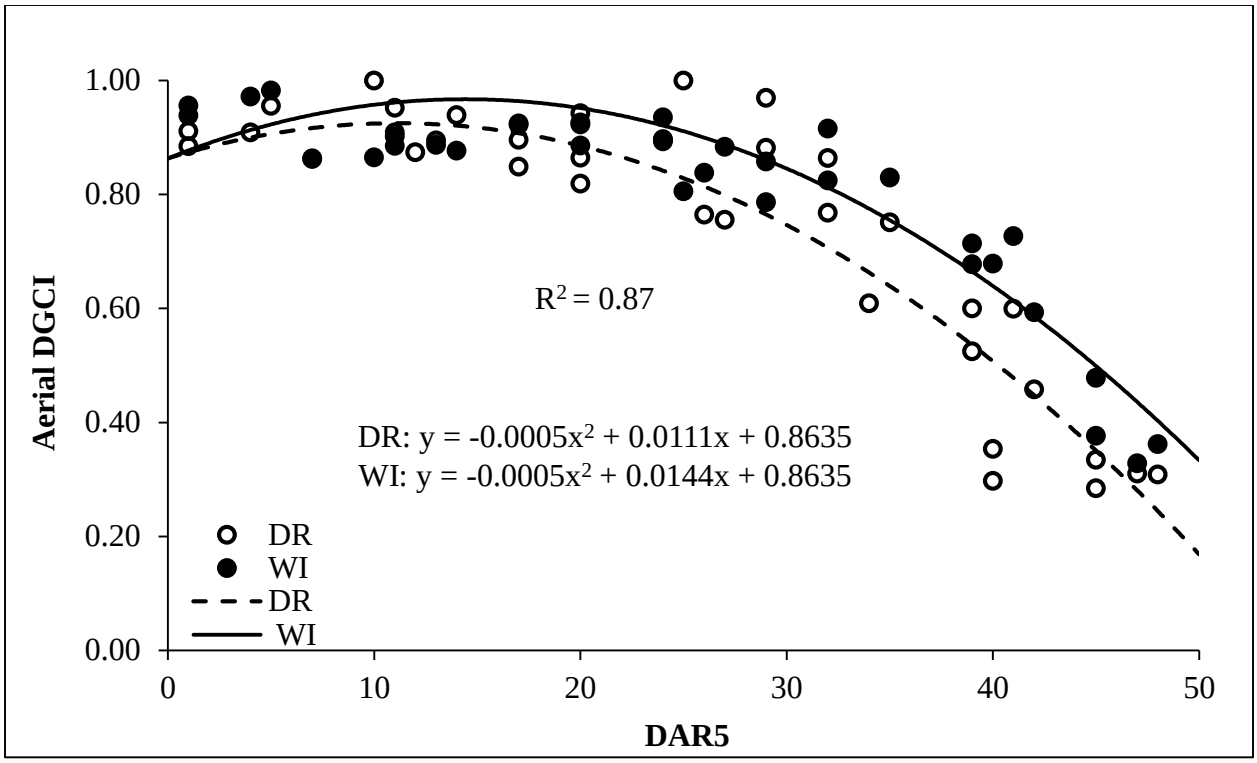

Figure 2_15 Aerial DGCI versus days after R5 (DAR5) across genotypes (NS) in Fayetteville 2014.

Both G_DGCI and aerial DGCI decreased in the late reproductive stages of soybean in all years, which was similar to the response of leaf N concentration versus DAR5 (refer to **Appendix**—**Table A1** to **A3**, **Figure A1** to **A3**), showing that leaves gradually lost their greenness and began yellowing as N was remobilized from leaves to seeds during reproductive stages. However, only aerial DGCI was able to identify the significant effect showing the aerial DGCI was lower in DR treatment at any given DAR5 for all years, which showed that aerial imaging method had high sensitivity compared to ground level method in detecting differences among treatments. G_DGCI and aerial DGCI measurements are two different methods for evaluating the greenness of a soybean canopy. Aerial DGCI measurements had higher sensitivity to identify the differences among treatments, but there was a general agreement between the two measurements (refer to **Appendix**—**Table A4** to **A6**, **Figure A4** to **A6**).

D. G_DGCI and Aerial DGCI versus Est_HI

G_DGCI decreased with increasing est_HI in all years (**Figure 2_16**, **2_17**, and **2_18**) with ANCOVA accounting for between 66 and 84% for all variation (**Table 2_17**, **2_18**, and **2_19**). As mentioned above, in 2012, genotypes AG24-30 and S25-T8 were not included in the data analysis since they had only two HI samples. Irrigation did not show a significant difference in any of the three years, but genotype did. There was a linear decrease in G_DGCI in 2012 and 2013, and a quadratic decrease in 2014.

Aerial DGCI decreased with increasing est_HI in all years (**Figure 2_19**, **2_20**, and **2_21**) with ANCOVA accounting for between 79 and 99% for all variation (**Table 2_20**, **2_21**, and **2_22**). In 2012, genotypes AG24-30 and S25-T8 were not included in the data analysis since they had only two HI samples. Genotype S33-K5 was also not counted due to insufficient aerial DGCI data

Table 2_17 ANCOVA for ground DGCI (G_DGCI) associated with genotype, estimated harvest index (est_HI) in Fayetteville 2012. Non-significant interactions were removed from the model stepwise. MG2 was not included in this model because it only had two harvest index samples. Letters b and c represented the linear slope and intercept for each genotype across water treatments in this model.

G_DGCI

Source	DF	Mean Square	F Value	Pr > F	Adj. R^2
Irri	1	0.0117	1.25	0.2696	
Geno	2	0.0795	8.47	0.0007	0.66
Est_HI	1	0.9126	97.22	<.0001	

$y = bx + c$

Geno	Relative MG	Irri	b	c
S33-K5	3.3	DR/WI	0.8791	0.6732
P94Y40	4.4	DR/WI	0.8791	0.7533
P95Y50	5.5	DR/WI	0.8791	0.6154

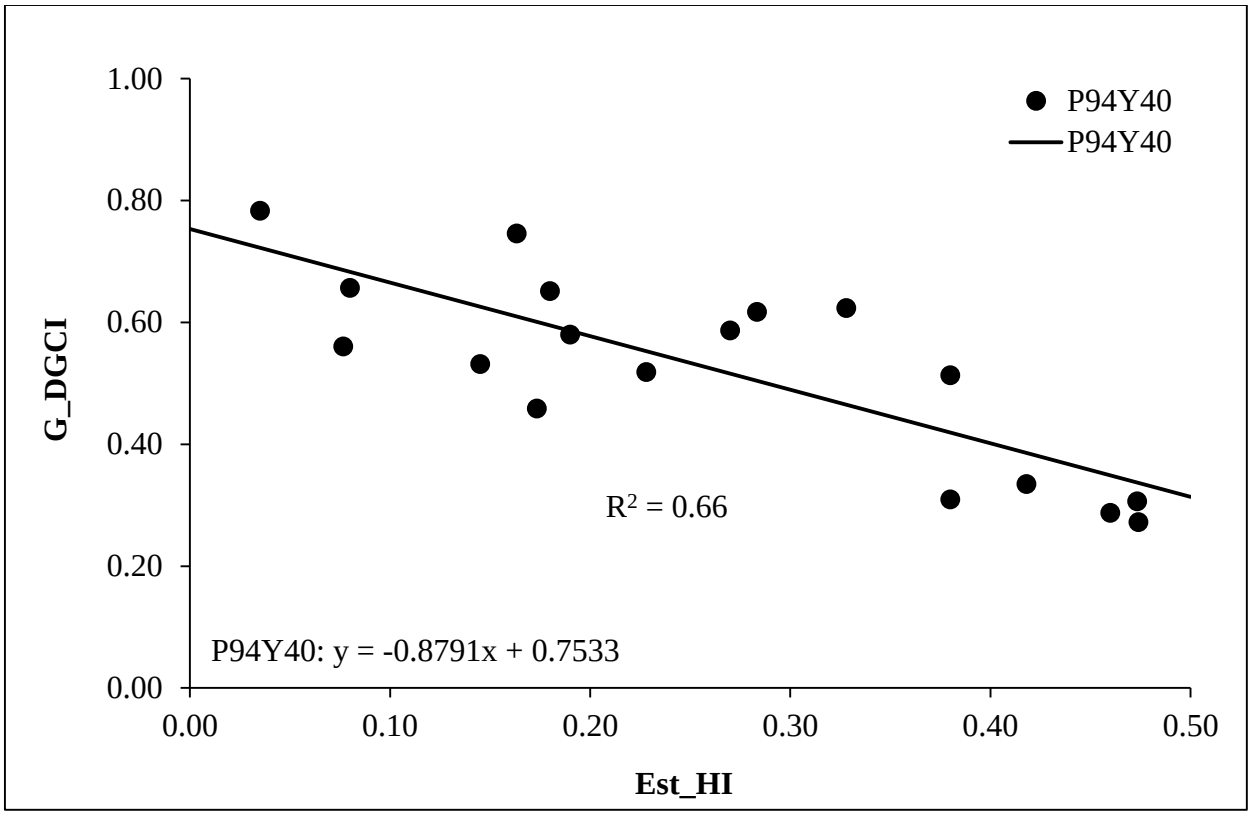

Figure 2_16 Ground DGCI (G_DGCI) versus estimated harvest index (est_HI) over water treatments (NS) in Fayetteville 2012. Genotype P94Y40 was used to represent the response of G_DGCI to est_HI, which was similar to other genotypes (not included in the figure).

Table 2_18 ANCOVA for ground DGCI (G_DGCI) associated with genotype, estimated harvest index (est_HI), and their interaction of est_HI*genotype in Fayetteville 2013. Non-significant interactions were removed from the model stepwise. Letters b and c represented the linear slope and intercept for each genotype across water treatments in this model.

G_DGCI

Source	DF	Mean Square	F Value	Pr > F	Adj. R^2
Irri	1	0.0141	1.29	0.2612	0.84
Geno	4	0.1278	11.64	<.0001	
Est_HI	1	2.6566	241.94	<.0001	
Est_HI*geno	4	0.0351	3.19	0.0192	

$y = bx + c$

Geno	Relative MG	Irri	b	c
S25-E5	2.5	DR/WI	-1.1781	0.9790
S35-C3	3.5	DR/WI	-1.2438	0.9021
P93Y72	3.7	DR/WI	-1.2069	0.9021
P94Y40	4.4	DR/WI	-1.8081	0.9622
P95Y50	5.5	DR/WI	-0.7731	0.5975

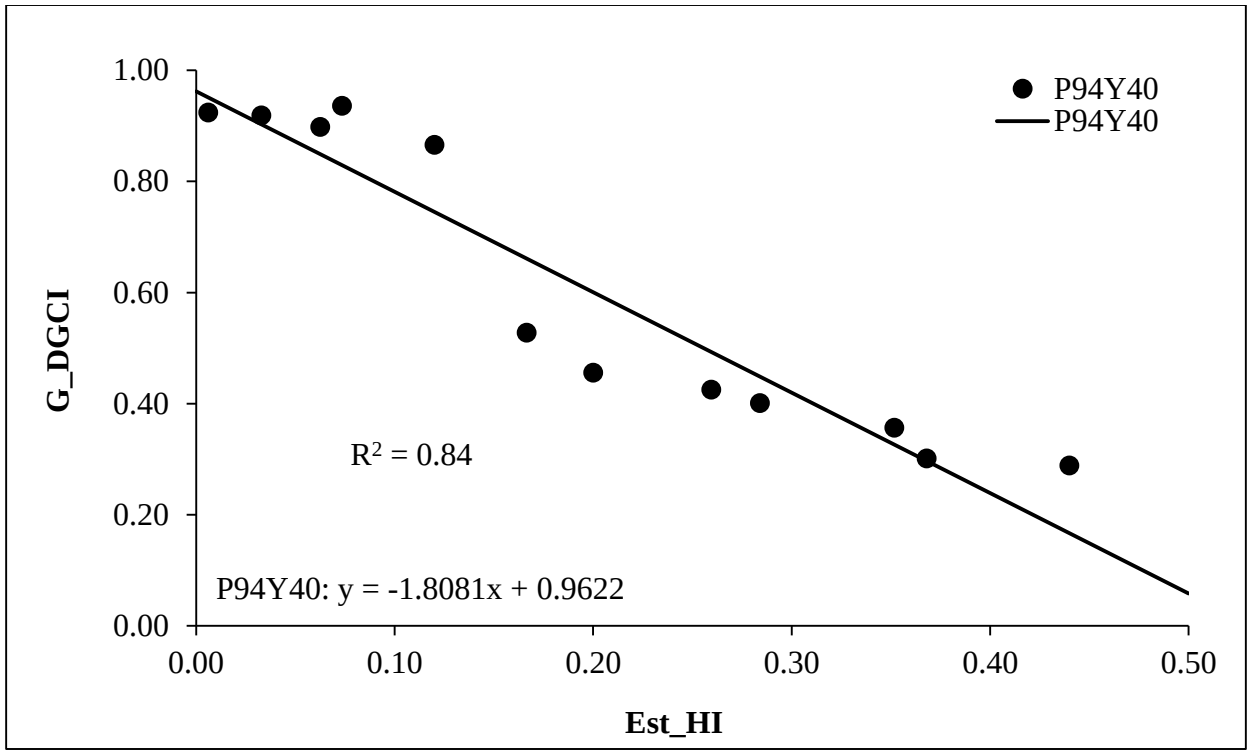

Figure 2_17 Ground DGCI (G_DGCI) versus estimated harvest index (est_HI) over water treatments (NS) in Fayetteville 2013. Genotype P94Y40 was used to represent the response of G_DGCI to est_HI, which was similar to other genotypes (not included in the figure).

Table 2_19 ANCOVA for ground DGCI (G_DGCI) associated with genotype, estimated harvest index (est_HI), est_HI*genotype, est_HI*est_HI, and est_HI*est_HI*genotype in Fayetteville 2014. Non-significant interactions were removed from the model stepwise. Letters a, b and c represented the quadratic and linear slopes and intercept for each genotype across water treatments in this model.

G_DGCI

Source	DF	Mean Square	F Value	Pr > F	Adj. R^2
Irri	1	0.0030	0.4	0.5281	0.75
Geno	4	0.0716	9.47	<.0001	
Est_HI	1	0.3258	43.08	<.0001	
Est_HI*geno	4	0.0383	5.06	0.0015	
Est_HI*est_HI	1	0.5327	70.44	<.0001	
Est_HI*est_HI*geno	4	0.0257	3.4	0.0145	

$y = ax^2 + bx + c$

Geno	Relative MG	Irri	a	b	c
S25-E5	2.5	DR/WI	-2.9104	1.7078	0.4856
S35-A5	3.5	DR/WI	-5.1810	2.6590	0.4471
R2 36X82N	3.6	DR/WI	-8.8771	5.1901	0.0524
P46T21R	4.6	DR/WI	-3.8946	1.3188	0.7454
AG5532	5.5	DR/WI	-2.1363	0.1006	0.8833

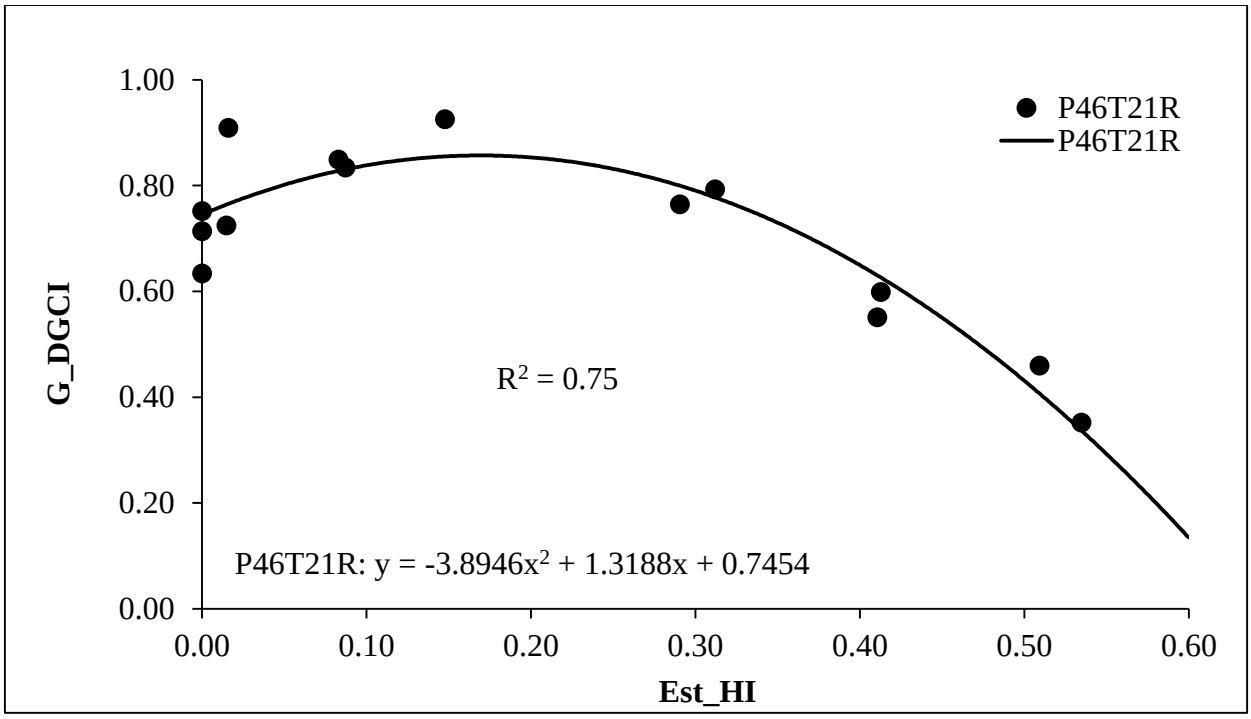

Figure 2_18 Ground DGCI (G_DGCI) versus estimated harvest index (est_HI) across water treatments (NS) in Fayetteville 2014. Genotype P41T21R was used to represent the response of G_DGCI to est_HI, which was similar to other genotypes (not included in the figure).

Table 2_20 ANCOVA for aerial DGCI associated with irrigation, genotype, irri*geno, estimated harvest index (est_HI), est_HI*irri, est_HI*geno, est_HI*irri*geno, est_HI*est_HI*irri and est_HI*est_HI*geno in Fayetteville 2012. Non-significant interactions were removed from the model stepwise. Only MG 4 and 5 were used in this model because MG 2 only had two HI samples and MG 3 only had 2 aerial DGCI data points in DR. Letters a, b and c represented the quadratic and linear slopes and intercept for each genotype under different water treatments in this model.

Aerial DGCI

Source	DF	Mean Square	F Value	Pr > F	Adj. R^2
Irri	1	0.0554	54.05	<.0001	
Geno	1	0.2144	209.27	<.0001	
Irri*geno	1	0.0805	78.61	<.0001	
Est_HI	1	0.1090	106.44	<.0001	
Est_HI*irri	1	0.0242	23.61	0.0007	0.99
Est_HI*geno	1	0.0890	86.87	<.0001	
Est_HI*irri*geno	1	0.0748	72.97	<.0001	
Est_HI*Est_HI*irri	1	0.0238	23.22	0.0007	
Est_HI*Est_HI*geno	1	0.0388	37.89	0.0001	

$y = ax^2 + bx + c$

Geno	Estimate MG	Irri	a	b	c
P94Y40	4.4	DR	2.4826	-3.4549	1.0797
		WI	9.5108	-9.0532	2.1813
P95Y50	5.5	DR	-5.5237	0.1823	0.5570
		WI	1.5045	-0.9763	0.5529

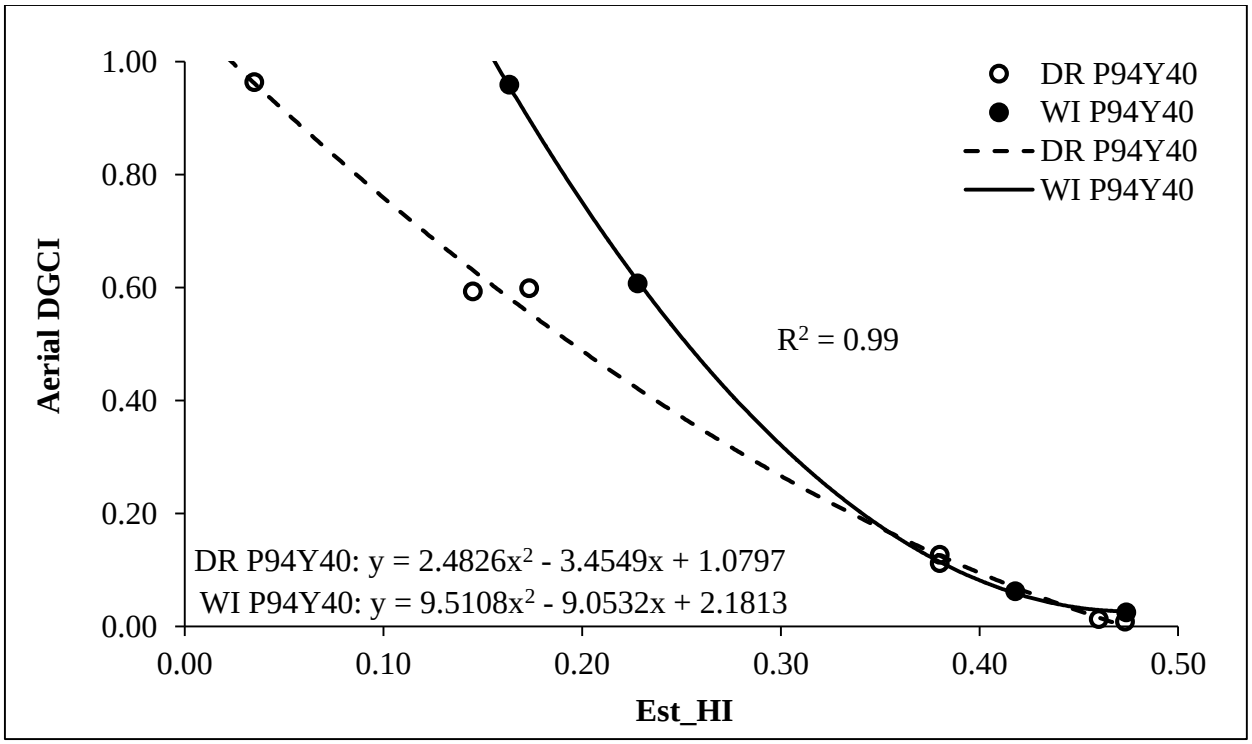

Figure 2_19 Aerial DGCI versus estimated harvest index (est_HI) in Fayetteville 2012. Genotype P94Y40 was used to represent the response of aerial DGCI to est_HI, which was similar to other genotypes (not included in the figure).

Table 2_21 ANCOVA for aerial DGCI associated with irrigation, genotype, and estimated harvest index (est_HI)*est_HI in Fayetteville 2013. Non-significant interactions were removed from the model stepwise. Letters a and c represented the quadratic slope and intercept for each genotype under different water treatments in this model.

Aerial DGCI

Source	DF	Mean Square	F Value	Pr > F	Adj. R^2
Irri	1	0.1602	21.83	<.0001	
Geno	4	0.0299	4.07	0.0100	0.79
Est_HI*Est_HI	1	0.7102	96.76	<.0001	

$y = ax^2 + c$

Geno	Estimate MG	Irri	a	c
S25-E5	2.5	DR	-2.2690	1.0468
		WI	-2.2690	1.1941
S35-C3	3.5	DR	-2.2690	1.0567
		WI	-2.2690	1.2040
P93Y72	3.7	DR	-2.2690	1.0244
		WI	-2.2690	1.1717
P94Y40	4.4	DR	-2.2690	0.9613
		WI	-2.2690	1.1086
P95Y50	5.5	DR	-2.2690	0.8769
		WI	-2.2690	1.0242

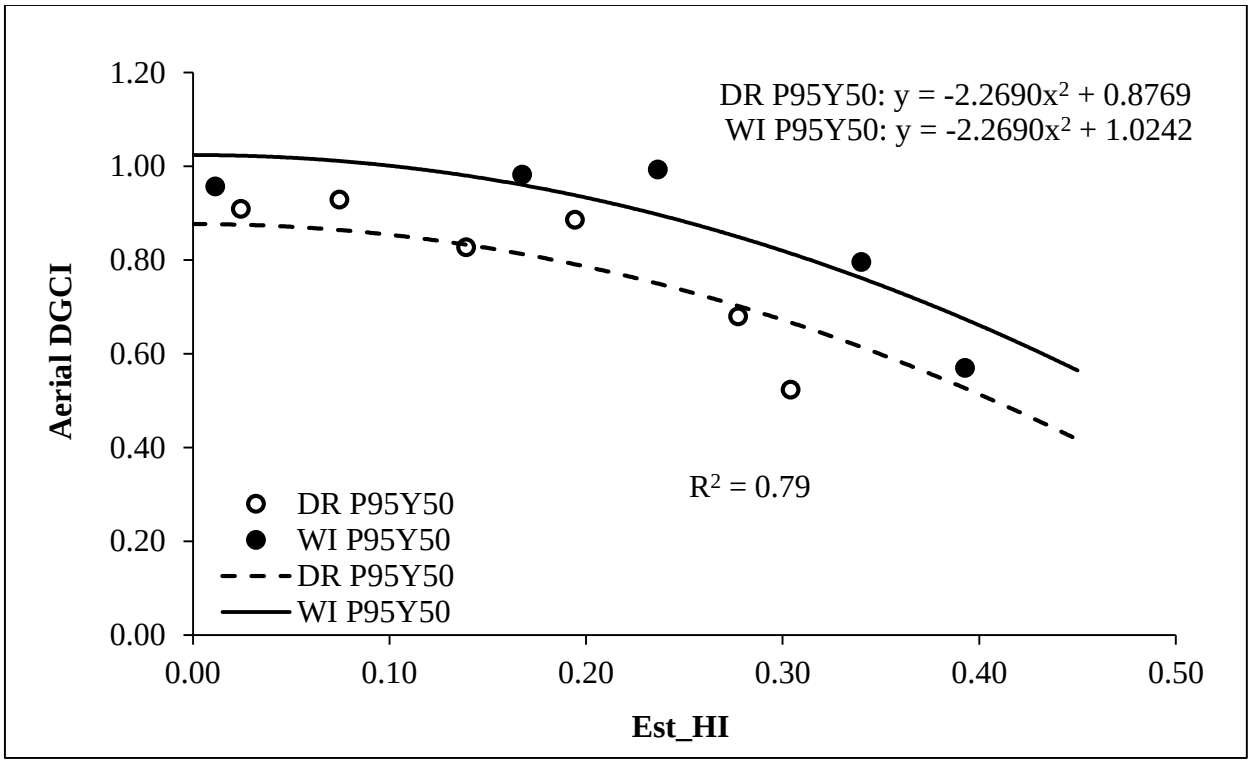

Figure 2_20 Aerial DGCI versus estimated harvest index (est_HI) in Fayetteville 2013. Genotype P95Y50 was used to represent the response of aerial DGCI to est_HI, which was similar to other genotypes (not included in the figure).

Table 2_22 ANCOVA for aerial DGCI associated with estimated harvest index (est_HI), and est_HI*irrigation in Fayetteville 2014. Non-significant interactions were removed from the model stepwise.

Aerial DGCI

Source	DF	Mean Square	F Value	Pr > F	Adj. R^2
Irri	1	0.0147	2.47	0.1211	
Geno	4	0.0088	1.49	0.2161	
Est_HI	1	0.1175	19.8	<.0001	0.88
Est_HI*irri	1	0.0743	12.52	0.0008	
Est_HI*est_HI	1	0.5600	94.35	<.0001	

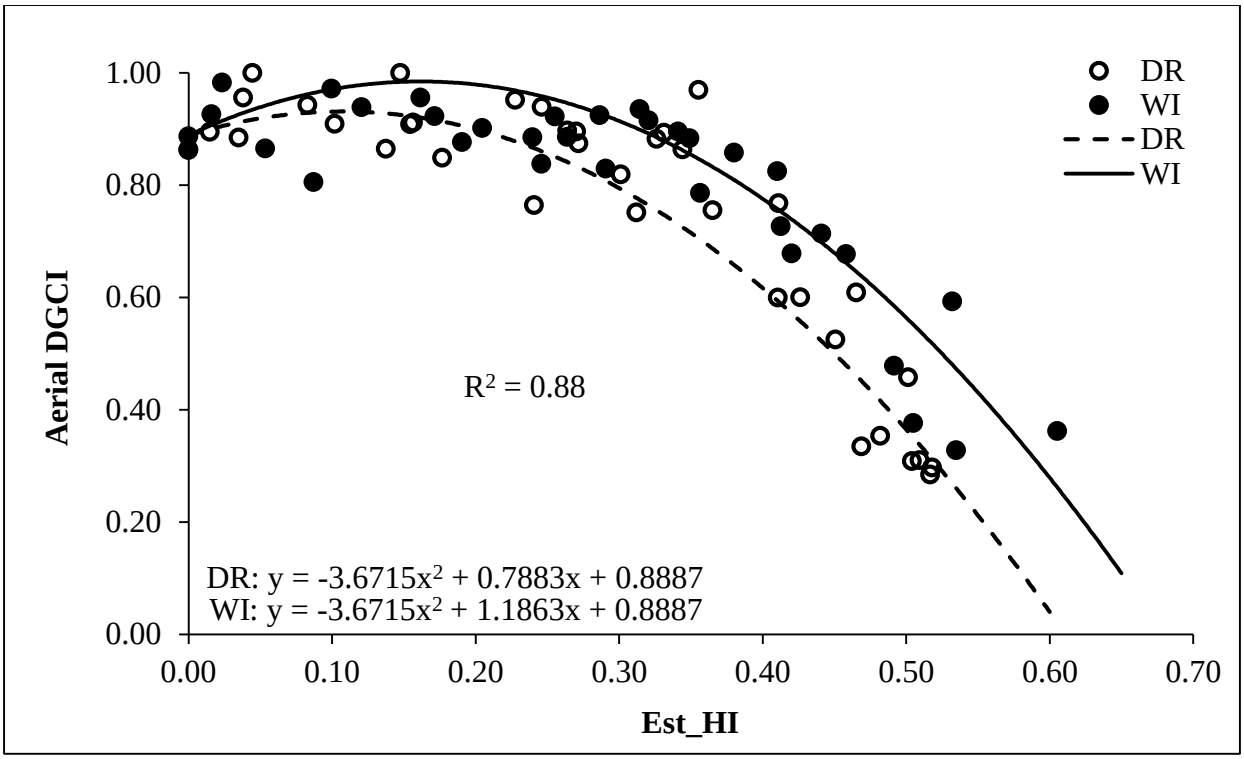

Figure 2_21 Aerial DGCI versus estimated harvest index (est_HI) across genotypes and water treatment (genotype × water treatment interaction: NS) in Fayetteville 2014.

points in 2012. In 2012 and 2013, there was a quadratic decrease in aerial DGCI that differed among genotypes and between irrigation treatments. In contrast, in 2014, aerial DGCI decrease quadratically and was not affected by either irrigation or genotype, but aerial DGCI was affected by the interaction of est_HI with irrigation. Aerial DGCI values under WI treatment in all years were higher than the values under DR treatment.

G_DGCI and aerial DGCI decreased with increasing est_HI from 0 to 0.5, which was consistent with the response of leaf N concentration to est_HI (refer to **Appendix**—**Table A7** to **A9**, **Figure A7** to **A9**), indicating N was remobilized from leaves to seeds during the seedfill period resulting in the loss of greenness. This is an alternative method of evaluating senescence response to drought. Since remobilization from leaves to seeds is the underlying reason that there is a change in "greenness", changes in DGCI may be closely associated with HI.

E. Yield

Grain yield was significantly affected by the main effects of irrigation and genotype in 2012 (**Table 2_23**) and 2014 (**Table 2_25**) and by the interaction of irrigation and genotype in 2013 (**Table 2_24**). In 2012, averaged yield was 3210 kg ha^{-1} for WI and 2132 kg ha^{-1} for DR treatments (**Figure 2_22**). The MG 4 cultivar, P94Y40, had the highest yield (3747 kg ha^{-1}), followed by the MG 5 cultivar (P95Y50) with a yield of 2885 kg ha^{-1} (**Figure 2_23**). The MG 2 and 3 cultivars had the lowest yield in 2012. In 2013, MG 3 cultivars (S35-C3 and P93Y72) had the highest yield under both DR and WI treatments (**Figure 2_24**), and the MG 5 cultivar (P95Y50) had the lowest yield for both WI and DR treatments. In 2014, the WI treatment had significantly higher yield (4528 kg ha^{-1}) than the DR treatment (3740 kg ha^{-1}) (**Figure 2_25**). The MG 5 (AG5532) and MG 3 (R2 36X82N) cultivars had significant higher yield than other cultivars (**Figure 2_26**).

Table 2_23 ANOVA for grain yield associated with irrigation treatment and genotype, but not with their interaction in Fayetteville 2012.

Yield (kg ha^{-1})

Source	DF	Mean Square	F Value	Pr > F	Adj. R^2
Rep	4	160836	0.70	0.5996	
Irri†	1	14530362	240.57	<.0001	
Rep (Irr), Err_a	4	60401	0.26	0.9003	0.82
Geno	4	4450424	19.29	<.0001	
Irri*Geno	4	285748	1.24	0.3144	

† The effect of irrigation was tested using Rep (Irr) as the error term.

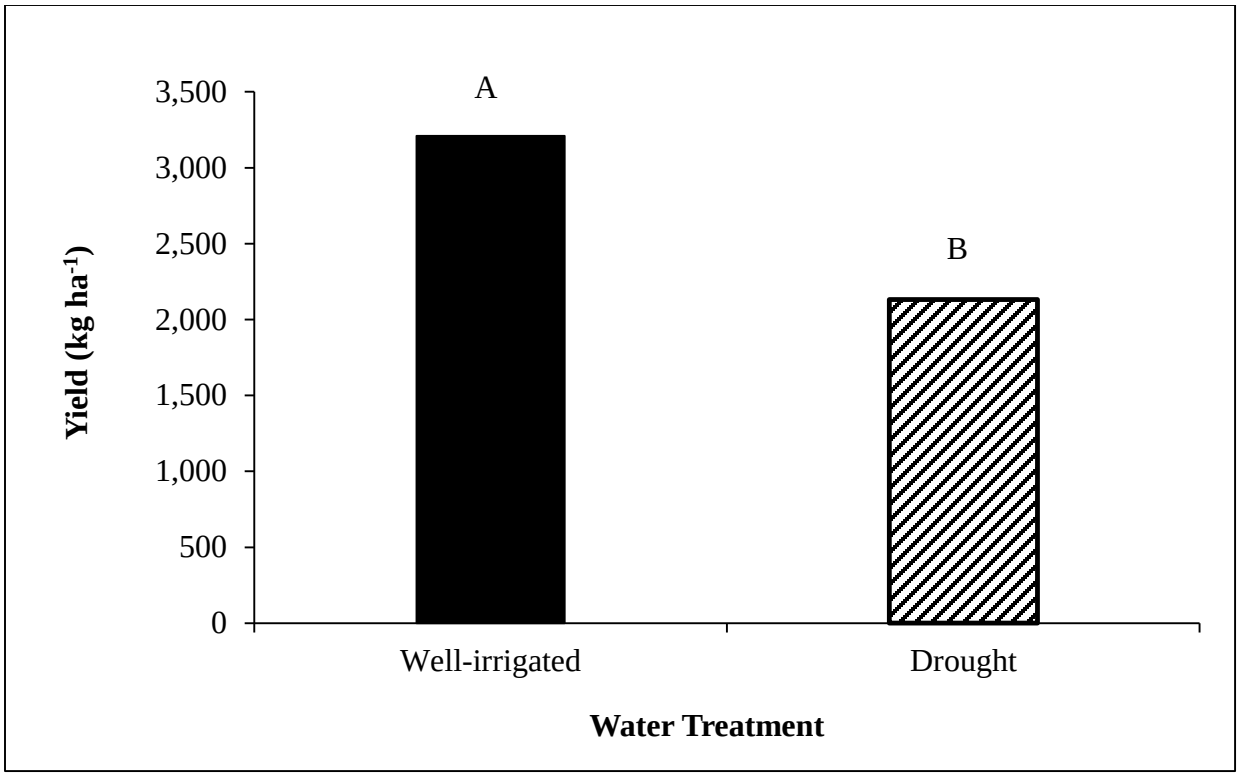

Figure 2_22 Soybean grain yield for well-irrigated and drought treatments across genotypes (genotype × water treatment interaction, NS) in Fayetteville 2012. Different letters above the bars denote significant differences (P≤0.05) as determined by an LSD.

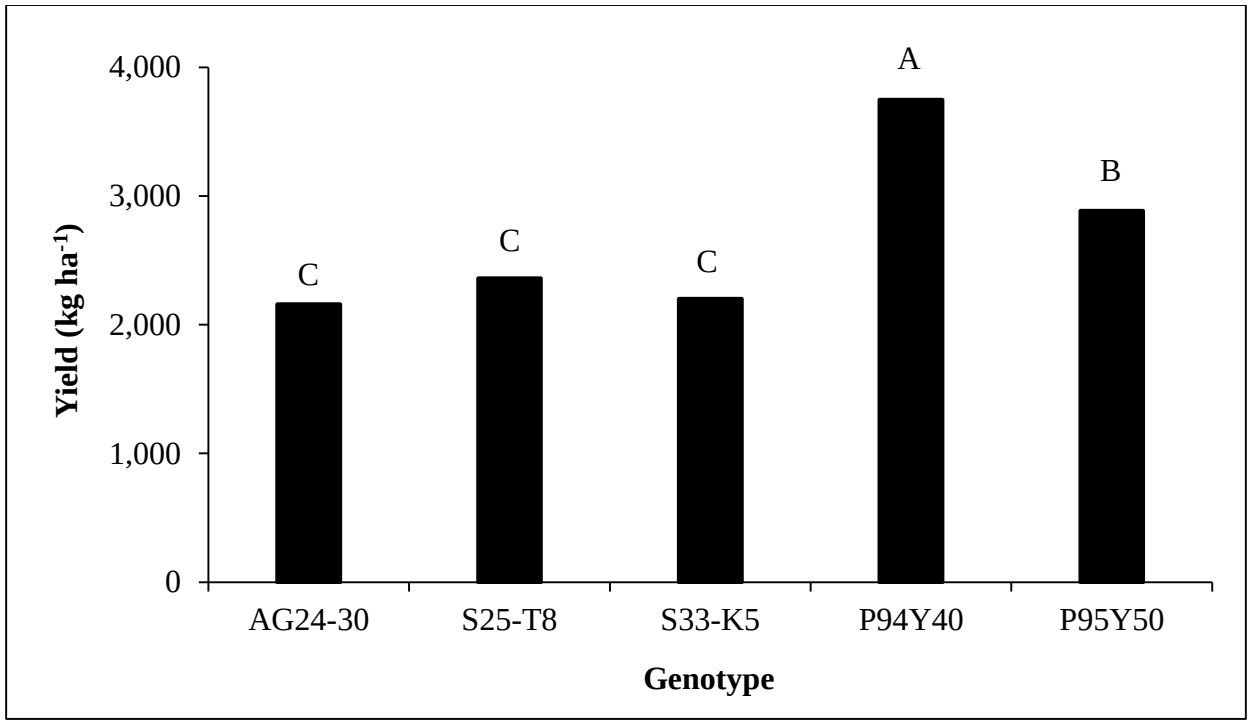

Figure 2_23 Grain yields versus genotype, averaged over water treatment (genotype × water treatment interaction, NS) in Fayetteville 2012. Different letters above the bars denote significant differences (P≤0.05) as determined by an LSD.

Table 2_24 ANOVA for grain yield associated with irrigation treatment, genotype and their interaction in Fayetteville 2013.

Yield (kg ha^{-1})

Source	DF	Mean Square	F Value	Pr > F	Adj. R^2
Rep	4	248670	1.09	0.3771	
Irri†	1	12374644	63.08	<.0001	
Rep (Irr), Err_a	4	196178	0.86	0.4972	0.85
Geno	4	4990339	21.94	<.0001	
Irri*Geno	4	1022978	4.50	0.0056	

† The effect of irrigation was tested using Rep (Irr) as the error term.

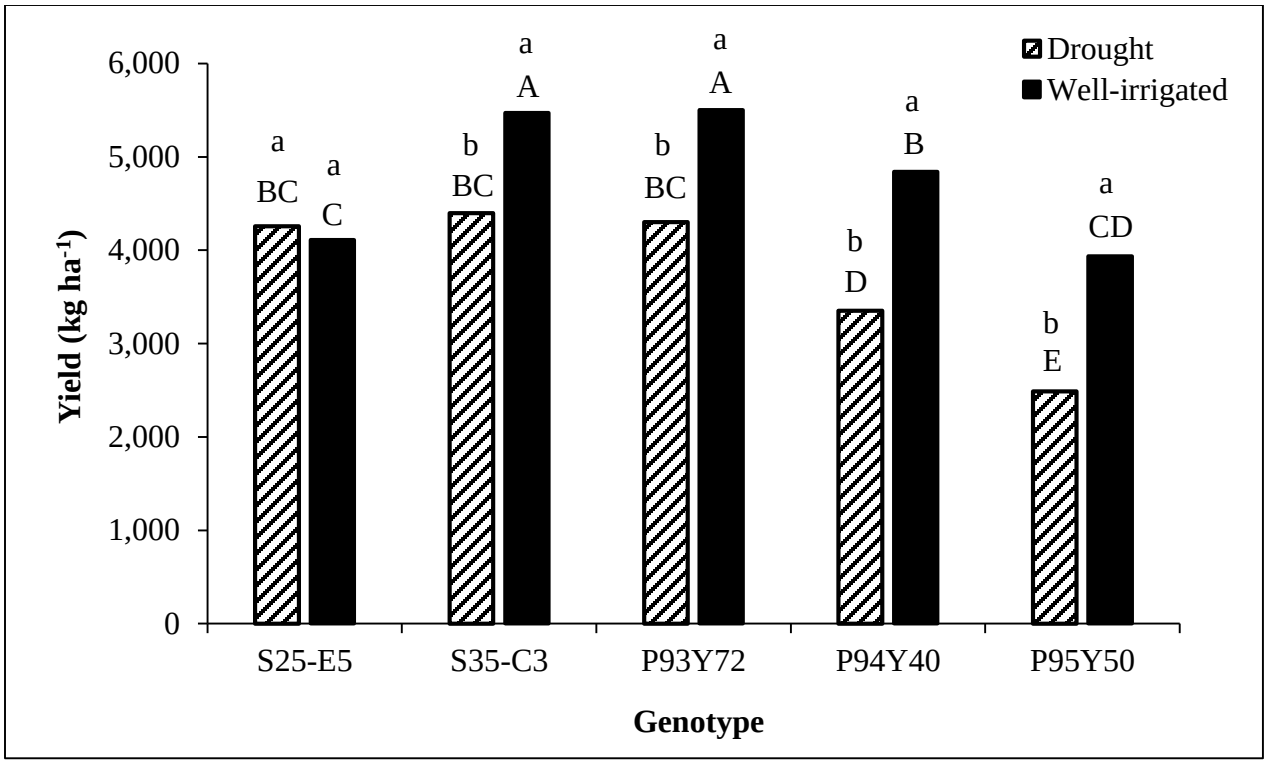

Figure 2_24 Grain yields versus genotype in Fayetteville 2013. Different capital letters above each bar denote significant differences (P≤0.05) among genotypes within a water treatment as determined by an LSD. Different lower case letters above bars represent significant differences (P≤0.05) within a genotype between water treatments as determined by an LSD.

Table 2_25 ANOVA for grain yield associated with irrigation treatment and genotype, but not with their interaction in Fayetteville 2014.

Yield (kg ha^{-1})

Source	DF	Mean Square	F Value	Pr > F	Adj. R^2
Rep	4	20997	0.06	0.9930	
Irri†	1	7728270	12.82	<.0001	
Rep (Irr), Err_a	4	602770	1.73	0.1695	0.62
Geno	4	935410	2.68	0.0500	
Irri*Geno	4	815157	2.33	0.0776	

† The effect of irrigation was tested using Rep (Irr) as the error term.

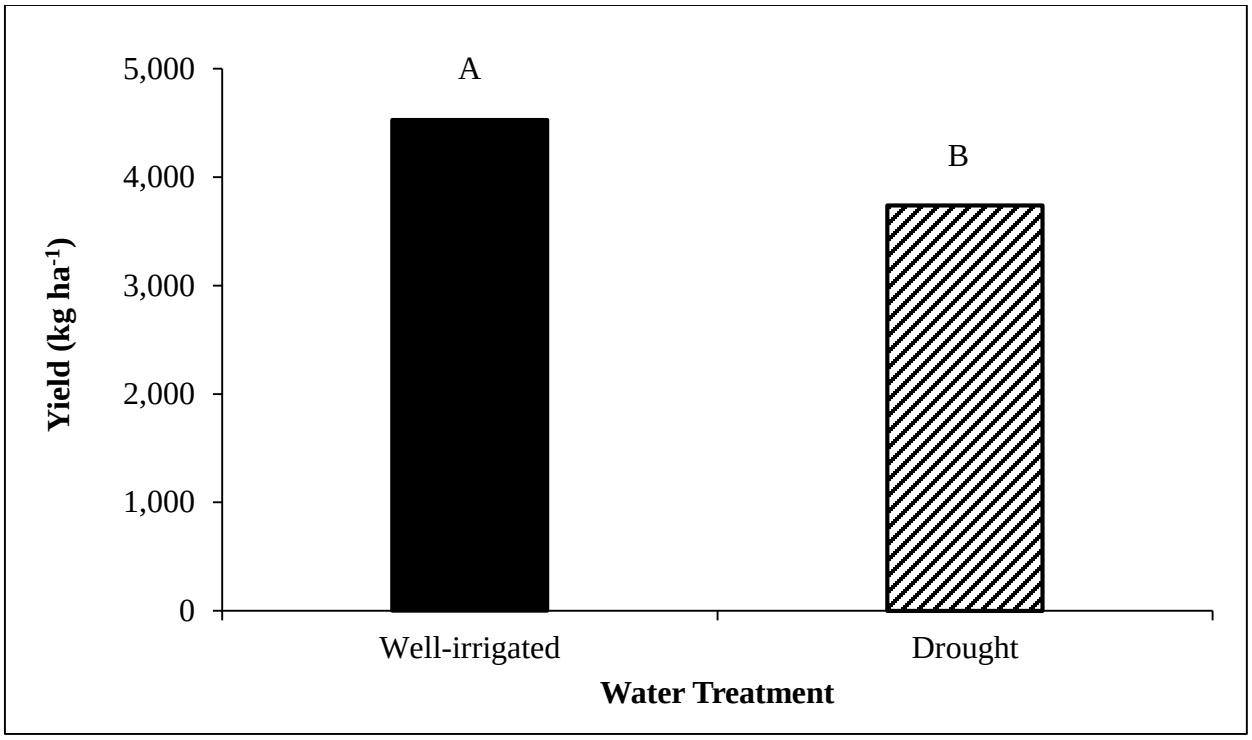

Figure 2_25 Soybean grain yield for well-irrigated and drought treatments averaged over genotypes (genotype × water treatment interaction, NS) in Fayetteville 2014. Different letters above the bars denote significant differences ($P \leq 0.05$) as determined by an LSD.

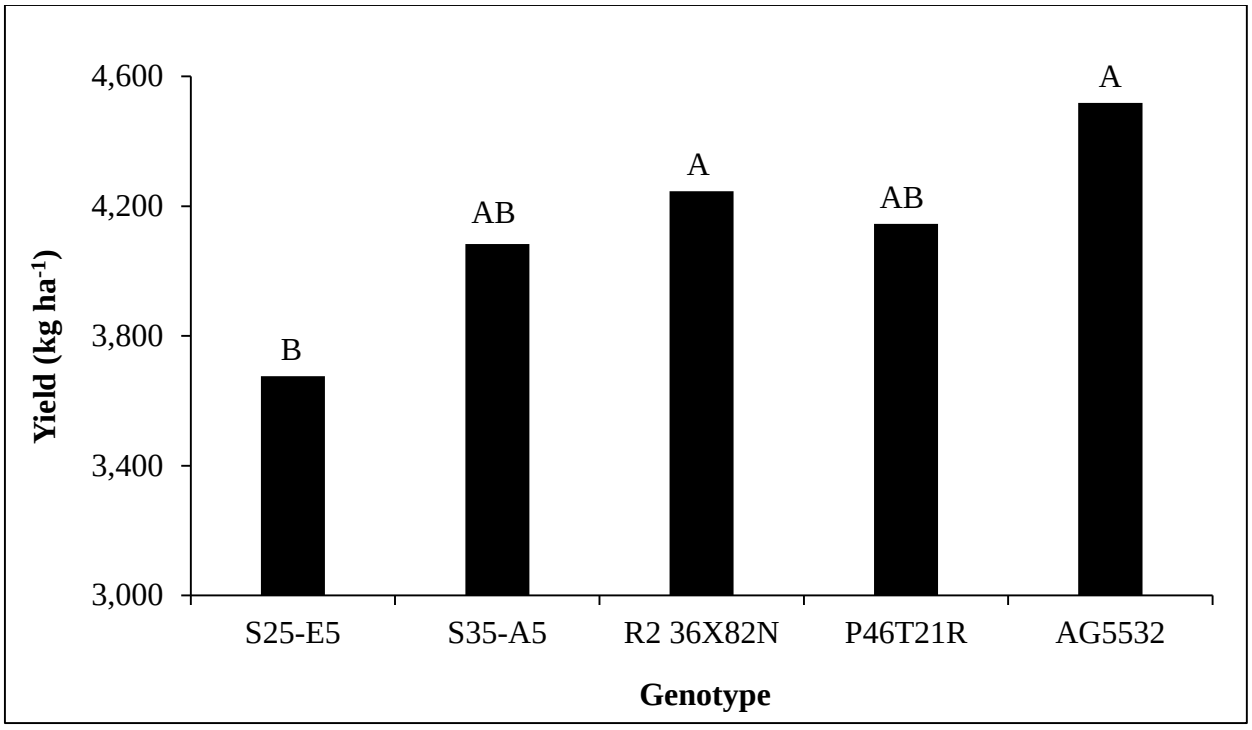

Figure 2_26 Grain yields versus genotype averaged over irrigation (genotype × water treatment interaction, NS) in Fayetteville 2014. Different letters above the bars denote significant differences (P≤0.05) as determined by an LSD.

Discussion

G_DGCI decreased with increasing leaf N concentration for all years. The two main factors, irrigation treatments and genotypes did not show any differences in the response of G_DGCI to leaf N concentration in all 3 years. G_DGCI increased with increasing leaf N concentration ranging from 1.5 to 4.5%. At leaf N concentration greater than 4.5%, there was a slight decline in G_DGCI. Likewise, aerial DGCI increased with increasing leaf N concentration, but over a wider range of leaf N from 1.5 to 5%. Over 5% of leaf N concentration, aerial DGCI also slightly decreased. However, aerial images were able to separate the difference among genotypes and irrigation treatments for leaf N concentration in 2013. The results indicated that the aerial DGCI method had advantages compared to ground DGCI measurements.

The measurements of aerial DGCI and G_DGCI generally followed the same trends (refer to **Appendix**—**Table A4** to **A6**, **Figure A4** to **A6**) G_DGCI and aerial DGCI decreased with increasing DAR5 as well as with est_HI. These responses were similar to the decrease in leaf N concentration versus DAR5 and est_HI, which are indicative of N remobilization from leaves to seed causing leaf yellowing. However, aerial DGCI identified lower aerial DGCI values for the DR treatment than for the WW treatment at any given DAR5 or est_HI value for all years. In contrast, G_DGCI versus DAR5 or est_HI were not affected by water treatments for the 3 years. Therefore, aerial DGCI measurements have advantages over G_DGCI measurements for identifying effects of drought. The reason for the greater sensitivity of aerial DGCI might be that aerial images covered a larger area than ground images so that aerial DGCI may be more representative than G_DGCI. Another reason could be the angle differences when images were taken. Ground images were taken at an oblique angle with the canopy, but the aerial images were

taken vertically above the top of the canopy, which may allow a better assessment of leaf senescence through different strata in the canopy.

Ground imaging measurements covered about 1 m^2 of the top portion of the canopy for each plot whereas aerial images covered a large number of plots each measurement date. Thus, ground imaging was time-consuming. However, aerial image measurements were highly dependent on weather conditions and required training for flying. Because aerial images discriminated the difference of greenness between water treatments and among genotypes, this method ensures the possibility for characterizing soybean genotypes that senesce slowly and are less affected by drought stress. The results indicated that aerial DGCI measurements has the promise to identify drought tolerance traits of soybean.

The results in the present study are comparable to previous studies. Rorie et al. (2011a; 2011b) reported a close association between DGCI and leaf N concentration in corn that reached a plateau at high leaf N concentration. Hoyos-Villegas et al. (2014) tested the response of DGCI in soybean to drought by using rooting barriers placed at different depths and found that DGCI values declined with a rooting barrier at 0.3 m compared with the control treatment. Hastened senescence with increased drought conditions (due to shallow rooting) are similar to the results from aerial DGCI in this study. Normalized difference vegetation index (NDVI), as an indicator of drought, was also able to differentiate the developmental stages during the year with early senescence in soybean (Hoyos-villegas and Fritschi, 2013). NDVI increased with the increasing vegetation water content during the vegetative stages of soybean, indicating the relationship between NDVI and greenness/senescence (Jackson et al., 2004), which was similar with the results in this study.

Results from this study suggest that aerial imaging technology for soybean canopy could be used in a breeding program to differentiate different soybean genotypes and identify lines that senesce slowly so that promising genotypes can be crossed with elite lines. This technology also opens the possibility of identifying QTL and genes associated with slow senescence under drought. Developing drought tolerant crops will allow plants to have high water use efficiency, high yield resulting in improved profitability, and will have the potential to improve crop performance under water-limited conditions.

Literature Cited

Aber, J.S., and S.W. Aber. 2002. Unmanned small-format aerial photography from kites for acquiring large-scale, high-resolution, multiview-angle imagery. In: The International Archives of the Photogrammetry, Remote Sensing and Spatial Information Sciences, Pecora 15/Land Satellite Information IV/ISPRS Commission I/FIEOS, Denver, CO, USA.

Board, J.E., and C.S. Kahlon. 2011. Soybean yield formation: what controls it and how it can be improved. p. 1-36. In: (eds. A. Hany, El-Shemy) Soybean Physiology and Biochemistry, InTech, doi: 10.5772/17596. http://www.intechopen.com/books/soybean-physiology-and-biochemistry/soybean-yield-formation-what-controls-it-and-how-it-can-be-improved (accessed 31 May 2016).

Boike, J., and K. Yoshikawa. 2003. Mapping of periglacial geomorphology using kite/balloon aerial photography. Permafrost Periglac. 14:81-85.

Durand, J.L., J.E. Sheehy, and F.R. Minchin. 1987. Nitrogenase activity, photosynthesis and nodule water potential in soyabean plants experiencing water deprivation. J. Exp. Bot. 38:311-321.

FAO. 2015. Food and Agriculture Organization of the United Nations Statistics Division. http://faostat3.fao.org/home/E (accessed 30 Jul. 2015).

Fehr, W.R., and C.E. Caviness. 1977. Stages of soybean development. Cooperative Extension Service, Agriculture and Home Economics Experiment Station, Iowa State University, Ames, Iowa.

French, A.N., T.J. Schmugge, and W.P. Kustas. 2002. Discrimination of senescent vegetation using thermal emissivity contrast. Remote Sens. Environ. 74:249-254.

Godfray, H.C.J., J.R. Beddington, I.R. Crute, L. Haddad, D. Lawrence, J.F. Muir, J. Pretty, S. Robinson, S.M. Thomas, and C. Toulmin. 2010. Food security: The challenge of feeding 9 billion people. Science 327:812-818.

Handcock, R.N., A. Gillespie, K.A. Cherkauer, J.E. Kay, S.J. Burges, and S.K. Kampf. 2006. Accuracy and uncertainty of thermal-infrared remote sensing of stream temperatures at multiple spatial scales. Remote Sens. Environ. 100:427–440.

Hoyos-villegas, V., J.H. Houx, S.K. Singh, and F.B. Fritschi. 2014. Ground-based digital imaging as a tool to assess soybean growth and yield. Crop Sci. 54:1756-1768.

Hoyos-villegas, V., and F.B. Fritschi. 2013. Relationships among vegetation indices derived from aerial photographs and soybean growth and yield. Crop Sci. 53:2631-2642.

Jackson, T.J., D. Chen, M. Cosh, F. Li, M. Anderson, C. Walthall, P. Doriaswamy, E.R. Hunt. 2004. Vegetation water content mapping using landsat data derived normalized difference water index for corn and soybeans. Remote Sens. Environ. 92:475-482.

Jones, H.G., R. Serraj, B.R. Loveys, L.Z. Xiong, A. Wheaton, and A.H. Price. 2009. Thermal infrared imaging of crop canopies for the remote diagnosis and quantification of plant responses to water stress in the field. Funct. Plant Biol. 36:978-989.

King, C.A., and L.C. Purcell. 2006. Genotypic variation for shoot N concentration and response to water deficits in soybean. Crop Sci. 46:2396-2402.

Mastrodomenico, A.T., and L.C. Purcell. 2012. Soybean nitrogen fixation and nitrogen remobilization during reproductive development. Crop Sci. 52:1281-1289.

Miyamoto, M., K. Yoshino, T. Nagano, T. Ishida, and Y. Sato. 2004. Use of balloon aerial photography for classification of Kushiro wetland vegetation, northeastern Japan. Wetlands 24:701-710.

NASS, 2015. United States Department of Agriculture, National Agricultural Statistics Service. http://quickstats.nass.usda.gov/ (accessed 16 Sep. 2015).

NCDC, 2016. National Climatic Data Center, National Oceanic and Atmospheric Administration. https://www.ncdc.noaa.gov/data-access/land-based-station-data/land-baseddatasets /climate-normals/1981-2010-normals-data (accessed 6 Apr. 2016).

Primicerio, J., S.F.D. Gennaro, E. Fiorillo, L. Genesio, E. Lugato, A. Matese, and F.P. Vaccari. 2012. A flexible unmanned aerial vehicle for precision agriculture. Precision Agric. 13:517-523.

Purcell, L.C. 2000. Soybean canopy coverage and light interception measurements using digital imagery. Crop Sci. 40:834-837.

Purcell, L.C. 2009. Physiological responses of N_2 fixation to drought and selecting genotypes for improved N_2 fixation. p. 211-238. In: (eds. H.B. Krishnan and D.W. Emerich) Nitrogen Fixation in Crop Production. Agronomy Monograph. 52. ASA CSSA SSSA, Madison, WI.

Purcell, L.C., J.T. Edwards, and K.R. Brye. 2007. Soybean yield and biomass responses to cumulative transpiration: Questioning widely held beliefs. Field Crops Res. 101:10-18.

Purcell, L.C., and C.A. King. 1996. Drought and nitrogen source effects on nitrogen nutrition, seed growth, and yield in soybean. J. Plant Nutr. 196:969-993.

Ray, D.K., N.D. Mueller, P.C. West, and J.A. Foley. 2013. Yield trends are insufficient to double global crop production by 2050. PLOS ONE 8: e66428. doi: 10.1371/journal.pone. 0066428.

Rorie, R.L., L.C. Purcell, D.E. Karcher, and C.A. King. 2011a. The assessment of leaf nitrogen in corn from digital images. Crop Sci. 51:2174-2180.

Rorie, R.L., L.C. Purcell, M. Mozaffari, D.E. Karcher, C.A. King, M.C. Marsh, and D.E. Longer. 2011b. Association of "greenness" in corn with yield and leaf nitrogen concentration. Agron. J. 103:529-535.

Royal Society. 2009. Reaping the benefits: science and the sustainable intensification of global agriculture. Royal Society, London. https://royalsociety.org/~/media/Royal_Society_Content/policy/publications/2009/4294967719.pdf (accessed 29 May 2016).

Rundquist, D.C., and S.A. Samson. UNL. A guide to the practical use of aerial color-infrared photography in agriculture. Educational Circular 8. University of Nebraska-Lincoln. http://www.casde.unl.edu/activities/cir-uses/ (accessed 17 Sep. 2015).

Sinclair, T.R., and C.T. Dewit. 1976. Analysis of the carbon and nitrogen limitations to soybean yield. Agron. J. 68:319-324.

USDA. 2012. Economic Research Service: Soybeans & oil crops, background. United States Department of Agriculture. http://www.ers.usda.gov/topics/crops/soybeans-oil-crops/background.aspx (updated 10 Oct. 2012).

USDA. 2014a. Soybean-irrigated, crop acreage, yield, and production, by county, 2013-2014. United States Department of Agriculture, National Agricultural Statistics Service, Delta Regional Office: Arkansas. http://www.nass.usda.gov/Statistics_by_State/Arkansas/Publications/County_Estimates/14_AR_soybean_irrigated.pdf (accessed 17 Sep. 2015).

USDA. 2014b. Soybean-nonirrigated, crop acreage, yield, and production, by county, 2013-2014. United States Department of Agriculture, National Agricultural Statistics Service, Delta Regional Office: Arkansas. http://www.nass.usda.gov/Statistics_by_State/Arkansas/Publications/County_Estimates/14_AR_soybean_nonirrigated.pdf (accessed 17 Sep. 2015).

USDA. 2015. Crop production 2014 summary. United States Department of Agriculture. http://www.usda.gov/nass/PUBS/TODAYRPT/cropan15.pdf (updated 5 Feb. 2015).

USSEC. 2008. How the global oilseed and grain trade works. US Soybean Export Council. Soyatech, LLC, Southwest Harbor, Maine, US.

CHAPTER III

EVALUATION OF SOYBEAN RESPONSE TO DROUGHT USING INFRARED THERMOGRAPHY AND CARBON AND OXYGEN ISOTOPIC METHODS

Abstract

Drought stress limits crop growth and yield in soybean, but there are relatively few tools available to assess the ability of different genotypes to tolerate drought. Aerial infrared image analysis, carbon isotope discrimination ($\Delta^{13}C$) and oxygen isotope composition ($\delta^{18}O$) were evaluated as potential tools for identifying drought tolerance in soybean. Drought effects were evaluated during reproductive stages of soybean in an experiment with ten soybean genotypes including five slow- and five fast-wilting genotypes that were derived from a population of Benning×PI416937. The experiment was in the field with a line source irrigation system that included full irrigation and two deficit-irrigation treatments with increasing severity, deficit irrigation 1 and deficit irrigation 2. When the canopy was completely closed, relative canopy temperature was determined from infrared images taken with aerial platforms 50 to 75 m above the experiment. $\Delta^{13}C$ and $\delta^{18}O$ were measured from soybean leaves ($\Delta^{13}C$ only) sampled at late R5 and from seed (both $\Delta^{13}C$ and $\delta^{18}O$) at maturity as surrogate measurements for water use efficiency (WUE) and transpiration, respectively. The $\Delta^{13}C$ values from leaf and seed generally decreased with decreasing water availability (i.e., higher WUE). In contrast, as water availability decreased, the $\delta^{18}O$ values and relative canopy temperature generally increased. Moreover, slow-wilting soybean genotypes generally had lower $\Delta^{13}C$, $\delta^{18}O$ and canopy temperature compared to fast-wilting genotypes. However, $\delta^{18}O$ values were not consistent over years. The results indicate that the determination of $\Delta^{13}C$, and canopy temperature were promising tools for rapid characterization of drought-related traits in soybean.

Introduction

Soybean serves as one of the most important food sources globally (FAO, 2015). The United States has the largest soybean production and export in the world (USDA, 2015). Greater than 90% of the U.S. oil seed is soybean (USDA, 2012). Hence, soybean is a main crop supporting U.S. agricultural production. Based on the USDA National Agricultural Statistics Service (NASS), in last 10 years from 2005 to 2014 the average soybean grain yields in the U.S. and Arkansas were 2892 kg ha^{-1} (43 bu ac^{-1}), and 2636 kg ha^{-1} (39.2 bu ac^{-1}), respectively (NASS, 2015). Moreover, Arkansas soybean grain yields under irrigated and non-irrigated management in last 10 years averaged 2892 kg ha^{-1} (43 bu ac^{-1}) and 1809 kg ha^{-1} (26.9 bu ac^{-1}) (NASS, 2015). As shown for Arkansas, irrigation can ameliorate drought-induced yield losses, but more than 90% of the agricultural area in the U.S. is non-irrigated (Board and Kahlon, 2011). In addition, agriculture requires more than two-thirds of the global freshwater, and the demand for freshwater is predicted to increase 25% by 2030 (UN Global Compact, 2015) due to the predicted population increase worldwide (Royal Society, 2009). The ability to produce more grain in the future with less water available for agriculture remains a daunting and elusive goal.

Drought stress is considered one of the most severe abiotic problems limiting soybean yield (Heatherly and Elmore, 1986). Drought during seedfill causes premature senescence resulting in a shortened seedfill period (de Souza et al., 1997). One trait of great interest that may provide soybean with drought tolerance is slow-wilting under water-limited conditions. Slow-wilting genotypes had the least yield loss under drought stress (Sloane et al., 1990) because they conserve soil moisture when soil moisture is plentiful, which can then be used during a drought (King et al., 2009; Ries et al., 2012). The first symptom observed in soybean caused by drought is canopy wilting (King et al., 2009). Soybean genotypes differ in the beginning and severity of wilting to

drought stress (King et al., 2009; Sloane et al., 1990). Canopy wilting has been used to select soybean genotypes with drought tolerance (Abdel-Haleem et al., 2012; Charlson et al., 2009; King et al., 2009). The severity of canopy wilting corresponds to the rate of transpiration which is related to the canopy temperature (Jones et al., 2009). Hence, measurement of canopy temperature using aerial infrared photography may be used to study water relations of plants (Jones et al., 2009).

There are numerous articles in which carbon isotope discrimination was used to study water relations of plants (Araus et al., 1998; Condon et al., 1990; Condon et al., 2004; O'Leary, 1988). Carbon isotope discrimination is negatively related to water use efficiency (Farquhar and Richards, 1984; Condon et al., 1990). Slow wilting soybean genotypes are hypothesized to have high water use efficiency compared to fast wilting genotypes because slow wilting genotypes can conserve soil moisture when water is plentiful and continue transpiration when drought occurs.

Farquhar et al. (1982) described a simple equation to describe carbon isotope discrimination in C3 plants:

$$\Delta^{13}C = a + (b - a)\, C_i/C_a \qquad [8]$$

where a is the discrimination for diffusion of $^{12}CO_2$ and $^{13}CO_2$ through stomata (~4.4‰), and b is the discrimination regulated by RuBisCo during carboxylation of CO_2 into the initial photosynthetic products (~27‰). Ci/Ca refers to the ratio of CO_2 in the leaf and the atmosphere, respectively, as described in Eq. [4] and Eq. [5] in Chapter I. Thus, Eq. [8] can be simplified by substituting terms a and b with 4.4 (‰) and 27 (‰):

$$\Delta^{13}C\ (‰) \approx 4.4 + 22.6\, C_i/C_a \qquad [9]$$

$\Delta^{13}C$ is positively related to C_i/C_a whereas WUE at leaf level is negatively related to C_i/C_a (Eq. [5] in Chapter I). Therefore, $\Delta^{13}C$ and WUE are inversely related.

Oxygen isotope composition of plant tissue is often used to study the isotopic changes in leaf water or dry matter due to transpiration and photosynthesis. Oxygen isotope composition in either leaf water or leaf dry biomass is positively related to both transpiration and stomatal conductance (Madhava et al., 2010).

A negative correlation between carbon isotope discrimination and oxygen isotope composition has been reported in several articles (Barbour and Farquhar, 2000; Cernusak et al., 2003; Xu et al., 2000). The combination of carbon isotope discrimination as a surrogate for water use efficiency and oxygen isotope composition as a surrogate for transpiration potentially makes a powerful tool for identifying soybean genotypes with high water use efficiency that also have relatively high transpiration rates.

The primary hypothesis of this research is that slow-wilting genotypes will have a greater WUE due to the conservation of soil moisture when soil water is plentiful resulting in a decrease in both $\Delta^{13}C$ and $\delta^{18}O$. A corollary of this hypothesis is that canopy temperature will be lower in slow-wilting genotypes under drought stress because of continued transpiration of soil moisture that is conserved prior to drought. The objective of this study was to evaluate the differences in $\Delta^{13}C$, $\delta^{18}O$, and infrared temperature under well-watered and drought conditions among genotypes that were known to differ in how quickly they wilt under drought conditions.

Materials and Methods

A field experiment was conducted at the Main Experiment Station in Fayetteville, Arkansas (36º05' N, 94º10' W) on a Captina silt loam soil (Fine-silty, siliceous, active, mesic Typic Fragiudults) in 2012, 2013, and 2014. The experimental design was a split-plot arrangement of treatments with four replications. Each replication included three different water treatments: full irrigation and two deficit-irrigation treatments with increasing severity, deficit irrigation 1 and deficit irrigation 2. Ten different soybean genotypes (**Table 3_1**) were selected from the cross between 'Benning', which is a US elite cultivar with fast canopy wilting, and PI 416937, which is a Japanese genotype with slow canopy wilting (Abdel-Haleem et al., 2012).

Soybean was planted at 2 June 2012, 8 June 2013, and 17 June 2014. In 2012, plots consisted of four rows that were 6.1 m in length with 0.46 m between rows. In 2013 and 2014, plots consisted of seven rows that were 6.1 m in length with 0.19 m between rows. The narrower row spacing in 2013 and 2014 ensured quick canopy closure. The seeding density was 30 seed m^{-2} in all 3 years. An overhead sprinkler irrigation system was installed in the middle of the field. Full irrigation, deficit irrigation 1 and deficit irrigation 2 plots were symmetrically arranged on both sides of the central irrigation pipe. The closer the plots were to the pipe, the more water the plots received, and vice versa. An irrigation scheduling program (Purcell et al, 2007) was used to estimate soil-water deficits, and irrigation was applied when the estimated soil-water deficit of the fully irrigated treatment reached 30 mm. A total of 84 rain gauges were placed in the field to record the irrigation amount and rainfall. The total irrigation amount per rain gauge for each water treatment for the growing season was calculated based on the rain gauge amounts. The percent of deficit for individual water treatment was calculated using Eq [10]

Table 3_1 Genotypes and wilting types evaluated in 2012, 2013 and 2014 in Fayetteville, AR.

Genotype	Wilting Type
G00BP-84	Fast
G00BP-110	Fast
G00BP-200	Fast
G00BP-223	Fast
G00BP-245	Fast
G00BP-53	Slow
G00BP-60	Slow
G00BP-169	Slow
G00BP-214	Slow
G00BP-216	Slow

Deficit (%) = 100 – [(Irrigation amount/rain gauge for individual water treatment + rainfall) × 100 / (Irrigation amount/rain gauge for full irrigation + rainfall)] [10]

Approximately, 1 week after emergence, stand counts were made in each plot by counting the number of plants in 1 m of two central rows and averaging the two measurements. Light interception was measured twice a week after emergence until canopy closure by analyzing digital images of the canopy (Purcell, 2000). After canopy closure, aerial infrared images were taken once a week using a kite or a tethered balloon as an aerial platform at heights ranging from 50 to 75 m. At late R5, three leaves were sampled from three different plants in each plot for carbon isotope discrimination analysis. The three leaves were the third fully-developed leaf from the top of the plant. At maturity, all the plots were end trimmed, and the central five rows were harvested. Yield was adjusted to moisture content of 130 g kg^{-1}, and average seed mass was determined from a sample of 100 seed.

Leaf samples were coarse ground through a 6 mm sieve using a Wiley mill grinder. A 0.75 g sample of coarse-ground material was transferred to a 15-ml centrifuge tube (VWR cat. No. 89039-666) containing two 9-mm stainless steel beads. Samples were shaken for 10 min at 1500 rpm with a 2010 Geno Grinder (SPEX SamplePre). A subsample of approximately 25 seed were finely ground in a coffee grinder. A 250 mg subsample was shaken at 1500 rpm for 1 min with the Geno Grinder.

Between 2 and 5 mg of the fine leaf and seed sample was weighed and analyzed by the UC Davis Stable Isotope Facility for carbon isotope composition (δ_p). The value of δ_p is the deviation of carbon isotopic abundance in plant tissue from the international standard V-PDB, (Vienna PeeDee Belemnite). Carbon isotope discrimination ($\Delta^{13}C$) was then calculated as described by Farquhar et al. (1989):

$$\Delta^{13}C = (\delta_a - \delta_p)/(\delta_p + 1) \quad [14]$$

where δ_a is the deviation of carbon isotopic composition for the free atmosphere from V-PDB which is about -8‰ (Farquhar et al., 1989).

Between 0.4 and 0.8 mg of ground soybean seed was also weighed and analyzed for oxygen isotopic composition ($\delta^{18}O$) (UC Davis Stable Isotope Facility), which is the deviation of oxygen isotopic abundance in plant tissue from the international standard, Vienna-Standard Mean Oceanic Water (VSMOW) (Rohling, 2007; Gonfiantini, 1984).

$$\delta^{18}O = (R_p - R_{st})/R_{st} = R_p/R_{st} - 1 \quad [15]$$

In Eq [15], R_p and R_{st} are the oxygen isotopic ratio ($^{18}O/^{16}O$) in the plant sample and the standard, respectively. The $\delta^{18}O$ values were directly used in the statistically analysis.

The infrared camera used in this research was the FLIR Tau 640 (FLIR, Goleta CA), which detects wavelength from 8 to 14 μm, and has a 640 × 480 National Television System Committee (NTSC) video output. The lens was either 25 mm (2012) or 13 mm (2013 and 2014) with an aperture of f1.1, with a 640 × 480 resolution, and a pixel size of 17 microns. The Tau 640 is small and light weight (110 g). Sensitivity is most often measured by a parameter called Noise Equivalent Differential Temperature (NEdT). The Tau 640 has a high NEdT which is less than 50 mK at f/1.0 with FLIR proprietary noise reduction. This means that sequential differences in shades of gray differ by approximately 0.05 °C (i.e., 50 mK). There are 256 different shades of gray (0 to 255) that the camera distinguishes from white to black. Therefore, there is a range of approximate 12.8 °C (256 × 0.05 °C) at specific focal plane temperatures.

A 25 mm lens with a narrow field of view (FOV) of 25° × 20° was used in 2012. The width of the linesource experiment was approximately 26 m. Therefore, the camera had to be lifted

around 60 m in order to capture the width of the experiment if perfectly aligned. In 2013 and 2014, a 13 mm lens with a wide FOV of 69° × 56° was used so that the camera only needed to be lifted in 20 m if perfectly aligned. The camera was powered by a 7.4v, 2s lithium polymer battery with the voltage stepped down to 5v. The analog video stream was recorded using a digital video recorder (www.foxtechfpv.com, model DV02). The infrared camera, battery and recorder were mounted on a picavet (http://www.armadale.org.uk/kitebasic.htm, **Figure 3_1**), which dampened motion of the camera while suspended from the kite or balloon.

Either a tethered balloon or kite was used for taking aerial photographs in this research, depending upon wind conditions. The tethered balloon was approximately 2 m in diameter and was purchased from Southern Balloon (www.southernballoon.com). Helium was used to inflate the balloon. Three dacron (34 kg test weight) strings were fixed onto the balloon, and each of the strings was attached to a roller that allowed string to be released or taken up easily. The balloon was used on calm days with wind speeds 2 m s^{-1} or less. A parafoil kite (www.peterlynn.com) with a surface area of 2 m^2 was used as the aerial platform at wind speeds exceeding 9 m s^{-1}. A Levitation Delta kite (www.intothewind.com) with a 2.74 m span was used at intermediate wind speeds between 2 to 9 m s^{-1}.

After the kite or balloon was about 5 m high, the picavet was attached to the string of the kite or to one string of the balloon, and the camera was turned on. String was then released from the kite or balloon until the camera was approximately 75 m high. The camera was centered above the field and slowly walked down the length of the field. Infrared image data were collected between 10 am to 2 pm once a week when the sky was clear and unobstructed by clouds.

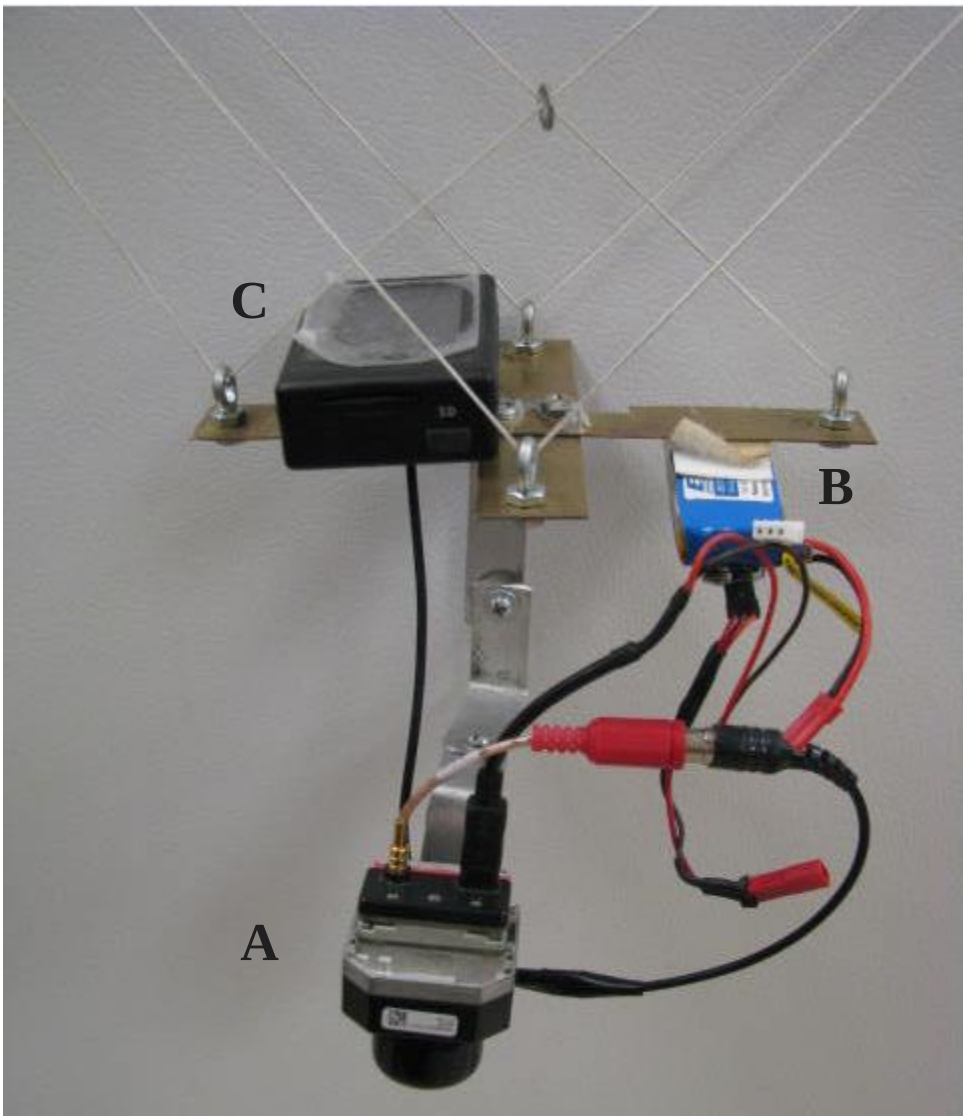

Figure 3_1 Picavet system with infrared camera (A), battery (B) and recorder (C).

Screen captures from the infrared video stream were processed using GIMP 2.8 (http://gimp.org) software. Captured images were rotated in GIMP to align the plots horizontally on the screen. Once the plots in the image were in the horizontal direction, the central five rows of individual seven-row plots were cropped. By selecting "Colors", "Info" functions in sequence a histogram window displayed the distribution of relative temperature values for all pixels in the selected area. The mean value of all the pixels in the selected area was used as the relative canopy temperature. Depending upon the height at which the image was taken, relative canopy temperature measurements for each plot was based upon an average of 6000 to 8000 pixels, which was about half of the total pixels for an individual plot.

Statistical Analysis

Data were analyzed by year and measurement date using analysis of variance (ANOVA) for $\Delta^{13}C$, $\delta^{18}O$, relative canopy temperature, and yield. The effects in the whole model included irrigation, wilting, genotype(wilting), irrigation*wilting, irrigation*genotype(wilting). Fisher's protected LSD ($p \leq 0.05$) was used to separate means. Pearson correlation analysis was used to evaluate relationships among leaf $\Delta^{13}C$, seed $\Delta^{13}C$, $\delta^{18}O$, yield, and relative canopy temperature.

Results

A. Environmental Data and Calculation of Deficit for Different Water Treatments

The environmental conditions on measurement dates including daily maximum and minimum temperature, total solar radiation and soil water deficit for the fully-irrigated treatment are summarized in **Table 3_2**. **Table 3_3** shows the deficit percentage for all three water treatments.

Table 3_2 Environmental conditions on measurement dates for aerial infrared imaging including daily maximum and minimum temperature (T_{max}, T_{min}), total solar radiation and soil water deficit for fully-irrigated treatment.

Date	T_{max} (°C)	T_{min} (°C)	Solar Radiation (MJ m^{-2} d^{-1})	Soil Water Deficit (mm)
08/01/13	31.3	20.2	21.04	30.06
08/30/13	35.2	23.2	19.45	31.07
09/06/13	32.2	13.3	23.38	30.61
08/05/14	31.0	18.0	22.48	32.00
08/06/14	31.0	17.0	23.25	12.00
08/13/14	28.0	11.0	24.99	30.87
08/21/14	33.0	23.0	18.53	30.09
08/22/14	34.0	24.0	18.44	32.00
08/28/14	33.0	18.0	21.92	32.00
09/04/14	32.0	23.0	16.98	11.41
09/09/14	31.0	19.0	18.28	28.70
09/25/14	27.0	8.0	20.51	32.00
10/01/14	23.9	8.9	17.35	32.00

Table 3_3 Irrigation amounts, rainfall, and estimated deficit irrigation amounts for different water treatments from 2012 through 2014.

Year	Irrigation Amount/Rain Gauge (mm)			Rainfall (mm)	Deficit (%)		
	Full	Deficit 1	Deficit 2		Full	Deficit 1	Deficit 2
2012	449	276	136	276	0	24	43
2013	125	85	47	335	0	9	17
2014	114	86	54	237	0	8	17

The estimated deficit percentage ranged from 8% (2014) to 24% (2012) for the deficit 1 treatment, and the deficit 2 treatment ranged from 17% (2014) to 43% (2012).

B. Carbon Isotope Discrimination and Oxygen Isotope Composition

The ANOVA for $\Delta^{13}C$ of soybean leaf and seed and $\delta^{18}O$ of soybean seed are summarized in **Table 3_4**. The estimated $\Delta^{13}C$ and $\delta^{18}O$ values for the main effects of irrigation and wilting are shown in the table as well. In 2012, the $\Delta^{13}C$ analysis of leaf tissue showed significant effects of irrigation and genotype(wilting), while the $\Delta^{13}C$ analysis of seed showed significant effects of irrigation, wilting type, and irrigation*genotype(wilting). Similarly, in 2013 and 2014, the analysis identified more significant effects in seed than in leaf. For the $\delta^{18}O$ of seed, irrigation and genotype(wilting) showed significant effects in 2012, and wilting type and genotype(wilting) were significant in 2013. However, in 2014, none of these effects were significant. Leaf $\Delta^{13}C$ in 2012 and seed $\Delta^{13}C$ in 2013 decreased with increasing drought stress. Seed $\delta^{18}O$ in 2012 increased with decreasing water availability. Slow-wilting genotypes had lower leaf $\Delta^{13}C$ in 2013 and 2014 compared to fast-wilting genotypes.

Figure 3_2 illustrates the genotype (wilting) effect of leaf $\Delta^{13}C$ for each genotype and irrigation in 2012. In 2012, there was relatively large variation of leaf $\Delta^{13}C$ among genotypes. In the slow wilting group, G00BP216 had considerately less leaf $\Delta^{13}C$ than others. Leaf $\Delta^{13}C$ in 2012 decreased with decreased water availability, which is consistent with drought increasing WUE. In 2013 and 2014, leaf $\Delta^{13}C$ was lower for slow-wilting genotypes than fast-wilting (**Table 3_4**), which is consistent with slow-wilting genotypes had higher WUE than fast-wilting genotypes.

Figure 3_3 shows the response of seed $\Delta^{13}C$ in 2012 to the three-way interaction of irrigation and genotype within wilting whereas **Figure 3_4** and **3_5** show the response to the two-way interaction of genotype within wilting for 2013 and 2014. In **Figure 3_3**, seed $\Delta^{13}C$ values

Table 3_4 Analysis of variance (ANOVA) for carbon isotope discrimination ($\Delta^{13}C$) of soybean leaf and seed and oxygen isotope composition ($\delta^{18}O$) of soybean seed from 2012 to 2014 in Fayetteville, AR.

Effects		$\Delta^{13}C$ Analysis of Leaf			$\Delta^{13}C$ Analysis of Seed			$\delta^{18}O$ Analysis of Seed		
		2012	2013	2014	2012	2013	2014	2012	2013	2014
Irri		**	NS	NS	***	**	NS	***	NS	NS
Wilt		NS	*	***	***	NS	***	NS	**	NS
Irri*wilt		NS	NS	NS	NS	NS	NS	NS	NS	NS
Geno(wilt)		***	NS	NS	NS	**	**	*	*	NS
Irri*geno(wilt)		NS	NS	NS	**	NS	NS	NS	NS	NS
Irri	Full	20.6 a	20.4	20.1	20.8 a	20.1 a	20.0	27.9 b	25.2	24.8
	Deficit 1	20.3 a	20.5	20.1	20.5 b	19.8 b	19.9	27.9 b	25.2	24.8
	Deficit 2	19.8 b	20.1	20.1	19.9 c	19.7 b	19.9	28.7 a	25.6	25.1
Wilt	Fast	20.3	20.4 a	20.3 a	20.5 a	19.9	20.2 a	28.3	25.6 a	24.8
	Slow	20.2	20.2 b	20.0 b	20.2 b	19.8	19.7 b	28.1	25.1 b	25.0

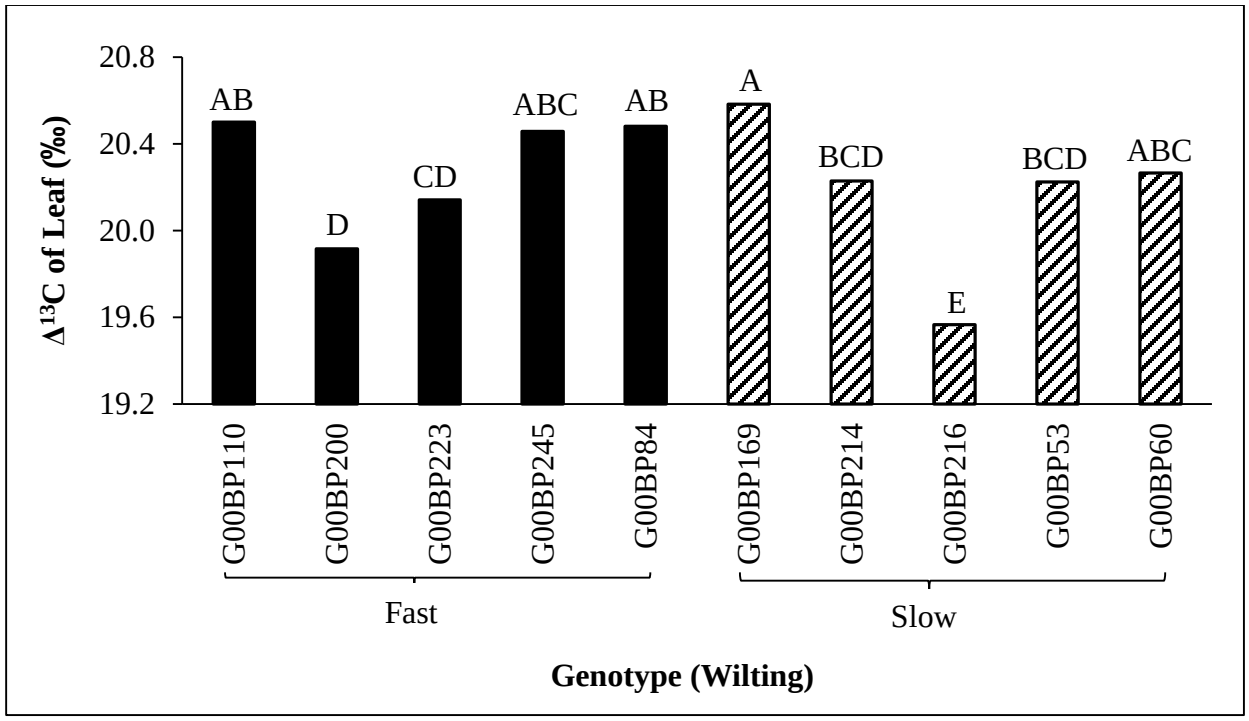

Figure 3_2 The response of carbon isotope discrimination ($\Delta^{13}C$) of leaf for each genotype averaged across water treatments in Fayetteville 2012. Different letters above the bars denote significant differences ($P \leq 0.05$) as determined by an LSD.

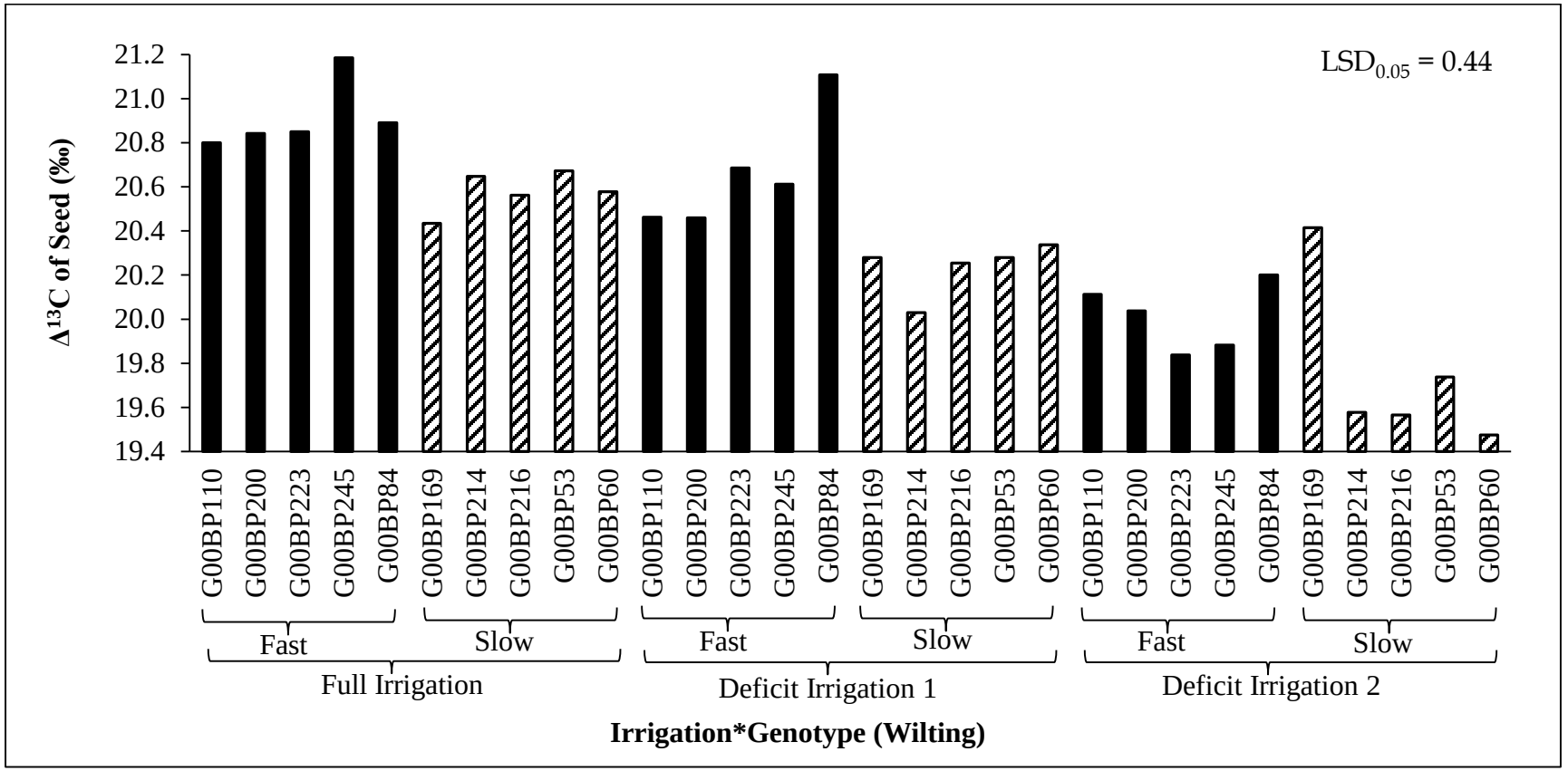

Figure 3_3 The response of carbon isotope discrimination ($\Delta^{13}C$) of seed for each genotype under different water treatments in Fayetteville 2012.

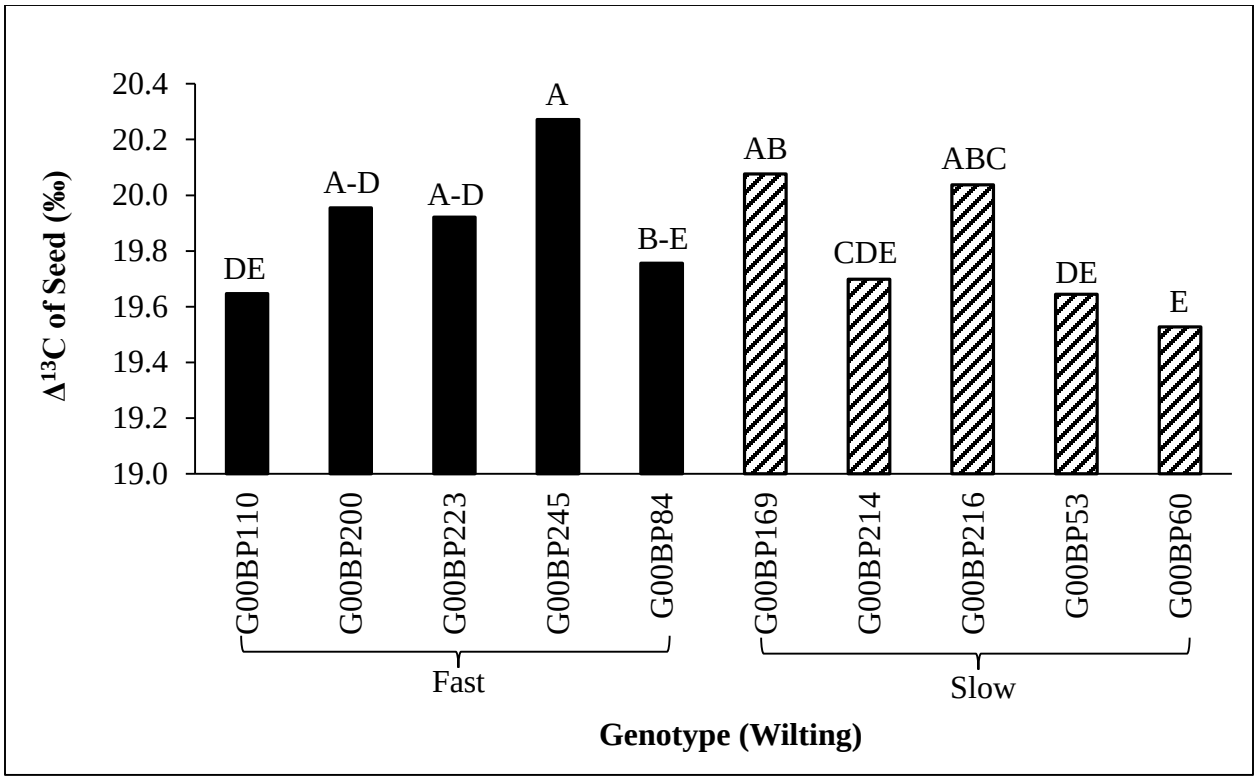

Figure 3_4 The response of carbon isotope discrimination ($\Delta^{13}C$) of seed for each genotype averaged across replications and irrigation treatments in Fayetteville 2013. Different letters above the bars denote significant differences ($P \leq 0.05$) as determined by an LSD.

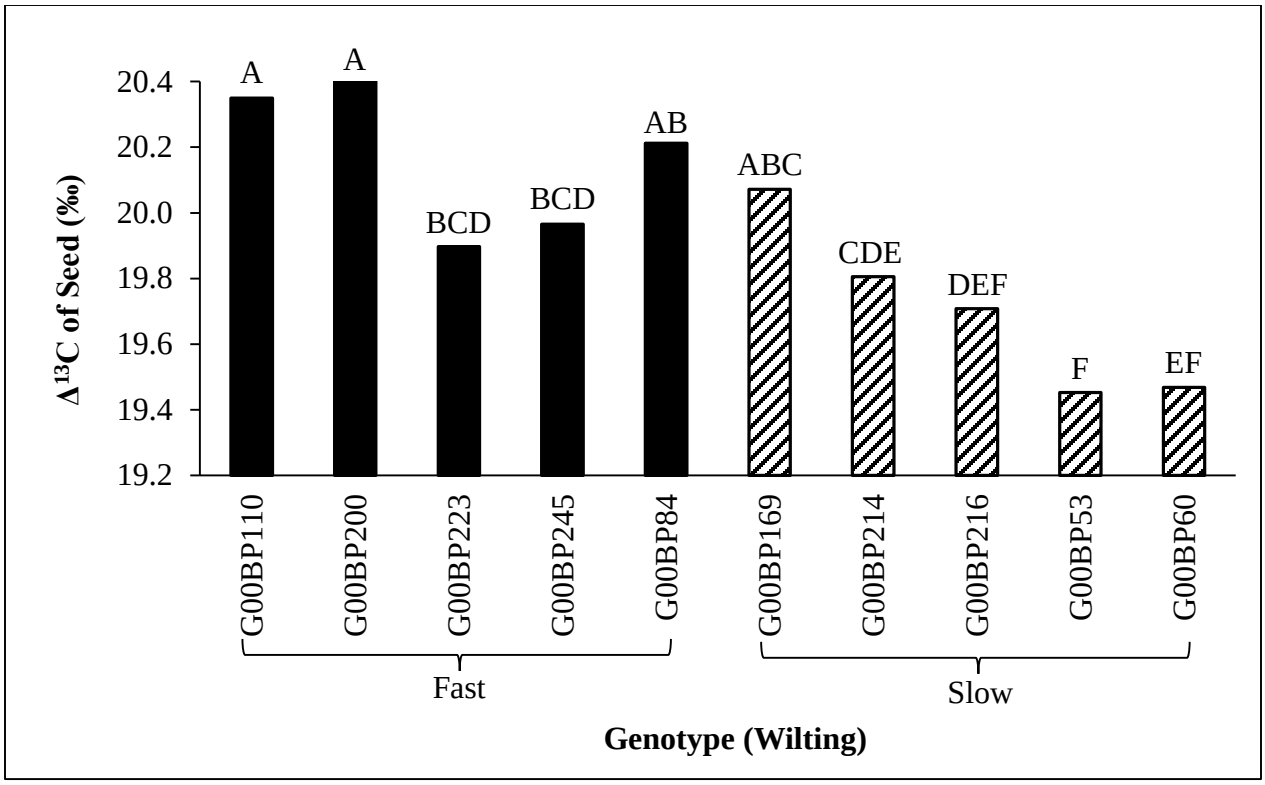

Figure 3_5 The response of carbon isotope discrimination ($\Delta^{13}C$) of seed for each genotype averaged across replications and irrigation treatments in Fayetteville 2014. Different letters above the bars denote significant differences ($P \leq 0.05$) as determined by an LSD.

generally decreased with increasing drought stress, which also indicates that drought increased WUE. Slow-wilting genotypes generally had lower $\Delta^{13}C$ values than fast-wilting genotypes under each water treatment, which is consistent with slow-wilting genotypes having higher WUE than fast-wilting genotypes. In 2013, fast-wilting genotype G00BP245 had higher $\Delta^{13}C$ values than slow-wilting genotypes G00BP214, 53, and 60; fast-wilting genotype G00BP200, 223 and 245 had significantly higher $\Delta^{13}C$ than slow-wilting genotype G00BP60 (**Figure 3_4**). In 2014, all fast-wilting genotypes showed significantly higher $\Delta^{13}C$ values than slow-wilting genotypes G00BP53 and 60 (**Figure 3_5**). Likewise, fast-wilting G00BP110 and G00BP200 had higher $\Delta^{13}C$ values than all slow-wilting genotypes except G00BP169.

ANOVA of $\delta^{18}O$ of soybean seed is shown in **Table 3_4** for 2012 to 2014. **Figure 3_6 and 3_7** show the response of $\delta^{18}O$ for the two-way interaction of genotype (wilting) for 2012 and 2013. There was no significant effect of treatments on $\delta^{18}O$ in 2014. Seed $\delta^{18}O$ in 2012 was significantly higher for the deficit irrigation 2 treatment than full and deficit irrigation 1 treatments (**Table 3_4**); these results are in contrast to those of Madhava et al. (2010) who found that $\delta^{18}O$ of dried leaf biomass decreased in cowpea as drought stress increased and as transpiration decreased. In 2012, $\delta^{18}O$ value for slow-wilting genotype G00BP60 was less than the value for fast-wilting genotypes G00BP110, G00BP223, G00BP245, and G00BP84 and lower than slow-wilting genotypes G00BP216 and G00BP53 (**Figure 3_6**). In 2013, slow-wilting genotypes (except G00BP169) had lower $\delta^{18}O$ values than genotype G00BP110 (**Figure 3_7**).

C. Relative Canopy Temperature

Aerial infrared images were taken on 30 Aug and 6 Sep in 2013, and 5 Aug, 6 Aug, 13 Aug, 21 Aug, 22 Aug, 28 Aug, 4 Sep, 9 Sep, 25 Sep, and 1 Oct in 2014 to determine the relative canopy temperature. Data collected on 5 Aug, 6 Aug, 13 Aug, 6 Sep, and 25 Sep in 2014, however,

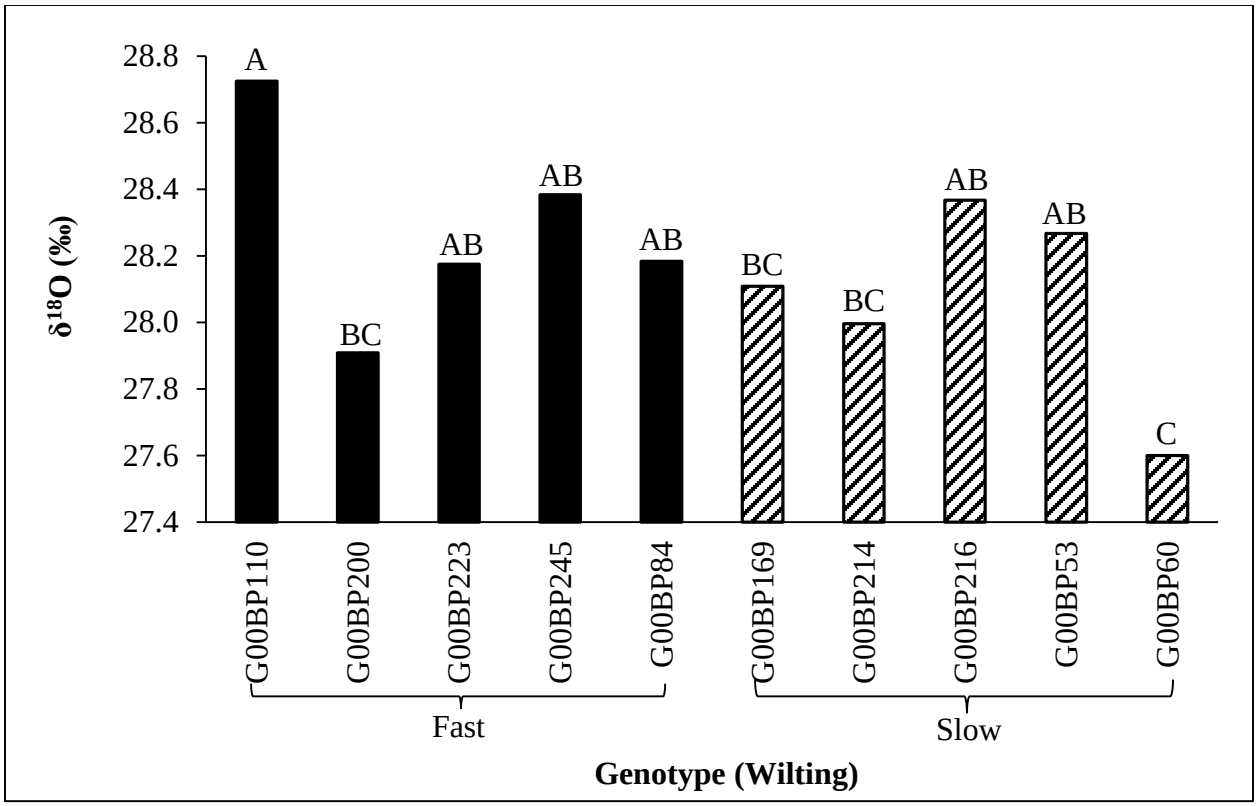

Figure 3_6 The response of oxygen isotope composition ($\delta^{18}O$) of soybean seed for each genotypes averaged across replications and water treatments in Fayetteville 2012. Different letters above the bars denote significant differences ($P \leq 0.05$) as determined by an LSD.

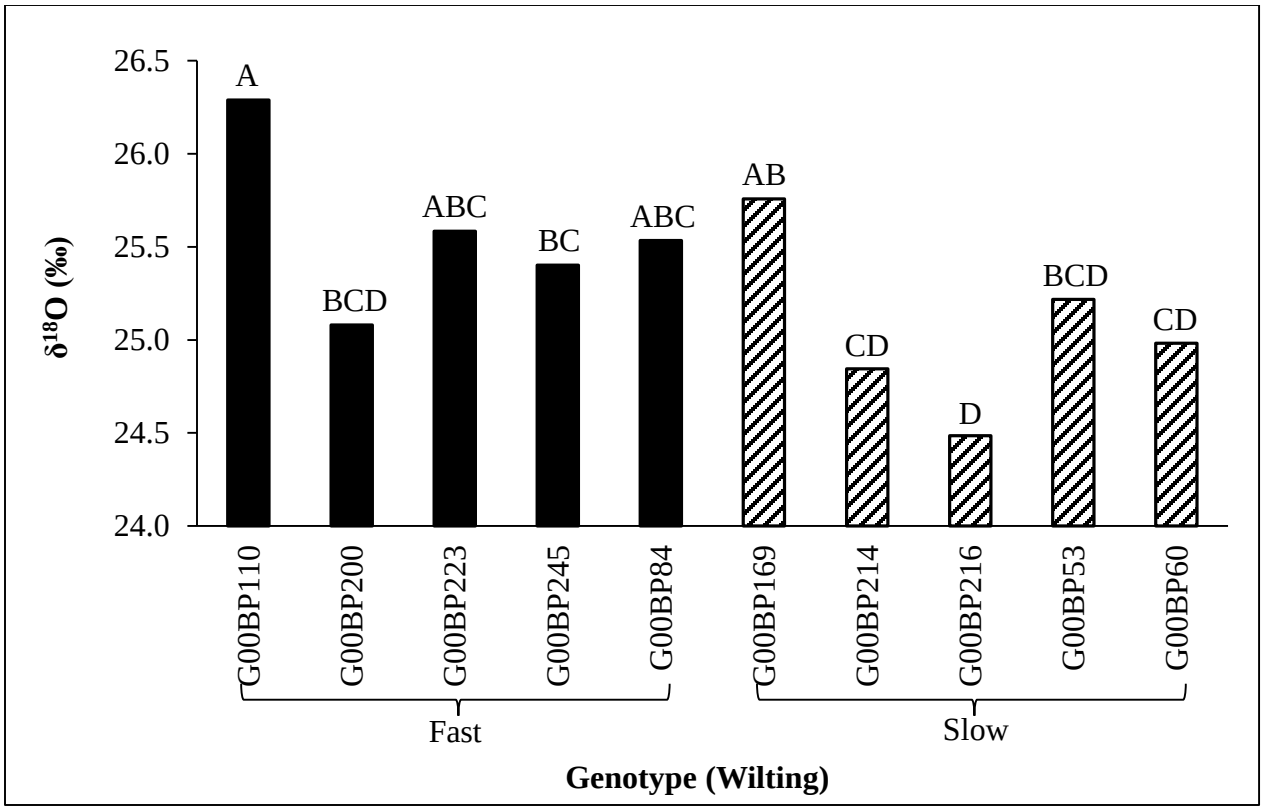

Figure 3_7 The response of oxygen isotope composition ($\delta^{18}O$) of soybean seed for each genotypes averaged across replications and water treatments in Fayetteville 2013. Different letters above the bars denote significant differences ($P \leq 0.05$) as determined by an LSD.

did not show any significant effects. **Table 3_5** shows the ANOVA for relative canopy temperature of soybean for dates in 2013 and 2014 that had significant effects. The large number of days in which temperature was not significant in 2014 could be because 2014 has a milder summer compared to 2013. Relative canopy temperature increased with the main effect of decreasing water availability on 30 Aug 2013, 21 Aug 2014, 22 Aug 2014, and 28 Aug 2014. Moreover, the main effect of wilting showed that slow-wilting genotypes had lower canopy temperature compared with fast-wilting genotypes on 4 Sep 2014 and 1 Oct 2014. On 6 Sep 2013 there was a significant interaction of relative canopy temperature between irrigation and genotype within wilting group, and, in general this response showed that as water availability decreased that canopy temperature increased and that within an irrigation treatment slow-wilting genotypes had a lower canopy temperature than fast-wilting genotypes (**Figure 3_8**).

D. Yield

The ANOVA for grain yield from 2012 to 2014 is summarized in **Table 3_6**. The main effect of irrigation did not affect grain yield in any of the three years, and only in 2013 the interaction with irrigation was significant. The main effect of wilting was significant for yield in 2012 and indicated that yield was significantly higher for slow-wilting than fast-wilting genotypes. In 2013, irrigation*genotype (wilting) was significant, and in 2014, genotype (wilting) was significant. **Figure 3_9** and **3_10** showed the yield response for each genotype under and across water treatments in 2013 and 2014, respectively. In 2013, there was considerable variation in yield among genotypes, but generally, slow-wilting genotypes had similar or greater yields within an irrigation treatment compared with fast-wilting genotypes (**Figure 3_9**). Likewise, in 2014, there was considerable variation in yield among genotypes, but generally, slow-wilting genotypes had

Table 3_5 The effects of relative canopy temperature for different imaging dates in Fayetteville AR 2013 and 2014. There is no infrared images in 2012.

	Dates	8/30/2013	9/6/2013	8/21/2014	8/22/2014	8/28/2014	9/4/2014	10/1/2014
Effects	Irri	*	***	**	***	***	NS	NS
	Wilt	NS	**	NS	NS	NS	*	*
	Irri*wilt	NS	*	NS	NS	NS	NS	NS
	Geno(wilt)	NS	NS	NS	NS	NS	NS	NS
	Irri*geno(wilt)	NS	*	NS	NS	NS	NS	NS
Irri	Full	72 b	62 c	46 b	34 b	47 b	62	93
	Deficit 1	91 ab	86 b	58 a	50 a	61 a	62	92
	Deficit 2	109 a	103 a	64 a	55 a	66 a	62	98
Wilt	Fast	94	94 a	57	48	59	67 a	98 a
	Slow	87	73 b	55	47	56	57 b	90 b

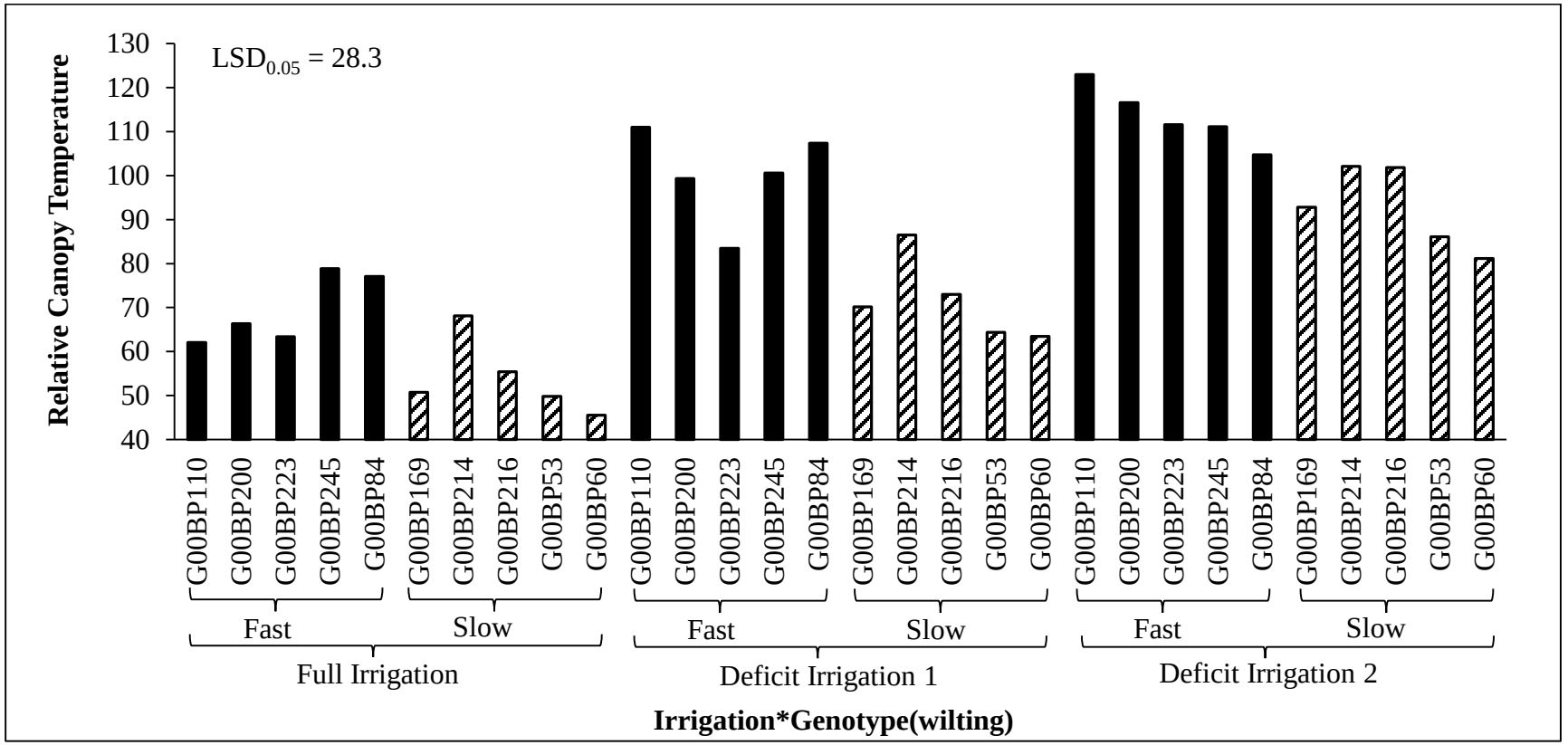

Figure 3_8 The response of relative canopy temperature for each genotype under different water treatments in Fayetteville AR on 6 Sep 2013.

Table 3_6 The effects of soybean yield and the mean values for irrigation and wilting effects in Fayetteville AR from 2012 through 2014.

Yield (kg ha^{-1})

Effects		2012		2013		2014	
		P Value	$LSD_{0.05}$	P Value	$LSD_{0.05}$	P Value	$LSD_{0.05}$
Irri		NS	-----	NS	-----	NS	-----
Wilt		*	242	*	302	**	168
Irri*wilt		NS	-----	*	566	NS	-----
Geno(wilt)		NS	-----	NS	-----	**	374
Irri*geno(wilt)		NS	-----	**	949	NS	-----
Irri	Full	3835		4523		4876	
	Deficit 1	3506		4215		4549	
	Deficit 2	3136		3977		4464	
Wilt	Fast	3351 b		4068 b		4463 b	
	Slow	3634 a		4408 a		4796 a	

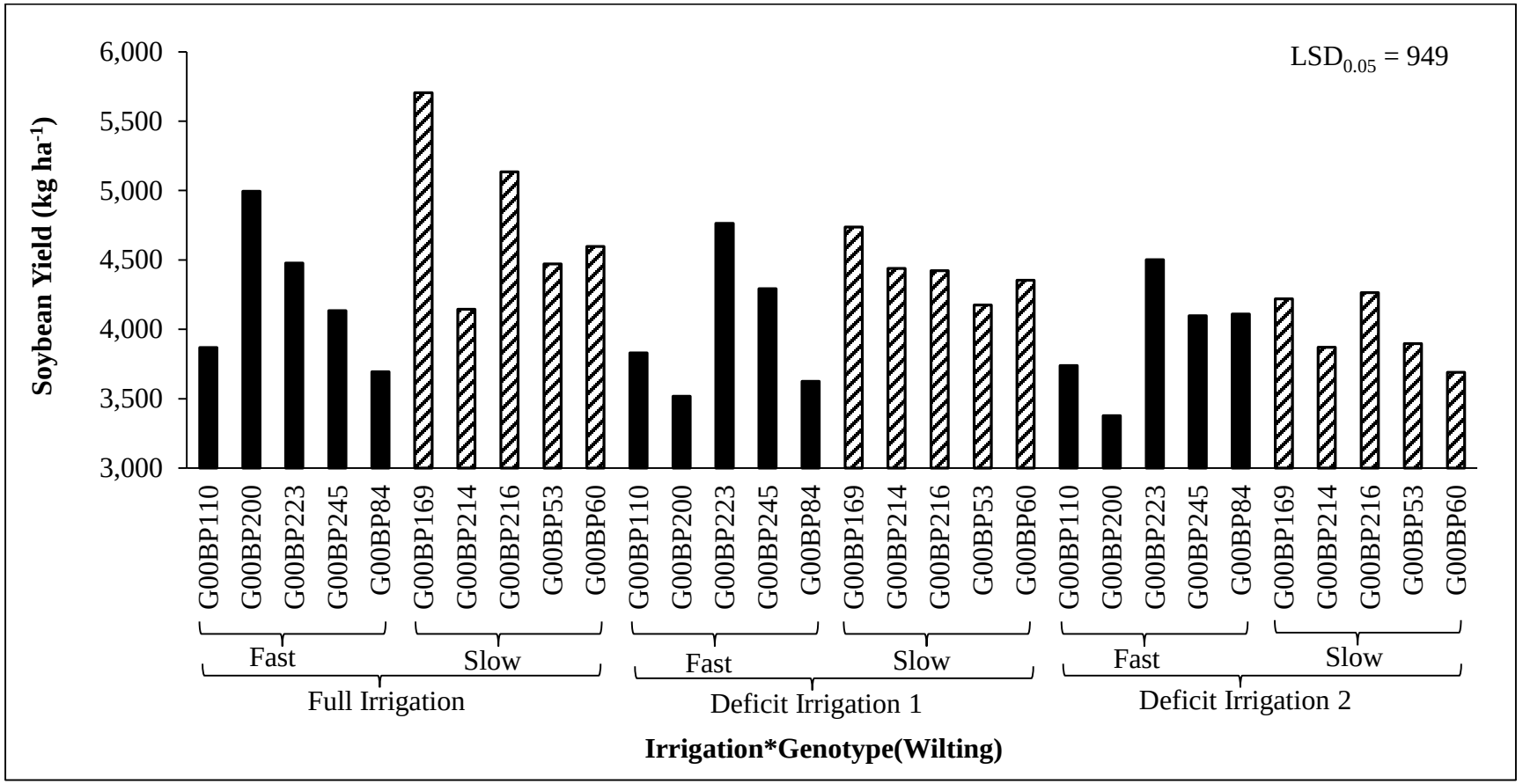

Figure 3_9 The response of soybean yield for each genotype under different water treatments averaged across replications in Fayetteville AR in 2013.

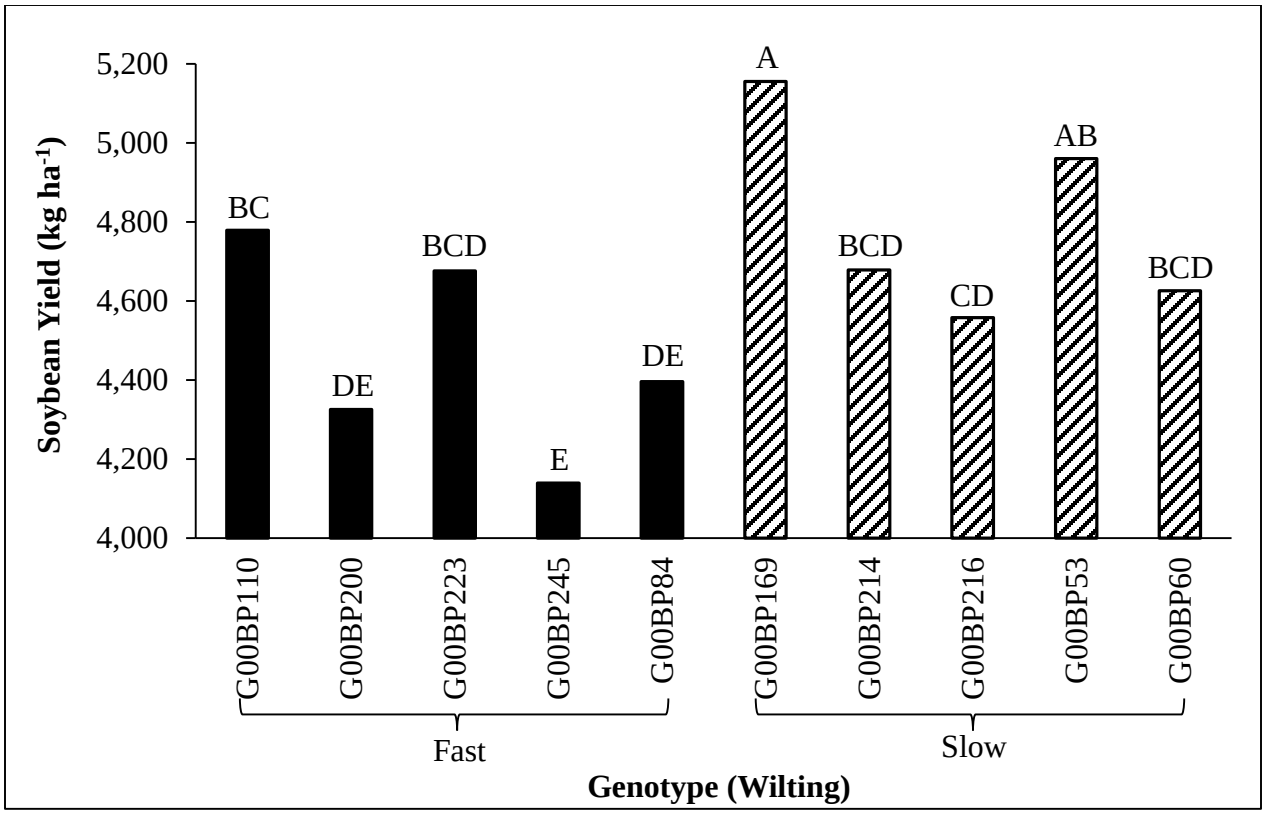

Figure 3_10 The response of soybean yield for each genotype averaged across replications and water treatments in Fayetteville AR in 2014. Different letters above the bars denote significant differences (P≤0.05) as determined by an LSD.

similar or greater yields than fast-wilting genotypes (**Figure 3_10**). In both 2013 and 2014, G00BP169 tended to be the highest yielding slow-wilting genotype, and G00BP223 tended to be the highest fast-wilting genotype.

E. Correlation among Variables

Table 3_7 shows the correlations among leaf $\Delta^{13}C$, seed $\Delta^{13}C$, seed $\delta^{18}O$, yield, and canopy temperature over years, over irrigation treatments, and by years. For canopy temperature, only the relations with yield are shown in the table. Leaf $\Delta^{13}C$ was positively correlated with seed $\Delta^{13}C$ over years (r=0.49***), by year (r=0.79*** in 2012, r=0.25 in 2013, and r=0.56** in 2014), and for the fully irrigated water treatment over years (r=0.61***). Seed $\Delta^{13}C$ and seed $\delta^{18}O$ were positively correlated over years (r=0.38***) and for the full irrigation (r=0.68***) and deficit irrigation 1 (r=0.67***) treatments over years, which is consistent with the hypothesis that increasing transpiration results in a decreased WUE (i.e. increased $\Delta^{13}C$). Similarly, there were negative correlations between seed $\Delta^{13}C$ and yield over years for the full irrigation treatment (r=-0.53**), deficit irrigation 1 treatment (r=-0.56**), and for the deficit irrigation 2 treatment (r=-0.02ns), which supports the hypothesis that yield and WUE were positively associated except under deficit irrigation 2 conditions.

There was a strong negative correlation between yield and seed $\delta^{18}O$ over years (r=-0.76***), and by irrigation treatments over years (r=-0.69*** for full irrigation, and -0.77*** for deficit irrigation 1, -0.84*** for deficit irrigation 2). When considering the relationship between yield and $\delta^{18}O$ by year and over irrigation treatments, only in 2012 was this significant (r=-0.60***). Therefore, it appears that the significant negative relationships between yield and $\delta^{18}O$ over all years and by years were due to differences among years that were not associated with water treatments. The year 2012 had severe drought which might be the reason for the differences

Table 3_7 Correlation coefficient among leaf $\Delta^{13}C$, seed $\Delta^{13}C$, seed $\delta^{18}O$, yield, and canopy temperature over year, over irrigation, by year and by irrigation. Only the negative coefficient between yield and canopy temperature were shown in the table.

Over Year & By Year		Variables	Leaf $\Delta^{13}C$	Seed $\Delta^{13}C$	Seed $\delta^{18}O$	Yield	Yield vs Temperature
Over year	**(n=90)**	Leaf $\Delta^{13}C$	1.00	0.49***	-0.02	0.07	**8/30/13**: -0.54**; **9/6/13**: -0.60***; **8/5/14**: -0.37*; **8/6/14:** -0.13; **8/13/14**: -0.27; **8/21/14**: -0.34; **8/22/14:** -0.57***; **8/28/14**: -0.57**; **9/4/14**: -0.38*; **9/9/14**: -0.35; 9/**25/14**: -0.47**; **10/1/14**: -0.62***.
		Seed $\Delta^{13}C$	0.49***	1.00	0.38***	-0.17	
		Seed $\delta^{18}O$	-0.02	0.38***	1.00	-0.76***	
		Yield	0.07	-0.17	-0.76***	1.00	
Over year by Irrigation	**Full (n=30)**	Leaf $\Delta^{13}C$	1.00	0.61***	0.48**	-0.51**	**8/30/13**: -0.61; **9/6/13**: -0.59; **8/5/14**: -0.30; **8/13/14**: -0.26; **8/22/14**: -0.37; **8/28/14**: -0.45; **9/4/14**: -0.48; **9/9/14**: -0.68*; **9/25/14**: -0.60; **10/1/14**: -0.52.
		Seed $\Delta^{13}C$	0.61***	1.00	0.68***	-0.53**	
		Seed $\delta^{18}O$	0.48**	0.68***	1.00	-0.69***	
		Yield	-0.51**	-0.53**	-0.69***	1.00	
	Deficit 1 (n=30)	Leaf $\Delta^{13}C$	1.00	0.19	0.07	-0.16	**8/30/13:** -0.47; **9/6/13**:-0.65*; **8/5/14**: -0.30; **8/22/14**: -0.32; **8/28/14**: -0.10; **9/4/14**: -0.18; **9/9/14**: -0.50; **9/25/14**: -0.78**; **10/1/14**: -0.89***.
		Seed $\Delta^{13}C$	0.19	1.00	0.67***	-0.56**	
		Seed $\delta^{18}O$	0.07	0.67***	1.00	-0.77***	
		Yield	-0.16	-0.56**	-0.77***	1.00	
	Deficit 2 (n=30)	Leaf $\Delta^{13}C$	1.00	0.22	-0.38*	0.39*	**9/6/13:** -0.06; **8/5/14**:-0.70*; **8/6/14**: -0.06; **8/13/14**: -0.31; **8/22/14**: -0.39; **8/28/14**: -0.29; **9/4/14**: -0.58; **9/9/14**: -0.49; **9/25/14**: -0.70*; **10/1/14**: -0.67*.
		Seed $\Delta^{13}C$	0.22	1.00	0.06	-0.02	
		Seed $\delta^{18}O$	-0.38*	0.06	1.00	-0.84***	
		Yield	0.39*	-0.02	-0.84***	1.00	
By Year	**2012 (n=30)**	Leaf $\Delta^{13}C$	1.00	0.79***	-0.45*	0.47**	No Temperature Data
		Seed $\Delta^{13}C$	0.79***	1.00	-0.48**	0.33	
		Seed $\delta^{18}O$	-0.45*	-0.48**	1.00	-0.60***	
		Yield	0.47**	0.33	-0.60***	1.00	
	2013 (n=30)	Leaf $\Delta^{13}C$	1.00	0.25	0.20	0.14	**8/30/13:** -0.54**; **9/6/13**: -0.60***
		Seed $\Delta^{13}C$	0.25	1.00	-0.20	0.52**	
		Seed $\delta^{18}O$	0.20	-0.20	1.00	-0.32	
		Yield	0.14	0.52**	-0.32	1.00	
	2014 (n=30)	Leaf $\Delta^{13}C$	1.00	0.56**	-0.34	-0.23	**8/5/14**:-0.37*; **8/6/14**: -0.13; **8/13/14**: -0.27; **8/21/14**: -0.34; **8/22/14:** -0.57***; **8/28/14**: -0.57**; **9/4/14**: -0.38*; **9/9/14**: -0.35; **9/25/14**: -0.47**; **10/1/14**: -0.62***.
		Seed $\Delta^{13}C$	0.56**	1.00	-0.12	-0.16	
		Seed $\delta^{18}O$	-0.34	-0.12	1.00	-0.16	
		Yield	-0.23	-0.16	-0.16	1.00	

among years.

Over all 3 years and all irrigation treatments, relative canopy temperature was significantly and negatively correlated with yield on eight out of 12 dates (-0.37*<r<-0.62***). By irrigation treatment, yield and relative canopy temperature were significantly and negatively associated on one date for the full irrigation treatment (r=-0.68*), three days for the deficit irrigation 1 treatment (-0.65*<r<-0.89***), and on three days for the deficit irrigation 2 treatment (-0.67*<r<-0.70*). These results also support the hypothesis that decreased water availability increased relative canopy temperature and resulted in decreased yield.

Discussion

Although $\Delta^{13}C$ from soybean leaf tissue had significant effects from ANOVA each year, the $\Delta^{13}C$ from seed had more significant effects for each year. Leaf $\Delta^{13}C$ values differed among irrigation treatments only in 2012 with a non-significant wilting effect; however, $\Delta^{13}C$ of seed was significantly affected by both irrigation treatment and wilting types. Except for significance in one of the main factors in 2013 and 2014, the seed $\Delta^{13}C$ also showed significant difference in the combination of genotype within wilting type. The reason for this difference between $\Delta^{13}C$ of leaf and seed might be that at late R5 when leaf samples were taken, the soybean plants had not been exposed to significant soil moisture stress. Additionally, since carbon in the seed is derived from many leaves over a very long period of time, seeds are likely a better integrator of $\Delta^{13}C$ over the course of the season. In 2012, both leaf $\Delta^{13}C$ and seed $\Delta^{13}C$ had more significant effects than in 2013 and 2014, which might be due to the seasonal weather conditions. During the growing season (June through September), the average maximum temperatures in 2012 was over than 30ºC for three months whereas the average maximum temperatures exceeded 30ºC for 2 months (2013) and 1 month (2014) (**Table 2_4**). Similarly, solar radiation was higher in 2012 than the other two years (**Table 2_4**), and soil water deficits were much greater in 2012 compared with 2013 and 2014 (**Figure 2_2**). High temperature, high solar radiation and a long period of severe soil water deficit likely impacted $\Delta^{13}C$ in 2012.

The $\Delta^{13}C$ values generally decreased (i.e., high WUE) with decreasing water availability. There was large variation of leaf $\Delta^{13}C$ in 2012 and seed $\Delta^{13}C$ in all 3 years among genotypes, but there was a trend that the average $\Delta^{13}C$ value of slow-wilting genotypes was lower than fast-wilting genotypes especially for 2014 seed. In 2013 and 2014, slow-wilting genotypes had lower leaf $\Delta^{13}C$ than fast-wilting genotypes. Previous research documented a negative relationship between $\Delta^{13}C$

and WUE. In the present research, slow-wilting genotypes had lower $\Delta^{13}C$ indicating a possible higher WUE than fast-wilting genotypes.

Due to the advantage of using soybean seed for the analysis of $\Delta^{13}C$, $\delta^{18}O$ was only analyzed from seed. The $\delta^{18}O$ values were significantly associated with irrigation treatments in 2012 and genotype within wilting in both 2012 and 2013. In contrast to previous reports by Madhava et al. (2010), the $\delta^{18}O$ values generally increased with decreasing water availability in 2012. The reason may be that the tissue used in this study (seed) is different with the previous research (leaf). Seed $\delta^{18}O$ values may be a reflection of transpiration, but there might be some other mechanisms that impact the ratio of ^{16}O and ^{18}O. There was large variability of $\delta^{18}O$ values among genotypes in 2012 and 2013. The genotypes G00BP60 in 2012 and G00BP214 and G00BP216 in 2013 had lower $\delta^{18}O$ values than other genotypes. In 2014, a very wet year, none of the treatment effects were significant.

The relative canopy temperature generally increased with increasing drought stress in five of the imaging dates. Moreover, slow-wilting genotypes had lower canopy temperature than fast-wilting genotypes in two of the imaging dates. These results were consistent with the hypothesis that drought stress causes an increase in relative canopy temperature and slow-wilting genotypes have lower temperature than fast-wilting genotypes. This is the first report that found the relationship between relative canopy temperature and drought stress as well as differences in canopy temperature and $\Delta^{13}C$ between wilting types. Additionally, grain yield was significantly higher for slow-wilting genotypes than fast-wilting in 2012. There was a large variation in yield among genotypes in 2013 and 2014, but overall, the average yield for slow-wilting genotypes was greater than for fast-wilting genotypes. Moreover, the grain yield was negatively correlated with

the relative canopy temperature. Previous literature indicates that cool canopies have higher yields in wheat (Pradhan et al., 2014; Ray and Ahmed, 2015).

Leaf and seed $\Delta^{13}C$ values were positively correlated. Seed $\Delta^{13}C$ was also positively correlated with $\delta^{18}O$ over years, which supports the hypothesis that increased transpiration is associated with decreased WUE (i.e. increased $\Delta^{13}C$). However, negative correlations between leaf $\Delta^{13}C$ and seed $\delta^{18}O$ were found both over the 3 years and in 2012 and 2014, which is consistent with previous reports (Barbour and Farquhar, 2000; Cernusak et al., 2003; Xu et al., 2000). Therefore, different plant tissues evaluated (seed or leaf) may cause different relationships between $\Delta^{13}C$ and $\delta^{18}O$.

There was a negative correlation between seed $\Delta^{13}C$ and grain yield under full irrigation and deficit irrigation 1 treatments, which is consistent with the hypothesis that yield and WUE were positively associated. This is the first report that shows the correlation between seed $\Delta^{13}C$ and yield in soybean. However, there are some articles that reported an inversely correlation between grain $\Delta^{13}C$ and yield in wheat (Araus et al., 2003; Misra et al., 2006). There was a strong negative correlation between yield and seed $\delta^{18}O$ over years and by irrigation treatments over years, which probably resulted from the differences among years. The severe drought in 2012 might be the reason for the differences among years. A consistent negative correlation between yield and relative canopy temperature also supports the hypothesis that decreased water availability increased relative canopy temperature, which caused canopy wilting and affected yield.

Literature Cited

Abdel-Haleem, H., T.E. Carter Jr., L.C. Purcell, C.A. King, L.L. Ries, P. Chen, W. Schapaugh Jr., T.R. Sinclair, and H.R. Boerma. 2012. Mapping of quantitative trait loci for canopy-wilting trait in soybean (Glycine max L. Merr). Theor. Appl. Genet. 125:837-846.

Araus, J.L., D. Villegas, N. Aparicio, L.F. Garcia del Moral, S. EI Hani, Y. Rharrabti, J.P. Ferrio, and C. Royo. 2003. Environmental factors determining carbon isotope discrimination and yield in durum wheat under Mediterranean conditions. Crop Sci. 43:170-180.

Araus, J.L., T. Amaro, J. Casadesus, A. Asbati, and M.M. Nachit. 1998. Relationships between ash content, carbon isotope discrimination and yield in durum wheat. Aust. J. Plant Physiol. 25:835-842.

Barbour, M.M., and G.D. Farquhar. 2000. Relative humidity- and ABA-induced variation in carbon and oxygen isotope ratios of cotton leaves. Plant Cell Environ. 23:473-485.

Board, J.E., and C.S. Kahlon. 2011. Soybean yield formation: what controls it and how it can be improved. p. 1-36. In: (eds. A. Hany, El-Shemy) Soybean Physiology and Biochemistry, InTech, doi: 10.5772/17596. http://www.intechopen.com/books/soybean-physiology-and-biochemistry/soybean-yield-formation-what-controls-it-and-how-it-can-be-improved (accessed 31 May 2016).

Cernusak, L.A., D.J. Arthur, J.S. Pate, and G.D. Farquhar. 2003. Water relations link carbon and oxygen isotope discrimination to phloem sap sugar concentration in *Eucalyptus globulus*. Plant Physiol. 131:1544-1554.

Charlson, D.V., S. Bhatnagar, C.A. King, J.D. Ray, C.H. Sneller, T.E. Carter Jr., and L.C. Purcell. 2009. Polygenic inheritance of canopy wilting in soybean [*Glycine max* (L.) Merr.]. Theor. Appl. Genet. 119:587-594.

Condon, A.G., G.D. Farquhar, and R.A. Richards. 1990. Genotypic variation in carbon isotope discrimination and transpiration efficiency in wheat leaf gas exchange and whole plant studies. Aust. J. Plant Physiol. 17:9-22.

Condon, A.G., R.A. Richards, G.J. Rebetzke, and G.D. Farquhar. 2004. Breeding for high water-use efficiency. J. Exp. Bot. 55:2447-2460.

de Souza, P.I., D. B. Egli, and W.P. Bruening. 1997. Water stress during seed filling and leaf senescence in soybean. Agron. J. 89:807-812.

FAO. 2015. Food and Agriculture Organization of the United Nations Statistics Division. http://faostat3.fao.org/home/E (accessed 30 Jul. 2015).

Farquhar, G.D., J.R. Ehleringer, and K.T. Hubick. 1989. Carbon Isotope discrimination and photosynthesis. Plant Mol. Biol. 40:503-537.

Farquhar, G.D., M.H. O'leary, and J.A. Berry. 1982. On the relationship between carbon isotope discrimination and the intercellular carbon dioxide concentration in leaves. Aust. J. Plant Physiol. 9:121-137.

Farquhar, G.D., and R.A. Richards. 1984. Isotopic composition of plant carbon correlates with water-use efficiency of wheat genotypes. Aust. J. Plant Physiol. 11:539–552.

Gonfiantini, R. 1983. Advisory group meeting on stable isotope reference samples for geochemical and hydrological investigations. IAEA, Vienna. http://www-naweb.iaea.org/naalihl/docs /pub/iaea-1984-gonfiantini_agmeeting-stableisotoperm.pdf (accessed 31 May 2016).

Heatherly, L.G., and C.D. Elmore. 1986. Irrigation and planting date effects on soybean grown on clay soil. Agron. J. 78:576-580.

Jones, H.G., R. Serraj, B.R. Loveys, L.Z. Xiong, A. Wheaton, and A.H. Price. 2009. Thermal infrared imaging of crop canopies for the remote diagnosis and quantification of plant responses to water stress in the field. Funct. Plant Biol. 36:978-989.

King, C.A., L.C. Purcell, and K.R. Brye. 2009. Differential wilting among soybean genotypes in response to water deficit. Crop Sci. 49:290-298.

Madhava, H.B., M.S. Sheshshayee, R. Devendra, T.G. Prasad, and M. Udayakumar. 2010. Oxygen (^{18}O) isotopic enrichment in the leaves as a potential surrogate for transpiration and stomatal conductance. http://www.iisc.ernet.in/currsci/jun10/articles12.htm (accessed 17 Sep. 2015).

Misra S. C., R. Randive, V.S. Rao, M.S. Sheshshayee, R. Serraj and P. Monneveux. 2006. Relationship between carbon isotope discrimination, ash content and grain yield in wheat in the peninsular zone of India. J. Agron. Crop Sci. 192:352-362.

NASS. 2015. United States Department of Agriculture, National Agricultural Statistics Service. http://quickstats.nass.usda.gov/ (accessed 16 Sep. 2015).

O'leary, M.H. 1988. Carbon isotope in photosynthesis. BioSci. 38:325-336.

Pradhan, G.P., Q. Xue, K.E. Jessup, J.C. Rudd, S. Liu, R.N. Devkota, and J.R. Mahan. 2014. Cooler canopy contributes to higher yield and drought tolerance in new wheat cultivars. Crop Sci. 54:2275-2284.

Purcell, L.C. 2000. Soybean canopy coverage and light interception measurements using digital imagery. Crop Sci. 40:834-837.

Purcell, L.C., J.T. Edwards, and K.R. Brye. 2007. Soybean yield and biomass responses to cumulative transpiration: Questioning widely held beliefs. Field Crops Res. 101:10-18.

Ray, J. and J.J. Ahmed. 2015. Canopy temperature effects on yield and grain growth of different wheat genotypes. IOSR-JAVS 8 II:48-55.

Ries, L.L., L.C. Purcell, T.E. Carter, Jr., J.T. Edwards, and C.A. King. 2012. Physiological traits contributing to differential canopy wilting in soybean under drought. Crop Sci. 52:272-281.

Rohling, E.J. 2007. Oxygen isotope composition of seawater. p. 1748–1756. In: (ed. S.A. Elias) Encyclopedia of Quaternary Science, 3, Elsevier.

Royal Society. 2009. Reaping the benefits: science and the sustainable intensification of global agriculture. Royal Society, London. https://royalsociety.org/~/media/Royal_Society _Content/policy/publications/2009/4294967719.pdf (accessed 29 May 2016).

Sadok, W., and T.R. Sinclair. 2010. Transpiration response of 'slow-wilting' and commercial soybean (Glycine max (L.) Merr.) genotypes to three aquaporin inhibitors. J. Exp Bot. 61:821-829.

Sloane, R.J., R.P. Patterson, and T.E. Carter. 1990. Field drought tolerance of a soybean plant introduction. Crop Sci. 30:118-123.

UN Global Compact, 2015. Increasing water demand. CEO Water Mandate, United Nations Global Compact. http://ceowatermandate.org/business-case/global-water-trends/increas ing-water-demand/ (accessed 17 Sep. 2015).

USDA. 2012. Economic Research Service: Soybeans & oil crops, background. United States Department of Agriculture. http://www.ers.usda.gov/topics/crops/soybeans-oil-crops/back ground.aspx (updated 10 Oct. 2012).

USDA. 2015. Economic Research Service: Soybeans & oil crops, trade. United States Department of Agriculture. http://www.ers.usda.gov/topics/crops/soybeans-oil-crops/trade.aspx (updated 7 May 2015).

Xu, Z.H., P.G. Saffigna, G.D. Farquhar, J.A. Simpson, R.J. Haines, S. Walker, D.O. Osborne, and D. Guinto. 2000. Carbon isotope discrimination and oxygen isotope composition in clones of the F1 hybrid between slash pine and Caribbean pine in relation to tree growth, water-use efficiency and foliar nutrient concentration. Tree Physiol. 20:1209-1218.

CHAPTER IV

CONCLUSION

Drought stress limits plant growth and yield production, and drought is considered as one of the most important factors limiting agricultural productivity all over the world. Freshwater demands will increase dramatically due to the predicted food requirement.

Some plants are able to resist drought stress, and this represents an important means of ameliorating drought effects on crop production. Drought stress often leads to an early senescence in soybean due to a shortened seedfill period. The first study of the present research was conducted with two different water treatments (WI and DR) and with five genotypes ranging from MGs 2 through 5. Weekly samples were made beginning at seedfill of leaf nitrogen concentration, and images from the ground and from 50 to 75 m above the ground to determine the dark green color index (DGCI), which is a measure of canopy greenness. Leaf nitrogen concentration, ground DGCI and aerial DGCI decreased during the seedfill period. Ground DGCI and aerial DGCI followed similar trends. However, changes of canopy color during reproductive stages due to drought were distinguished using aerial color photography, but were not when made from the ground.

Previous studies found that some soybean genotypes were slow to wilt under drought and that this trait was beneficial to yield. In the second experiment, five fast- and five slow-wilting soybean genotypes were tested under three different water treatments including a full irrigation treatment and two deficit-irrigation treatments of increasing severity. Measurements were made of $\Delta^{13}C$ of leaf at late R5 and seed at harvest, $\delta^{18}O$ of seed at harvest, and relative canopy temperature after canopy closure to evaluate the response of soybean under drought conditions. Aerial thermal photography was used to obtain the temperature data to identify soybean lines with a cooler canopy under drought. The $\Delta^{13}C$ values generally decreased (i.e., high WUE) with increasing drought stress. Slow-wilting genotypes had lower $\Delta^{13}C$ indicating a possible higher WUE than fast-wilting genotypes. The relative canopy temperature generally increased with decreasing water availability,

and slow-wilting genotypes had lower canopy temperature than fast-wilting genotypes. This study is the first to report the relationship between relative canopy temperature and drought stress as well as differences in canopy temperature and $\Delta^{13}C$ between wilting types.

By comparing ground imaging and aerial color imaging methods, ground imaging method was time-consuming, can only be used in small scale experiments, and cannot separate difference between water treatments. In contrast, aerial color imaging method was rapid, suitable for large scale studies, and was able to distinguish difference between water treatments. It was simple and rapid to take samples for carbon isotope discrimination and oxygen isotope composition; however, it was time-consuming to process the samples for these two methods. For isotope analysis, samples must be coarse ground, finely ground, and weighed for trace amounts as well as long time waiting (6 to 8 weeks) to get results back from the isotope laboratory. In addition, it costs approximately \$8 (^{13}C) and \$16 (^{18}O) for analysis of each sample. Fortunately, carbon isotope discrimination method separated differences between irrigation treatments and wilting types, but there were large variations for the oxygen isotope composition method. It was fast to obtain aerial infrared images for relative canopy temperature, but time-consuming to process the images, especially using ArcGIS. However, a computer program was developed in this research group to quickly separate individual plots and analyze the aerial images, which will simplify data processing. Relative canopy temperature also separated differences between irrigation treatments and wilting types. In general, relative canopy temperature and aerial color imaging methods are highly recommended for the future studies followed by carbon isotope discrimination and ground color imaging methods. Future research on tissues to be used for oxygen isotope composition is required before it can be used successfully for identifying drought tolerance.

The bottleneck of traditional breeding is screening large populations for traits of interest. These two studies indicate that aerial photography is able to identify different soybean genotypes that senesce or wilt slowly. This opens the possibility of using this technology as a selection tool in a breeding program. In the future, favorable genotypes can be crossed with elite lines to generate lines of interest. The aerial photography method also provides a broad perspective to identify QTL and genes which are associated with slow senescence or slow wilting under water-limited conditions. Developing drought tolerant crops, as a goal for many breeders, will allow plants to have high water use efficiency and high yield, resulting in improved profitability under drought conditions.

APPENDIX

A. Leaf N versus DAR5

As expected, leaf N concentration decreased with increasing DAR5 in all years (**Figure A1, A2,** and **A3**) with ANCOVA accounting for between 87 and 94% of the variation (**Table A1, A2,** and **A3**). In 2012, leaf N concentration decreased linearly and was not affected by irrigation, but the rate of decrease differed among genotypes (**Table A1**). In 2013, there was a quadratic decrease in leaf N concentration that differed among genotypes but was similar between irrigation treatments. In contrast, in 2014, leaf N concentration also decreased quadratically, but the intercept term for the drought treatment within each genotype was lower than for the irrigated, indicating earlier senescence (**Table A3**).

Table A1 ANCOVA for leaf N concentration associated with genotype (geno), days after R5 (DAR5) and their interactions in Fayetteville 2012. Non-significant interactions were removed from the model stepwise. Letters b and c represented the slope and intercept for each genotype across water treatments in the linear model.

Leaf N

Source	DF	Mean Square	F Value	Pr > F	Adj. R^2
Irri	1	0.0355	0.16	0.6917	0.87
Geno	4	0.9099	4.08	0.0061	
DAR5	1	61.0129	273.40	<.0001	
DAR5*geno	4	0.8615	3.86	0.0082	

y = bx + c

Geno	Relative MG	Irri	b	c
AG24-30	2.4	DR/WI	-0.0901	5.3234
S25-T8	2.5	DR/WI	-0.0938	5.3048
S33-K5	3.3	DR/WI	-0.0516	4.7331
P94Y40	4.4	DR/WI	-0.0748	5.5385
P95Y50	5.5	DR/WI	-0.0567	4.4581

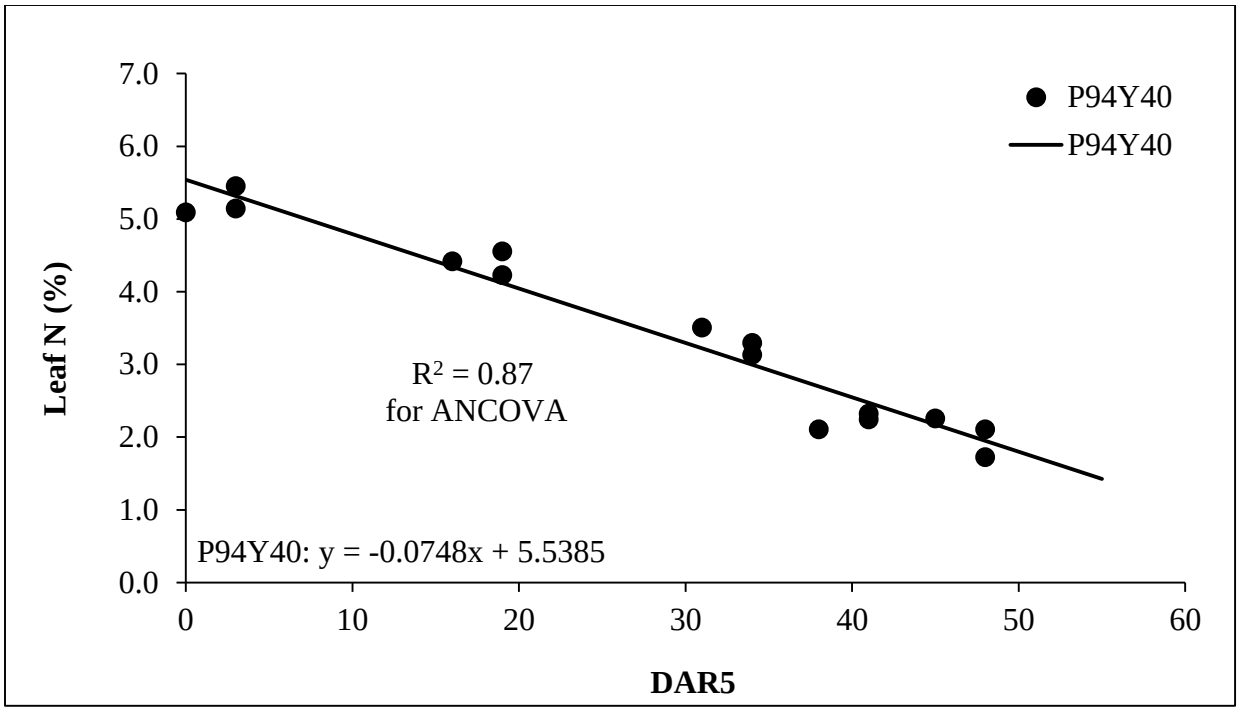

Figure A1 Leaf N concentration versus days after R5 (DAR5) across water treatments (NS) in Fayetteville 2012. P94Y40 was used to represent the response of leaf N concentration to DAR5, which was similar to other genotypes (not included in the figure).

Table A2 ANCOVA for leaf N concentration associated with days after R5 (DAR5)*genotype, DAR5*DAR5, and DAR5*DAR5*genotype in Fayetteville 2013. Non-significant interactions were removed from the model stepwise. Letters a, b and c represented the quadratic and linear slopes and intercept for each genotype across water treatments in this model.

Leaf N

Source	DF	Mean Square	F Value	Pr > F	Adj. R^2
Irri	1	0.0443	0.33	0.5662	
Geno	4	0.1583	1.19	0.3259	
DAR5*geno	5	0.4759	3.58	0.0072	0.94
DAR5*DAR5	1	7.8263	58.8	<.0001	
DAR5*DAR5*geno	4	0.9263	6.96	0.0001	

$y = ax^2 + bx + c$

Geno	Relative MG	Irri	a	b	c
S25-E5	2.5	DR/WI	-0.0025	0.0243	5.6946
S35-C3	3.5	DR/WI	-0.0026	0.0275	5.6946
P93Y72	3.7	DR/WI	-0.0022	0.0075	5.6946
P94Y40	4.4	DR/WI	-0.0041	0.091	5.6946
P95Y50	5.5	DR/WI	-0.0001	-0.0629	5.6946

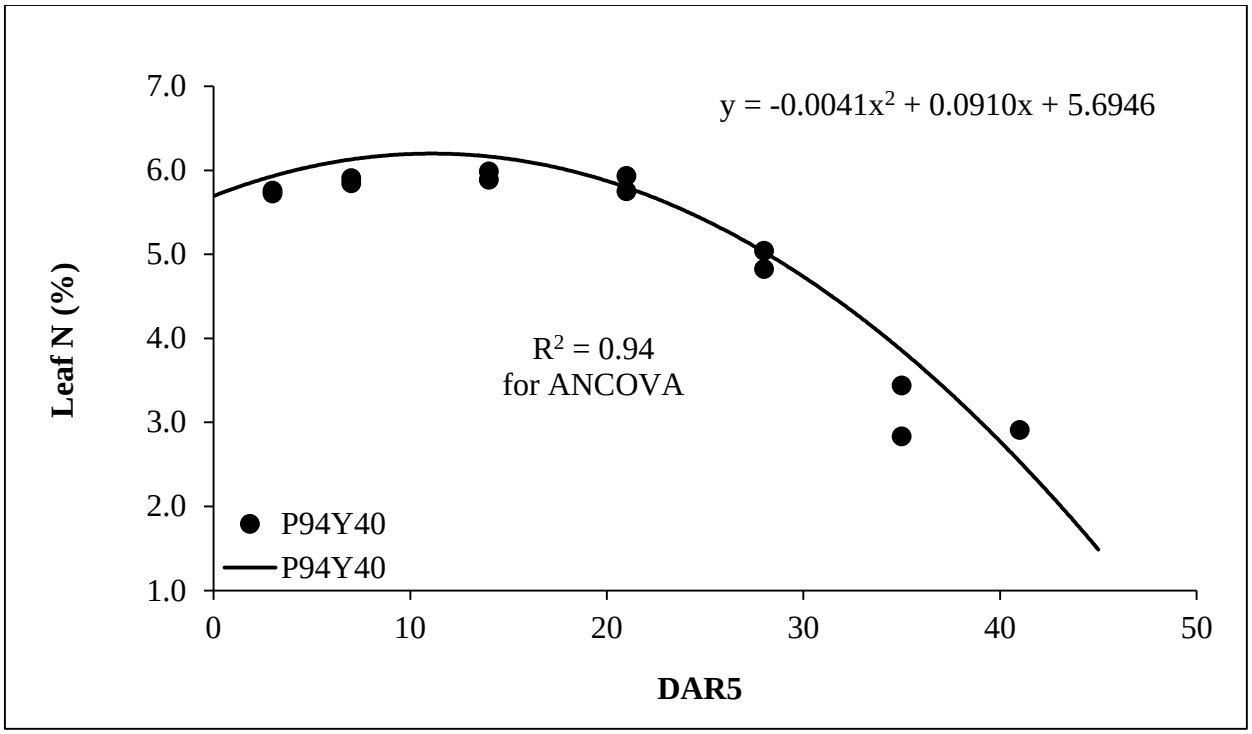

Figure A2 Leaf N concentration versus days after R5 (DAR5) across water treatments (NS) in Fayetteville 2013. P94Y40 was used to represent the response of leaf N concentration to DAR5, which was similar to other genotypes (not included in the figure).

Table A3 ANCOVA for leaf N concentration associated with irrigation, genotype and days after R5 (DAR5)*DAR5 in Fayetteville 2014. Non-significant interactions were removed from the model stepwise. Letters a and c represented the quadratic slope and intercept for each genotype under different water treatments in this model.

Leaf N

Source	DF	Mean Square	F Value	Pr > F	Adj. R^2
Irri	1	1.3507	8.74	0.0043	
Geno	4	1.1057	7.15	<.0001	0.92
DAR5*DAR5	1	112.6347	728.55	<.0001	

$y = ax^2 + c$

Geno	Relative MG	Irri	a	c
S25-E5	2.5	DR	-0.0018	5.6197
		WI	-0.0018	5.8942
S35-A5	3.5	DR	-0.0018	5.4464
		WI	-0.0018	5.7209
R2 36X82N	3.6	DR	-0.0018	5.5603
		WI	-0.0018	5.8349
P46T21R	4.6	DR	-0.0018	5.7699
		WI	-0.0018	6.0445
AG5532	5.5	DR	-0.0018	4.9866
		WI	-0.0018	5.2612

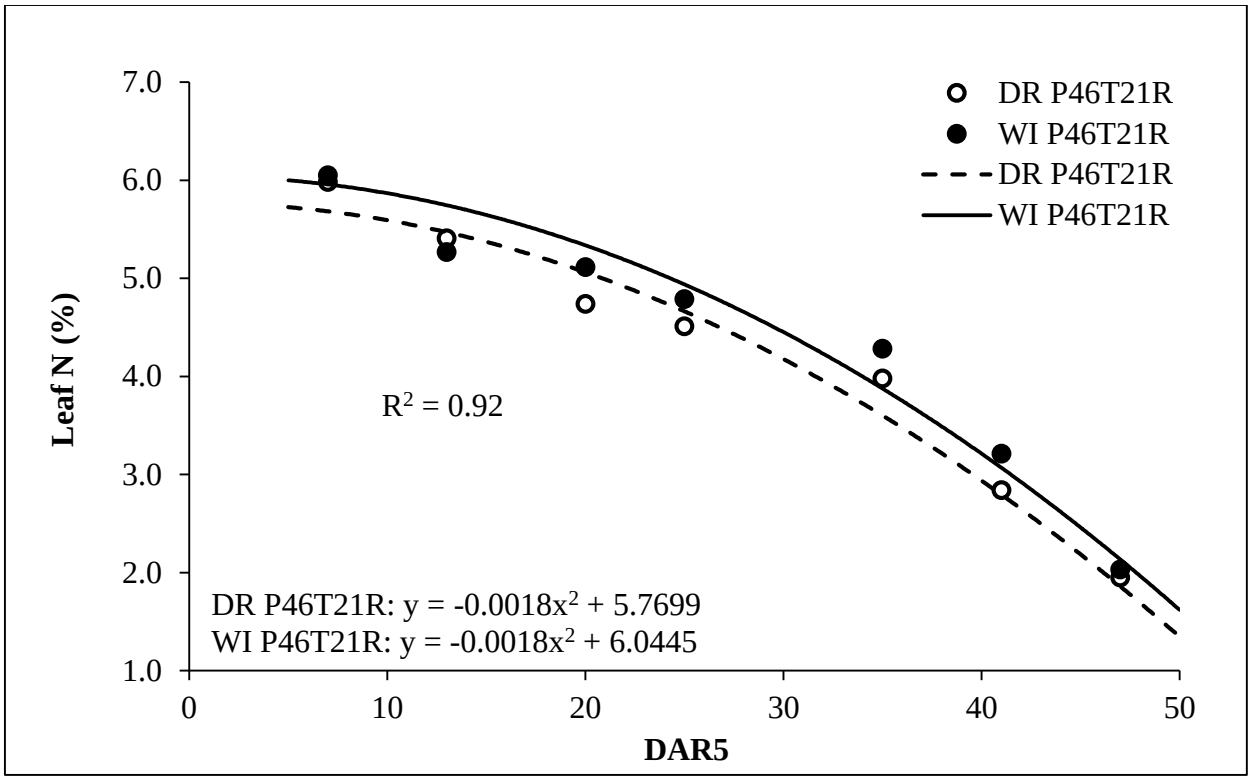

Figure A3 Leaf N concentration versus days after R5 (DAR5) for each genotype under different water treatments in Fayetteville 2014. Genotype P46T21R was used to represent the response of leaf N concentration to DAR5, which was similar to other genotypes (not included in the figure).

B. Aerial DGCI versus G_DGCI

As expected, aerial DGCI decreased with increasing G_DGCI in all years (**Figure A4**, **A5**, and **A6)** with ANCOVA accounting for between 62 and 70% of the variation (**Table A4, A5,** and **A6**). In 2012, aerial DGCI increased linearly and was not affected by irrigation, but the rate of decrease differed among genotypes. In 2013, there was still a linear increase in aerial DGCI that was not affected by irrigation but was affected by genotype and the interaction of irrigation and G_DGCI. The intercept for the DR within each genotype was lower than for WI, indicating earlier senescence. In contrast, in 2014, aerial DGCI increased quadratically and was not affected by either irrigation or genotype. This is just to show that there is general agreement between aerial DGCI and G_DGCI measurements.

Table A4 ANCOVA for aerial DGCI associated with genotype and ground DGCI (G_DGCI) in Fayetteville 2012. Non-significant interactions were removed from the model stepwise. Letters b and c represented the linear slope and intercept for each genotype across water treatments in this model.

Aerial DGCI

Source	DF	Mean Square	F Value	Pr > F	Adj. R^2
Irri	1	0.0619	1.81	0.1839	
Geno	4	0.1092	3.20	0.0198	0.62
G_DGCI	1	2.7997	81.99	<.0001	

$y = bx + c$

Geno	Relative MG	Irri	b	c
AG24-30	2.4	DR/WI	1.2374	-0.3563
S25-T8	2.5	DR/WI	1.2374	-0.2859
S33-K5	3.3	DR/WI	1.2374	-0.3150
P94Y40	4.4	DR/WI	1.2374	-0.1822
P95Y50	5.5	DR/WI	1.2374	-0.1243

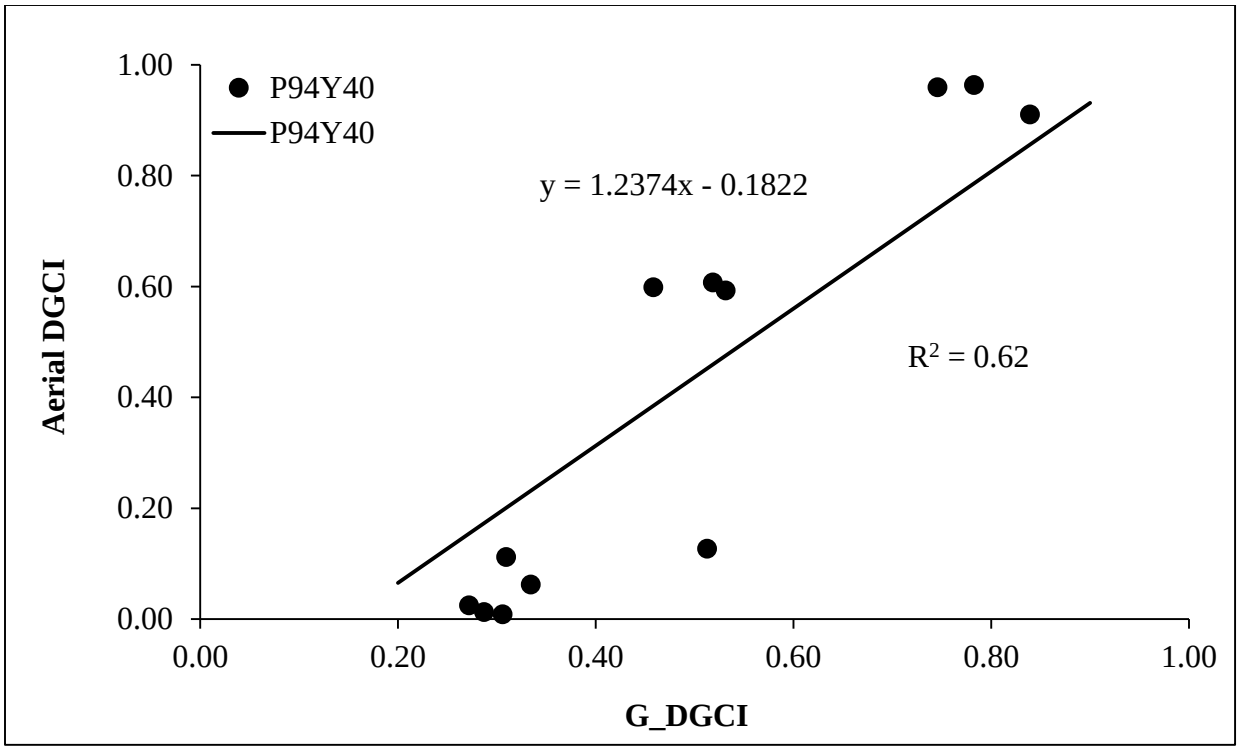

Figure A4 Aerial DGCI versus ground DGCI (G_DGCI) across water treatments (NS) in Fayetteville 2012. Genotype P94Y40 was used to represent the response of aerial DGCI to G_DGCI, which was similar to other genotypes (not included in the figure).

Table A5 ANCOVA for aerial DGCI associated with genotype and G_DGCI*irrigation in Fayetteville 2013. Non-significant interactions were removed from the model stepwise. Letters b and c represented the linear slope and intercept for each genotype under different water treatments in this model.

Aerial DGCI

Source	DF	Mean Square	F Value	Pr > F	Adj. R^2
Irri	1	0.0089	0.79	0.3813	
Geno	4	0.0474	4.23	0.0087	0.70
G_DGCI*irri	2	0.3068	27.42	<.0001	

$y = bx + c$

Geno	Relative MG	Irri	b	c
S25-E5	2.5	DR	1.7000	-0.1448
		WI	1.5333	0.0236
S35-C3	3.5	DR	1.7000	0.0124
		WI	1.5333	0.1808
P93Y72	3.7	DR	1.7000	0.0005
		WI	1.5333	0.1689
P94Y40	4.4	DR	1.7000	0.0905
		WI	1.5333	0.2590
P95Y50	5.5	DR	1.7000	0.0758
		WI	1.5333	0.2442

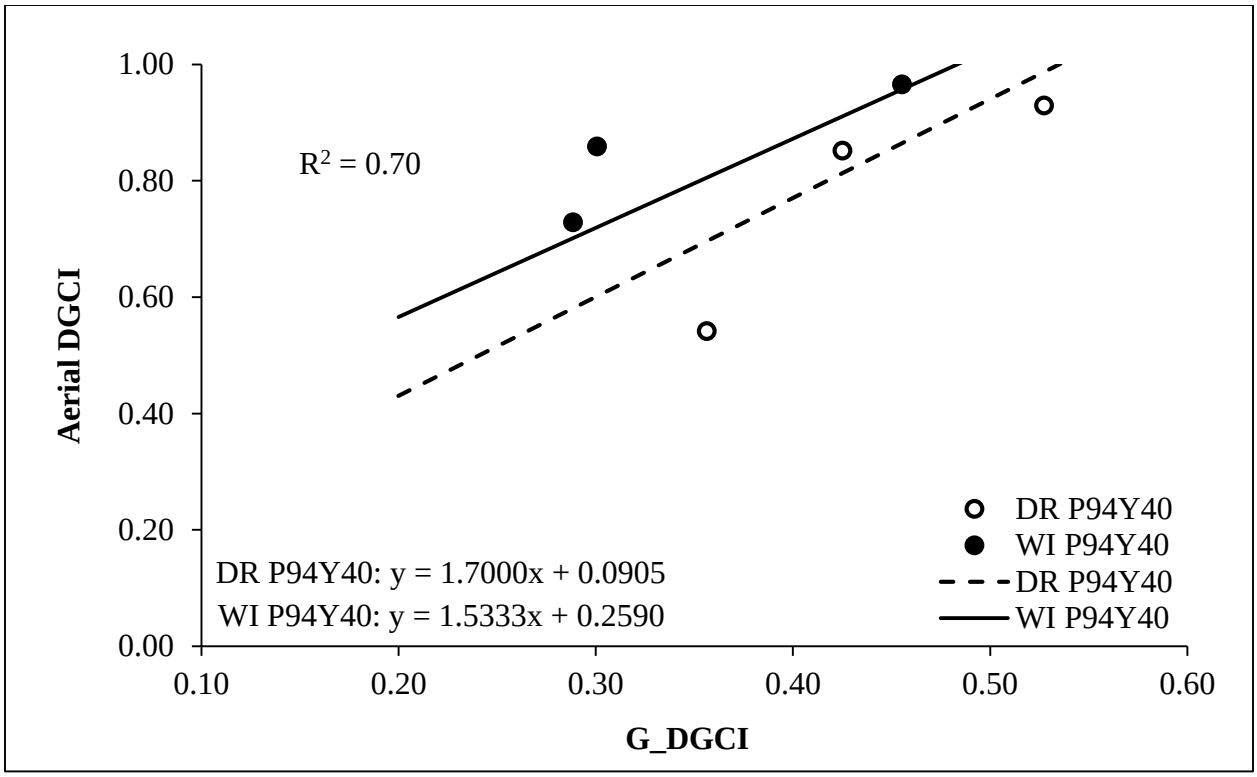

Figure A5 Aerial DGCI versus ground DGCI (G_DGCI) for each genotype under different water treatments in Fayetteville 2013. Genotype P94Y40 was used to represent the response of aerial DGCI to G_DGCI, which was similar to other genotypes (not included in the figure).

Table A6 ANCOVA for aerial DGCI associated with G_DGCI, and G_DGCI* G_DGCI in Fayetteville 2014. Non-significant interactions were removed from the model stepwise.

Aerial DGCI

Source	DF	Mean Square	F Value	Pr > F	Adj. R^2
Irri	1	0.0218	1.18	0.2808	0.62
Geno	4	0.0066	0.36	0.8356	
G_DGCI	1	0.2328	12.66	0.0007	
G_DGCI*G_DGCI	1	0.1087	5.91	0.0179	

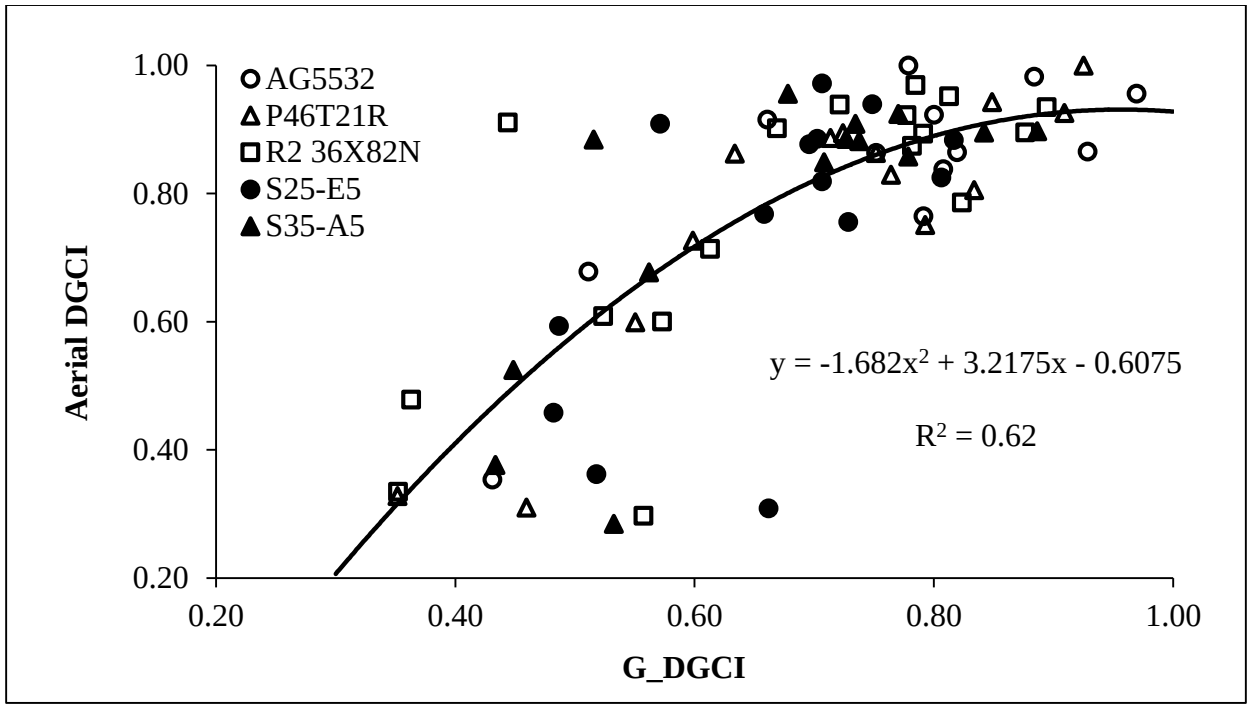

Figure A6 Aerial DGCI versus ground DGCI (G_DGCI) across genotypes and water treatments (genotype × water treatment interaction, NS) in Fayetteville 2014.

C. Leaf N versus Est_HI

Leaf N concentration decreased with increasing est_HI in all years with ANCOVA (**Figure A7, A8,** and **A9**) accounting for between 79 and 96% of the variation (**Table A7, A8,** and **A9**). In 2012, because only two HI samples were taken for AG24-30 and S25-T8, these two genotypes were not included for the data analysis. In 2012, leaf N concentration decreased linearly and was affected by either irrigation or genotype. In 2013, leaf N concentration decreased quadratically with increasing est_HI and was not affected by both irrigation and genotype, but was affected by interactions of est_HI and irrigation and est_HI and genotype. In 2014, there was a quadratic decrease in leaf N concentration that differed among genotypes and between irrigation treatments. The decrease in leaf N concentration in all years indicated that leaf N was remobilized and contributed to seed formation and enlargement. For all years, leaf N concentration under WI conditions was higher than that under DR conditions at est_HI from 0 to 0.5. That can explain the quick senescence of soybean plants under DR conditions compared to WI conditions. Leaf N versus est_HI method was highly similar with the method of G_DGCI and aerial DGCI versus est_HI, expecially with aerial DGCI versus est_HI. G_DGCI versus est_HI cannot identity the difference between irrigation treatments for all years, but both aerial DGCI and leaf N versus est_HI methods were able to detect the differences in water treatments for all 3 years.

Table A7 ANCOVA for leaf N concentration associated with irrigation treatment, genotype, estimated harvest index (est_HI) and interactions of est_HI with each main factor in Fayetteville 2012. Non-significant interactions were removed from the model stepwise. MG2 was not included because they only had two harvest index samples. Letters b and c represented the linear slope and intercept for each genotype under different water treatments in this model.

Leaf N

Source	DF	Mean Square	F Value	Pr > F	Adj. R^2
Irri	1	2.6203	9.45	0.0045	
Geno	2	2.3472	8.47	0.0012	
Est_HI	1	21.4126	77.25	<.0001	0.79
Est_HI*irri	1	1.3560	4.89	0.0347	
Est_HI*geno	2	1.0989	3.96	0.0297	

$y = bx + c$

Geno	Relative MG	Irri	b	c
S33-K5	3.3	DR	-2.2509	3.3237
		WI	-5.3005	4.6167
P94Y40	4.4	DR	-6.6843	5.1078
		WI	-9.7338	6.4008
P95Y50	5.5	DR	-3.3934	3.1490
		WI	-6.4429	4.4420

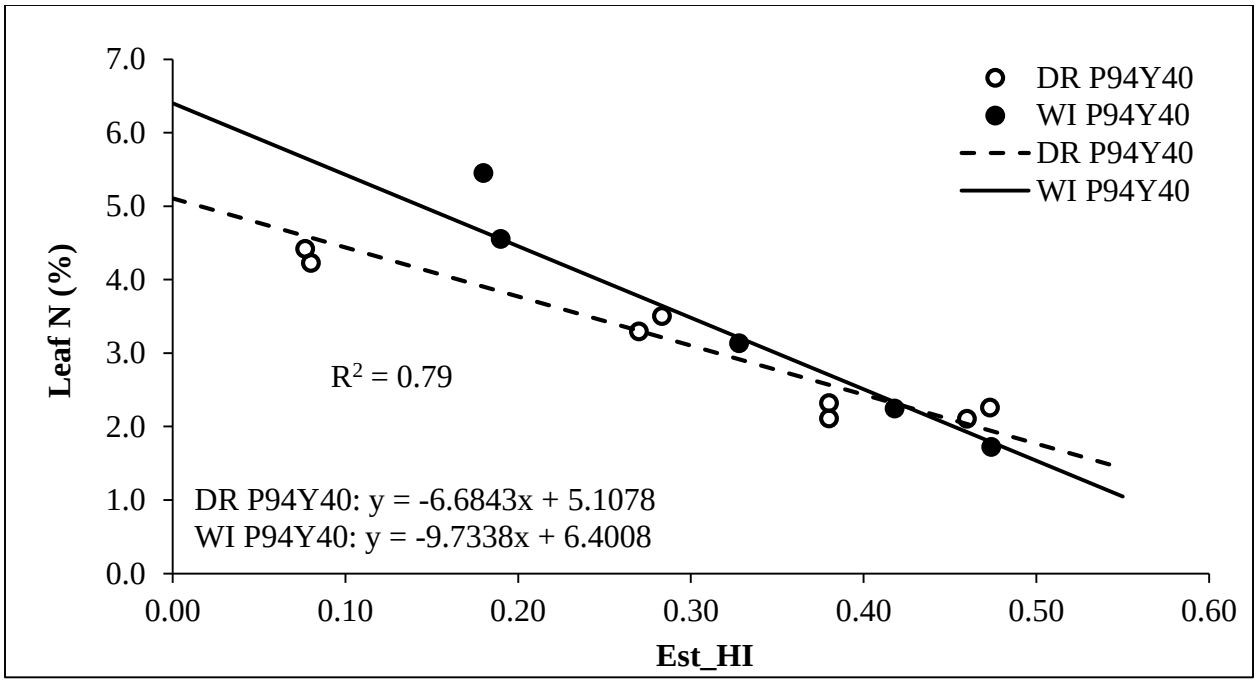

Figure A7 Leaf N concentration versus estimated harvest index (est_HI) for each genotype under different water treatments in Fayetteville 2012. MG2 was not included because they only had two harvest index samples. Genotype P94Y40 was used to represent the response of leaf N concentration to est_HI, which was similar to other genotypes (not included in the figure).

Table A8 ANCOVA for leaf N concentration associated with irrigation treatment*genotype, estimated harvest index (est_HI)*irrigation, est_HI*genotype, est_HI*est_HI, and est_HI*est_HI*genotype in Fayetteville 2013. Non-significant interactions were removed from the model stepwise. Letters a, b and c represented the quadratic and linear slopes and intercept for each genotype under different water treatments in this model.

Leaf N

Source	DF	Mean Square	F Value	Pr > F	Adj. R^2
Irri	1	0.0993	0.88	0.3518	
Geno	4	0.2629	2.34	0.0679	
Irri*geno	4	0.3155	2.81	0.0353	
Est_HI*irri	1	0.7634	6.79	0.012	0.96
Est_HI*geno	4	0.4221	3.76	0.0095	
Est_HI*est_HI	1	4.9718	44.23	<.0001	
Est_HI*est_HI*geno	4	0.3261	2.9	0.0309	

$y = ax^2 + bx + c$

Geno	Relative MG	Irri	a	b	c
S25-E5	2.5	DR	-14.3802	0.5664	6.1181
		WI	-14.3802	2.0873	5.6197
S35-C3	3.5	DR	-13.1230	-0.6596	5.9973
		WI	-13.1230	0.8613	5.6704
P93Y72	3.7	DR	-17.4835	0.4096	5.8323
		WI	-17.4835	1.9304	5.6813
P94Y40	4.4	DR	-28.5825	3.4834	5.7637
		WI	-28.5825	5.0042	5.7850
P95Y50	5.5	DR	-1.4390	-8.6634	5.0411
		WI	-1.4390	-7.1425	5.3533

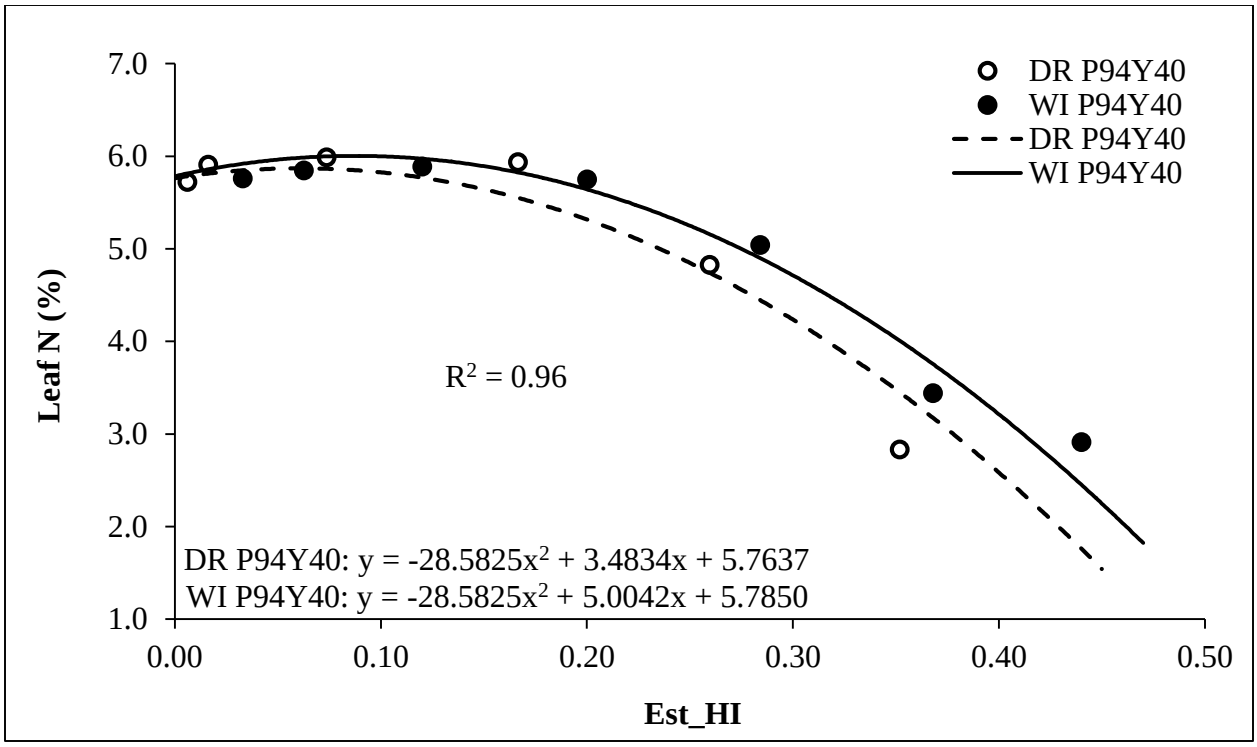

Figure A8 Leaf N concentration versus estimated harvest index (est_HI) for each genotype under different water treatments in Fayetteville 2013. Genotype P94Y40 was used to represent the response of leaf N concentration to est_HI, which was similar to other genotypes (not included in the figure).

Table A9 ANCOVA for leaf N concentration associated with irrigation, genotype and estimated harvest index (est_HI)*est_HI in Fayetteville 2014. Non-significant interactions were removed from the model stepwise. Letters a and c represented the quadratic slope and intercept for each genotype under different water treatments in this model.

Leaf N

Source	DF	Mean Square	F Value	Pr > F	Adj. R^2
Irri	1	1.5050	7.29	0.0088	0.89
Geno	4	3.1901	15.46	<.0001	
Est_HI*est_HI	1	109.2195	529.30	<.0001	

$y = ax^2 + c$

Geno	Relative MG	Irri	a	c
S25-E5	2.5	DR	-13.8467	5.9986
		WI	-13.8467	6.2884
S35-A5	3.5	DR	-13.8467	5.6400
		WI	-13.8467	5.9298
R2 36X82N	3.6	DR	-13.8467	5.9111
		WI	-13.8467	6.2010
P46T21R	4.6	DR	-13.8467	5.2424
		WI	-13.8467	5.5322
AG5532	5.5	DR	-13.8467	4.7756
		WI	-13.8467	5.0654

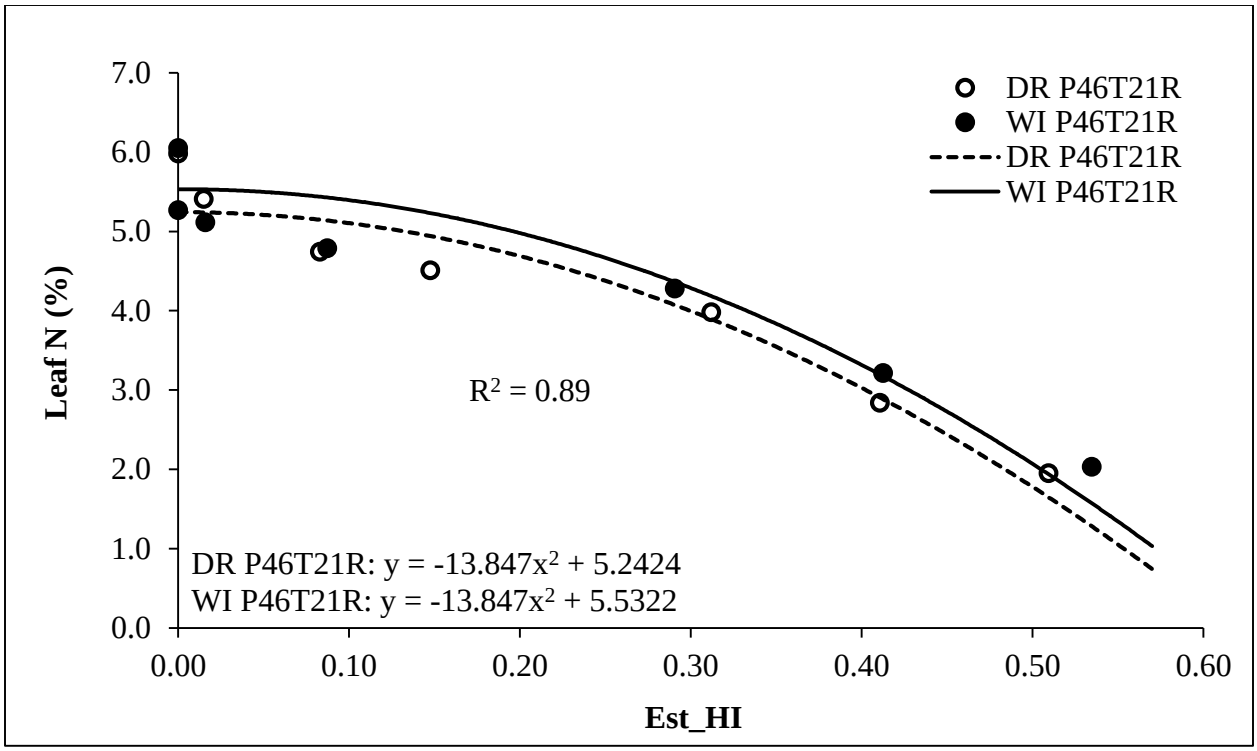

Figure A9 Leaf N concentration versus estimated harvest index (est_HI) for each genotype under different water treatments in Fayetteville 2014. Genotype P46T21R was used to represent the response of leaf N concentration to est_HI, which was similar to other genotypes (not included in the figure).